0 0 0 0 9 5 4 0 2 5 9 7

UC-25 ~~82~~
LBL-9264
c.1

THE COMPUTER SIMULATION OF MARTENSITIC TRANSFORMATIONS IN IDEALIZED SYSTEMS

RECEIVED
LAWRENCE
BERKELEY LABORATORY

JUN 28 1979

LIBRARY AND
DOCUMENTS SECTION

Sheree Hsiao-Ru Chen
(Ph. D. thesis)

June 1979

Prepared for the U. S. Department of Energy
under Contract W-7405-ENG-48

For Reference

Not to be taken from this room

LAWRENCE BERKELEY LABORATORY
UNIVERSITY OF CALIFORNIA

LBL-9264

LEGAL NOTICE

This report was prepared as an account of work sponsored by the United States Government. Neither the United States nor the United States Department of Energy, nor any of their employees, nor any of their contractors, subcontractors, or their employees, makes any warranty, express or implied, or assumes any legal liability or responsibility for the accuracy, completeness or usefulness of any information, apparatus, product or process disclosed, or represents that its use would not infringe privately owned rights.

THE COMPUTER SIMULATION OF MARTENSITIC TRANSFORMATIONS IN IDEALIZED SYSTEMS

by

Sheree Hsiao-Ru Chen

Materials and Molecular Research Division
Lawrence Berkeley Laboratory
University of California
Berkeley, California 94720

獻給

父母親

誰言寸草心

報得三春暉？……

To My Dear Parents

How can the growing grass

repay the sun which made it grow?.....

0 0 - 0 3 4 0 2 7 0 1

THE COMPUTER SIMULATION OF MARTENSITIC TRANSFORMATIONS IN IDEALIZED SYSTEMS

by

Sheree Hsiao-Ru Chen

ABSTRACT

Despite the engineering importance of martensitic transformations in solids, particularly steel, there exists very little theoretical work on the development of the martensitic transformation and the characteristics of the resulting microstructure. It is the purpose of the present thesis to advance the theory of the martensite transformation by constructing a computer model of a martensitic transformation in an idealized system. The model has its source in the general observation that the characteristics of martensitic transformations in solids are largely determined by the problem of accomodating the strain associated with the martensitic distortion of the crystal lattice. A review and adaptation of prior theoretical work leads to the development of a theory which allows the straightforward computation of the elastic energy associated with an arbitrary distribution of defects in an elastically anisotropic body under the assumption that the body has uniform elastic constants and that anharmonic effects may be neglected. These equations are cast into a form in which the energy is written as a simple sum of binary interactions in which the defects influence one another according to an elastic potential whose form can be readily calculated. At the same time that the energetic equations take a simple form the kinematics of the process involving the appearance of elastic inclusions are also

known to be simple since in a harmonic model an inclusion may be regarded as a simple sum of elementary inclusions which make it up. Given this theoretical foundation the martiensitic transformation is modeled as a transformation which occurs through the sequential formation of individual martensitic elements, each of which carries the elementary transformation strain. Statistical equations are developed which govern the selection of the transformation path, or specific sequence in which elementary martensite particles appear in the model, and which specify the kinetics of transformation along any known path. A useful representative path is defined, the "minimum energy" path. The resulting model is then used for the detailed simulation of a martensitic transformation in a pseudo two-dimensional system. Despite the simplicity of the model virtually all interesting qualitative aspects of the developing martensitic transformation are shown to be inherently present within it.

Acknowledgement

I would like to express my deepest gratitude to my advisor, Professor J. W. Morris Jr. and to Dr. A. G. Khachaturyan for their close collaboration in this work. Their guidance, enthusiasm and stimulating inspiration brought this work into being. It has been a most valuable and pleasurable experience for me to work with people, who are excellent scientists, who search for truth, and who are thoughtful and honest friends.

I would also like to express my sincere thanks to Professor Gareth Thomas and Professor Leo Falicov for their stimulating discussions and valuable advice on this work. Special thanks to Professor Gareth Thomas and Dr. B. Rao for their beautiful TEM micrographs which are shown in this thesis as illustrations of the experimental evidence.

Many thanks to the colleagues in our group and department who provided interesting discussions and a pleasant working atmosphere during the course of this work. A special deep appreciation is extended to Dr. Kenton Hanson for his useful discussion, as well as, constant help.

I am pleased to thank Mrs. Jeanne L. Shull for her careful preparation of this manuscript and to Mrs. Delores Nobles for her benevolent assistance.

I would like especially to thank my parents, my brothers and sisters and most of all my dearest husband. Their love, patience, understanding and encouragement through these years has been my great emotional support.

This work was supported by the Division of Materials Sciences, Office of Basic Energy Sciences, U.S. Department of Energy under contract No. W-7405-Eng.-48.

0 0 - 5 4 0 2 7 0 3

THE COMPUTER SIMULATION OF MARTENSITIC TRANSFORMATIONS IN IDEALIZED SYSTEMS

Table of Contents

ABSTRACT

Acknowledgement----------i

I. INTRODUCTION----------1

II. THE ELASTIC ENERGY OF A HETEROGENEOUS CRYSTAL----------10

A. The Macroscopic Elastic Theory----------11

B. The Microscopic Elastic Theory----------19

C. The Long-Wavelength Approximation----------44

D. Limit Transition to the Continuum Theory of Macroscopic Elastic Inclusion----------47

III. THE MARTENSITE TRANSFORMATION----------51

A. The Description of Martensite in Terms of Elementary Particles----------54

B. The Elastic Energy----------57

C. The Chemical Energy----------61

D. The Total Energy and the Thermoelastic Potential----------64

E. The Path and Kinetics of the Martensite Transformation------66

F. The Minimum-Energy Path----------75

IV. COMPUTER SIMULATION OF MARTENSITE TRANSFORMATION----------79

V. COMPUTER SIMULATION RESULTS----------83

A. The Single Nucleus Case----------83

B. Multi-Nucleus Case----------87

C. Variations on the Multi-Nucleus Case----------94

D. Variation of Array Size and Dimensionality----------97

E. The Introduction of Elastic Anisotropy and Dilatation-------99

VI. DISCUSSION ---- 103

A. Comparison with Experiment ---- 103

B. Extensions of the Model ---- 108

VII. CONCLUSIONS ---- 118

REFERENCES ---- 121

FIGURE CAPTIONS ---- 125

FIGURES ---- 128

0 0 0 5 4 0 2 7 0 4

I. INTRODUCTION

The Chinese have an adage "The shortest step may be the beginning of the longest journey". As long ago as 4,000 B.C., primitive men were using meteoric iron as a rare and valuable material. This 'heaven-sent iron' could be hammered and worked like native gold and copper but became harder than either of them and hence very useful for the manufacture of implements. This marked the initial use of "heaven-sent" martensitic iron.

Over the next four millenia men learned to win iron from its ores, to purify it and to join it into useful implements. However, these implements were for the most part soft and easily bent, lacking the hardness we associate with modern, industrial steel tools. The development of steel in the modern sense occurred at about the time of Christ. Many of its first and most important uses were military. We know that in the battle of Insubres (220 B.C.) the Romans, using weapons made of quenched carbon-containing iron, easily defeated Gallic forces armed with traditional wrought iron weapons. This and subsequent Roman military successes, which were due in no small part to their metallurgical superiority, amply demonstrated the advantages of quenched carbon-containing irons for the manufacture of useful implements. Though the Romans were not aware of the fact they were using some of the first man-made martensitic steels.

The term "martensite" is adapted from the name of the 19th century metallographer, A. Martens, who was among the first to study the correlation between the microstructure and properties of quenched carborized iron. He and other 19th century metallographers observed that when iron containing carbon is cooled rapidly from a temperature at which the high

temperature austenitic phase is stable, the usual nucleation and growth transformation to the soft "pearlitic" phase is avoided, and the body instead undergoes a very rapid transformation at low temperature to an extremely hard product phase.

In our more modern understanding martensite is not strictly a different phase of steel, but rather a unique microstructure which results from the special characteristics of the martensite transformation which gives it birth. The decomposition of the high temperature FCC austenitic phase on slow cooling involves a separation into two phases of different carbon content. The process hence requires diffusion. If the steel is cooled so rapidly that these diffusional processes cannot occur, however, the driving force for transformation from the high temperature FCC phase to the low BCC phase becomes so great that the steel eventually undergoes a very rapid diffusionless shear transformation to a nearly BCC structure with no change in composition. The mechanical character of the transformation introduces elastic strains and often high densities of dislocations, twins, or other defects into the lattice. These, combined with the distortions caused by the presence of the supersaturation of carbon, induce the high structural strength that engineers have found so useful since the time of the Romans.

We now know that the martensitic transformation in steel is only one example of a class of similar transformations that are found in a number of physical systems (Table I.).[1] Materials known to exhibit martensitic transformations include a variety of metal alloy systems, ferro-electric materials such as beryllium titanate, ceramic materials such as zirconium oxide, superconducting phases, and many others. The characteristics of the martensite product differ from system to system,

and are particularly sensitive to the crystallography of the initial and product phases. As a consequence of extensive experimental study over many years, it is known that a number of morphological, kinetic and crystallographic features are, however, common to a wide variety of martensitic transformations and their product phases. These can be summarized as follows:

- Morphologically, the martensitic phase usually forms as a thin plate, needle, or lath lying along a reasonably well defined habit plane of the parent crystal. The crystallographic axes of the martensitic phase show reproducible orientation relationships to those of the parent phase. The interior of the martensite platelet is dense with crystal defects, which may be either crystallographic twins or dislocations. If the martensite platelet impinges on a free surface, the latter will be deformed to exhibit a characteristic surface relief.

- Kinetically, the martensitic transformation is extremely rapid, with each platelet growing at speeds which approach the speed of sound. In general, the transformation begins with the rapid growth of a single platelet which then triggers the growth of further platelets by an autocatalytic process. The result is a "burst" of martensitic transformation which often produces a "click" audible in experiment.

- However, the martensitic transformation will usually not go to completion at its initiation temperature. To maintain the transformation and bring it essentially to completion, it is necessary that the temperature be decreased continuously. The temperature at which a martensitic transformation first begins is denoted the martensite start temperature, M_s, and that at which it essentially reaches completion is called the martensite finish temperature, M_f. It is, however, commonly

found that the last bit of high temperature phase is extremely difficult to remove through a martensitic transformation. Even after the transformation is sensibly complete, retained high temperature phase may still be found along the periphery of the martensite platelets.

- The martensitic transformation may be reversed by heating, but transformation hysteresis effects are usually observed. The reverse martensite transformation is initiated at a temperature A_s, and is completed at a higher temperature A_f, which may lie several hundreds of degrees above the M_s temperature at which the martensite transformation begins on cooling.

- In keeping with the mechanical character of the transformation, both the temperature at which the martensite formation occurs and the type and morphology of the martensite platelets which are formed are strongly influenced by the presence of applied stress. In iron, where the martensitic phase is ferromagnetic, these features are also influenced by the presence of magnetic fields.

While the martensitic transformation has been studied extensively experimentally and is reasonably well understood phenomenologically, its theoretical interpretation remains at a rather primitive analytical level. Significant progress has been made in understanding and interpreting the morphology and crystallographic orientation of isolated martensite particles. However, the nucleation and growth characteristics, autocatalytic phenomena and resultant martensite microstructure remain poorly understood. The resolution of these questions is of major engineering, as well as scientific, importance.

Studies on the crystallography of the isolated martensite platelets began with the work of Bain in 1924[2] and were developed by Kurdjumov and Sachs[3] and by Nishiyama[4] in the 1930's. The crystallographic relations found by these researchers successfully predicted the lattice correspondence between the martensite particle and the parent phase. The crystallographic relations do not, however, uniquely fix the details of the atomic displacements which occur, a subject which is still the topic of much discussion[5,6,7,8]. The habit plane of an isolated martensite particle can be obtained from its orientation following crystallographic models developed by Greninger and Troiano[9], Liebreman, Wechsler and Read[10], Bowles and Mackenzie[11], and later Wayman[12]. These models essentially begin from the hypothesis that the habit of a martensite plate will be a plane of lattice correspondence with the parent matrix which gives rise to an invariant plane strain, so as to minimize the elastic energy. An equivalent, but more direct approach was taken by Khachaturyan[13,14,15] who computed the elastic energy associated with a martensitic inclusion in an anisotropic medium as a function of its shape and habit, and derived results for the habit plane and structure of martensite crystals essentially identical to those obtained from the crystallographic theory. A similar analysis was performed by Shabata and Ono[16] who employed an alternative formulation for the elastic energy based on the Eshelby treatment[17,18]. As a consequence of this work, the shape and orientation of isolated particles may be said to be reasonably well established, and can be based alternatively on crystallographic or elastic energy formulations.

Our understanding of the initiation, growth and development of martensite is, however, not nearly so well developed. The nucleation of

the martensitic transformation in steel has been studied from the point of view of classical homogeneous nucleation theory by Kaufman and Cohen[19], Read and Breedes[1], Christian[20], and Easterling and Thölén[21]. These investigators treated the martensite nucleus as a discrete homogeneous particle involving an internal elastic distortion and a relatively high surface energy. They concluded that the activation energy required for homogeneous nucleation of martensite in bulk is far too high to be overcome purely by thermal fluctuations. This conclusion is supported by experimental evidence on the martensitic transformation in steel which also appears to shown that the martensitic transformation is heterogeneously nucleated. Specific mechanisms for heterogeneous nucleation were proposed by Frank[22], by Kaufman and Cohen[19] who suggested the presence of pre-existing embryos of the martensite phase, by Olson and Cohen[23], who proposed a mechanism involving cooperative faulting from groups of existing dislocations, and others. None of these models is widely accepted at the present time.

An alternative approach, which has been applied with some success to nonferrous systems, treats martensitic transformations which arise from "soft mode" mechanisms in which the parent phase becomes unstable with respect to infinitesimal distortions. Examples of martensitic transformations which appear to be of the soft mode type include transformations in A15 compounds, such as Nb_3Sn and V_3Ga, and the well known omega transformation in titanium alloys. Soft mode theories for the transformation of A15 compounds are particularly well developed. Labbe and Friedel[24] and Pytte[25,26] proposed models based on an instability with respect to a Jahn-Teller distortion of the parent phase. Gorkov[27-30] suggested a lattice instability due to the Peierls mecha-

nism of an energy gap opening near the Fermi Surface. Mattheiss[31] developed a successful Landau theory based on the Gorkov model. He also proposed a microscopic model using a band structure calculated by APW techniques which includes both the Jahn-Teller instability and the Peierls effect. This model predicts an elastic softening ($C11-C12 \rightarrow 0$) for the <110> transverse mode as the transition temperature is approached. Variations on the "soft mode" which involve instabilities with respect to finite atom displacements have been proposed by Clapp[32] and by Suzuki and Wuttig[33] among others.

While the crystallography, shape, and habit of isolated martensite particles may be regarded as well understood theoretically, and the problem of the initiation of the martensite transformation has at least been widely attacked, there exists virtually no prior theoretical work on the development of the martensitic transformation and the characteristics of the resulting microstructure. The absence of relevant theoretical work is perhaps not surprising given the complexity of martensitic transformation behavior, but is disconcerting since it is during the development of the martensitic transformation that the most interesting phenomenological apsects of the transformations appear and it is the final microstructure of the martensite phase which most strongly determines engineering properties.

It is the purpose of the present thesis to devise a more comprehensive treatment of the martensitic transformation by constructing a computer model of the martensitic transformation in an idealized system.

The model which will be developed here begins from the general observation that the characteristics of the martensite transformation are largely determined by the problem of accomodating the strain asso-

ciated with the distortion of the crystal lattice, and from the realization that, due largely to the work of Khachaturyan[34-38] we are now in possession of rather elegant theoretical tools which permit the comprehensive treatment of elastic distortions in the context of the linear elastic model. The model which is constructed and utilized here is set up essentially as follows:

The Khachaturyan formulation of the linear theory of elastic inclusions in anisotropic media permits the straightforward computation of the elastic energy associated with an arbitrary distribution of defects in an elastically anisotropic body having uniform elastic constants. Moreover, if the defects consist of elementary particles of a few discrete types, the equations can be cast into a form in which the energy becomes a simple sum of binary interactions in which the defects influence one another according to an elastic potential whose form can be readily calculated. At the same time as the equations take a simple form in a linear model, the kinematics of a process involving the appearance of elastic inclusions also become simple since in the linear model an inclusion may be regarded as the simple sum of elementary inclusions which make it up.

The martensitic transformation is hence modeled as a transformation which occurs through the formation of individual martensitic elements, each of which carries the elementary transformation strain. Since the energy associated with an arbitrary distribution of such martensitic elements can readily be calculated in a form which is particularly well adapted for solution in a digital computer, the model martensitic transformation can be allowed to proceed through the successive appearance of elementary martensite particles whose type and location is chosen by

the computer according to some reasonable energy criterion; for example. to provide the maximum rate of energy decrease or to follow the statistics of an assumed thermally activated process. The kinematics and governing equations of the model are developed in detail in subsequent sections. The model is then used for the detailed simulation of a martensitic transformation in a pseudo two-dimensional system. As we shall see, despite the simplicity of the model, virtually all interesting qualitative aspects of a developing martensitic transformation are inherently present within it.

The body of this work is developed in four sections. The first section contains a brief review of previous results concerning the elastic theory of phase transformations, the formulation of the equations giving the energy of a crystal lattice containing a distribution of substitutional defects from the lattice statics theory, the development of the long wavelength approximation to the microscopic elastic theory and the derivation of the limit transition to the continuum theory of the macroscopic elastic inclusion. In the second section this model is specified to the particular case of a martensitic transformation whose development is driven by the need to accomodate the elastic strain. In the third section the specific procedures for computer simulation of the martensitic transformation in a pseudo two-dimensional crystal lattice are discussed, and in the fourth section the results of the simulation are presented with particular emphasis on the qualitative reproduction of interesting features of martensitic transformations observed in bulk.

II. THE ELASTIC ENERGY OF A HETEROGENEOUS CRYSTAL

The theory of the elastic energy of a crystal containing defects has developed along two largely independent lines that lead, respectively, to the "macroscopic" elastic theory and to the "microscopic" or "lattice statics" theory. The former is most useful in the treatment of large inclusions, such as precipitate particles. The latter was developed to treat problems such as the elastic relaxation near point defects in crystal lattices.

The model which is constructed and utilized for the study of the martensitic transformation in the body of this thesis lies in the middle ground between these two formulations. The present section is included to lay the theoretical foundations for this model. In subsection A we review some salient features of the macroscopic elastic theory. In subsection B we define the microscopic, or "lattice statics" model, and reformulate it for the particular case of an anisotropic elastic body which contains an arbitrary distribution of substitutional defects. In subsections C and D we establish the correspondence between the microscopic and macroscopic approaches in the limit in which the defects are aggregated into large inclusions.

It is worthwhile to mention that the model described in this section is not only applicable to the martensitic transformation but also to a wide variety of phase transformation in metallurgical systems, such as order-disorder reactions, spinodal decomposition, tweed formation and precipitation reactions. The exploration of applications to these other transformation types is in progress at the present time.

A. The Macroscopic Elastic Theory

The first serious attempt to calculate the elastic energy of a coherent inclusion was apparently made by Eshelby[17], who considered an ellipsoidal inclusion in an isotropic medium. Eshelby obtained a general solution for the elastic energy of an ellipsoidal inclusion in a matrix of similar elastic constants, and formulated a procedure which might be used when the elastic moduli are not the same. His work led to a variety of specific results which have subsequently proven to be of significant value to the theory of phase transformations. However, his real-space formulation of the problem is difficult to extend to cases involving non-ellipsoidal geometry, anisotropic elastic constants, or distributions of inclusions. These formal limitations are important, since many of the problems of greatest interest in the theory of phase transformations in solids involve distributions of inclusions whose configuration depends strikingly on the anisotropy of the matrix.

A general solution for the elastic energy of an arbitrary distribution of macroscopic elastic inclusions in an anisotropic matrix was obtained by Khachaturyan[14], who used a Fourier transform technique to solve the problem under an assumption of uniform elastic constants. The central result of the Khachaturyan treatment is that the elastic energy of an inclusion (or distribution of like inclusions) of arbitrary shape may be written in the compact form

$$E_{el} = \frac{1}{2} \iiint_{-\infty}^{\infty} B(\underset{\sim}{e}) \left|\tilde{\theta}(\underset{\sim}{k})\right|^2 \frac{d^3k}{(2\pi)^3} \qquad \text{(II-A-1)}$$

where $e = \underset{\sim}{k}/|\underset{\sim}{k}|$ is a unit vector, $B(\underset{\sim}{e})$ is a scalar elastic energy function which is independent of the shape or distribution of the inclusions and $|\tilde{\theta}(\underset{\sim}{k})|^2$ is an "intensity" factor which is independent of both the nature of the inclusion and the values of the elastic constants.

Specifically, the elastic energy function is given by

$$B(\underset{\sim}{e}) = \lambda_{ijk\ell}\varepsilon^{o}_{ij}\varepsilon^{o}_{k\ell} - \underset{\sim}{e}_i\sigma^{o}_{ij}\Omega_{jk}(\underset{\sim}{e})\sigma^{o}_{k\ell}\underset{\sim}{e}_\ell \qquad \text{(II-A-2)}$$

where i, j, k, ℓ are cartesian indices (which are to be summed if repeated), $\lambda_{ijk\ell}$ are the elastic constants, ε^{o}_{ij} is the "transformation strain", i.e., the strain required to bring the matrix lattice into coincidence with that of the inclusion, σ^{o}_{ij} is the "transformation stress",

$$\sigma^{o}_{ij} = \lambda_{ijk\ell}\varepsilon_{k\ell} \qquad \text{(II-A-3)}$$

and Ω^{o}_{ij} is a Green's function whose reciprocal is related to the dynamical matrix in the long wavelength approximation:

$$\Omega^{-1}_{k\ell}(\underset{\sim}{e}) = \lambda_{ik\ell j}e_i e_j \qquad \text{(II-A-4)}$$

The function $B(\underset{\sim}{e})$ multiplied by the volume is, in fact, equal to the elastic energy of the inclusion when the inclusion is in the form of an infinite plate which is oriented so that its normal vector $\underset{\sim}{n}$ is parallel to $\underset{\sim}{e}$ and which is strained so as to provide an exact lattice correspondence with the matrix in the plane of the plate.

The "intensity" factor $|\tilde{\theta}(\underset{\sim}{k})|^2$ coincides with the Laue interference function which describes the intensity distribution in reciprocal space caused by scattering from the inclusion. The $\tilde{\theta}(\underset{\sim}{k})$ is the Fourier transform of the shape function

$$\theta(\underset{\sim}{r}) = \begin{cases} 1 \text{ for } \underset{\sim}{r} \text{ inside an inclusion} \\ 0 \text{ otherwise} \end{cases} \qquad \text{(II-A-5)}$$

The intensity factor satisfies the identity

$$\iiint_{-\infty}^{\infty} \frac{d^3k}{(2\pi)^3} |\tilde{\theta}(\underset{\sim}{k})|^2 = V \qquad \text{(II-A-6)}$$

where V is the volume of the inclusion.

As shown by Khatchaturyan and Shatalov[15], equations (II-A-1) may be generalized to the case of simultaneous distributions of inclusions of distinct types. The result is

$$E_{el} = 1/2 \sum_{pq} \iiint_{-\infty}^{\infty} B_{pq}(\underset{\sim}{e})\, \theta_{pq}(\underset{\sim}{k}) \frac{d^3k}{(2\pi)^3} \qquad \text{(II-A-7)}$$

where p and q label the different inclusion types,

$$B_{pq}(\underset{\sim}{e}) = \lambda_{ijk\ell}\varepsilon^{o}_{ij}(p)\ \varepsilon^{o}_{k\ell}(q) - e_i\sigma^{o}_{ij}(p)\ \Omega_{j\ell}\ (\underset{\sim}{e})\ \sigma^{o}_{\ell k}(q)\ e_k, \qquad \text{(II-A-8)}$$

and

$$\theta_{pq}(\underset{\sim}{k}) = \tilde{\theta}_p(\underset{\sim}{k})\ \tilde{\theta}^{*}_q(\underset{\sim}{k}) \qquad \text{(II-A-9)}$$

Many of the most important results of the macroscopic elastic theory follow directly from eq. II-A-1 or II-A-7. Examples include the following:

(1) The elastic energy is positive semi-definite (i.e. $E_{el} \geq 0$). It may easily be shown that

$$B(\underset{\sim}{e}) \geq 0. \qquad \text{(II-A-10)}$$

The vanishing of $B(\underset{\sim}{e})$ occurs only in the special case, discussed below, in which the transformation strain has an invariant plane perpendicular to $\underset{\sim}{e}$.

(2) The preferred shape of an inclusion is an infinitely thin plate with a habit plane specified by the normal vector, $\underset{\sim}{n}_o$.

Let $\underset{\sim}{n}_o$ be the direction for which $B(\underset{\sim}{e})$ takes on its minimum value

$$B(\underset{\sim}{e}) \geq B(\underset{\sim}{n}_o) \qquad \text{(II-A-11)}$$

The $\underset{\sim}{n}_o$ will be unique except for the degeneracy imposed by symmetry

considerations. From equation II-A-1

$$E_{el} = 1/2 \iiint_{-\infty}^{\infty} B(\underset{\sim}{e}) \; |\tilde{\theta}\,(\underset{\sim}{k})|^2 \; \frac{d^3k}{(2\pi)^3}$$

$$\geq 1/2 \; B(\underset{\sim}{n}_o) \iiint_{-\infty}^{\infty} |\tilde{\theta}\,(\underset{\sim}{k})|^2 \; \frac{d^3k}{(2\pi)^3} = 1/2 \; B(\underset{\sim}{n}_o) \; V \qquad \text{(II-A-12)}$$

Hence E_{el} takes its minimum value

$$E_{min} = 1/2 \; B(\underset{\sim}{n}_o) \; V \qquad \text{(II-A-13)}$$

when the intensity factor $|\tilde{\theta}\,(\underset{\sim}{k})|^2$ is non-zero only within an arbitrary thin rod of direction $\underset{\sim}{n}_o$, and hence when the shape factor, $\theta\,(\underset{\sim}{r})$, is non-zero only within an infinitely thin plate normal to $\underset{\sim}{n}_o$.

The coherent inclusions produced by phase transformations in solids are usually found to have the predicted thin-plate morphology. Exceptions occur when the lattice mismatch between the inclusion and the matrix (and hence the elastic energy) is small, or when the particle is so small that surface energy effects predominate.

(3) When the inclusion is plate-like but finite, its energy may be written as the sum of a volume term and a peripheral energy in which the peripheral energy is formally equivalent to the energy of a dislocation loop with an appropriate Burger's vector.

Let the precipitate be a thin plate with normal $\underset{\sim}{n}_o$.

$$E_e = 1/2 \iiint_{-\infty}^{\infty} B(\underset{\sim}{e}) \; |\tilde{\theta}\,(\underset{\sim}{k})|^2 \; \frac{d^3k}{(2\pi)^3}$$

$$= 1/2 \; B(\underset{\sim}{n}_c) \;\; V + 1/2 \iiint_{-\infty}^{\infty} \Delta B(\underset{\sim}{e}) \; |\tilde{\theta}\,(\underset{\sim}{k})|^2 \; \frac{d^3k}{(2\pi)^3} \qquad \text{(II-A-14)}$$

We now expand $B(\underset{\sim}{e})$ about $\underset{\sim}{n}_o$. Since $B(\underset{\sim}{n}_o)$ is a minimum, the first term in the expansion vanishes. To second order,

$$\Delta B(e) = B(\underset{\sim}{e}) - B(\underset{\sim}{n}_o)$$

$$\simeq 1/2\ (\partial^2\ B(e)/\partial e_i \partial e_j)_{\underset{\sim}{e}=\underset{\sim}{n}_o}\ \Delta e_i\ \Delta e_j \qquad \text{(II-A-15)}$$

$$\simeq 1/2\ \beta_{ij}(\underset{\sim}{n}_o)\ \ \Delta e_i\ \Delta e_j$$

where

$$\beta_{ij}(\underset{\sim}{n}_o) = (\partial^2 B(e)/\partial e_i \partial e_j)_{\underset{\sim}{e}=\underset{\sim}{n}_o} \qquad \text{(II-A-16)}$$

For a thin plate $|\tilde{\theta}(\underset{\sim}{k})|^2$ is small for angles larger than

$$\zeta \sim \frac{2\pi/2R}{2\pi/d} \sim \frac{d}{2R} = \frac{1}{\Lambda} \qquad \text{(II-A-17)}$$

where ζ is the angle between $\underset{\sim}{e}$ and $\underset{\sim}{n}_o$, d and R are the thickness and radius of the inclusion respectively, and Λ is the aspect ratio, 2R/d. By using (II-A-15) in (II-A-14) and confining the integration to small angles, it may be shown that

$$E_e = 1/2\ B(\underset{\sim}{n}_o)\ V + \oint \Gamma(\underset{\sim}{m})\ dl(\underset{\sim}{m}) \qquad \text{(II-A-18)}$$

where $\underset{\sim}{m}$ is a unit vector perpendicular to the element, $dl(\underset{\sim}{m})$, of the plate periphery and lying in the plane of the plate, and

$$\Gamma(m) = \frac{d^2}{4\pi}\ \ln\ (2R/d)\ \beta_{ij}(\underset{\sim}{n}_o)\ m_i m_j \qquad \text{(II-A-19)}$$

The function $\Gamma(\underset{\sim}{m})$ formally resembles the line tension of a dislocation line element of Burger's vector of the order $\varepsilon^o d$.

When the function $\Gamma(\underset{\sim}{m})$ is a constant, Γ, as it is, for example, in the case of a tetragonal inclusion in a cubic matrix, then the elastic energy can be written

$$E_e \simeq V \left\{ 1/2\ B(\underset{\sim}{n}_o) + \ [\frac{1}{\Lambda}\ \ln\ \Lambda] \right\} \qquad \text{(II-A-20)}$$

Where $\beta = \beta_{ij}(n_o)\ m_i m_j$ = constant. This relation allows the energy per unit volume to be phrased as a simple function of the aspect ratio.

(4) When the transformation strain has an invariant plane, the bulk elastic energy of a properly oriented plate is zero.

Let the transformation strain have the diadic form

$$\varepsilon^o_{ij} = (\ell_i n^o_j + n^o_i \ell_j) \qquad \text{(II-A-21)}$$

where $\underset{\sim}{\ell}$ and $\underset{\sim}{n}_o$ are unit vectors.

If we substitute (II-A-21) into (II-A-2)

$$\begin{aligned} B(\underset{\sim}{n}_o) &= \Lambda_{ijk\ell}(\ell_i n^o_j)\ (\ell_k n^o_\ell) \\ &\quad - n^o_i\ (\lambda_{ijk\ell}\ell_k n^o_\ell)\ \Omega_{js}(\underset{\sim}{n}_o)\ (\lambda_{spqr}\ell_q n^o_r)\ n^o_p \\ &= 1/2\ [\lambda_{ijk\ell} n^o_j n^o_\ell \ell_i \ell_k - \ell_k(\lambda_{ijk\ell} n^o_i\ n^o_\ell)\ \Omega_{js}(\underset{\sim}{n}_o)\ (\lambda_{spqr} n^o_r n^o_p\ )\ \ell_q] \end{aligned}$$

(II-A-22)

According to the definition of the tensor $\hat{\Omega}$

$$\lambda_{ijk\ell} n^o_i n^o_\ell = \Omega^{-1}_{jk}\ (\underset{\sim}{n}_o) \qquad \text{(II-A-23)}$$

$$\lambda_{spqr} n^o_r n^o_p = \Omega^{-1}_{sq}\ (\underset{\sim}{n}_o) \qquad \text{(II-A-24)}$$

substitution of (II-A-23) and (II-A-24) into (II-A-22), using the relation

$$\hat{\Omega}^{-1}_{i\ell}\ (\underset{\sim}{n})\ \Omega_{\ell j}\ (\underset{\sim}{n}) = \delta_{ij} \qquad \text{(II-A-25)}$$

results in the equation,

$$\begin{aligned} B(\underset{\sim}{n}_o) &= 1/2\ [\Omega^{-1}_{ik}\ (\underset{\sim}{n}_o)\ \ell_i \ell_k\ - \ell_k\ (\Omega^{-1}_{kj}\ (\underset{\sim}{n}_o)\ \Omega_{js}\ (\underset{\sim}{n}_o))\ \Omega^{-1}_{sq}(\underset{\sim}{n}_o)\ \ell_q] \\ &= 1/2\ [\Omega^{-1}_{ik}\ (\underset{\sim}{n}_o)\ell_i \ell_k\ - \ell_k\ \Omega^{-1}_{kq}\ (\underset{\sim}{n}_o)\ \ell_q] \\ &= 0 \end{aligned} \qquad \text{(II-A-26)}$$

Since $B(\underset{\sim}{e}) \geq 0$, the value $B(\underset{\sim}{n}_o) = 0$ provides the absolute minimum of $B(\underset{\sim}{e})$ and therefore

$$B(\underset{\sim}{n}_o) = \min B(\underset{\sim}{e}) = 0 \text{ and} \qquad \text{(II-A-27)}$$

$$E_e = 1/2 \min B(\underset{\sim}{e})\ V = 0. \qquad \text{(II-A-28)}$$

Hence an infinite thin plate lying in a plane of invariant strain has zero elastic energy.

The result (II-A-28) provides the connection between the elastic and crystallographic theories of the habit plane of martensite plates[15]. The crystallographic theories[10,11,12] are based on the assumption that the habit of martensite will be an invariant plane of the transformation. The elastic theory confirms the assumption that the invariant plane provides a minimum of the elastic energy.

It will also be noted from equation (II-A-18) or (II-A-20) that where an inclusion has a plate morphology with an invariant habit plane, the bulk elastic energy is equal to zero and the total energy is equal to the peripheral energy of the plate, which may be represented as the linear tension of a pseudo dislocation loop encircling it.

(5) When the matrix is cubic and contains a distribution of tetragonal inclusions, the elastic energy is minimized when the inclusions aggregate to form martensite-like crystals whose habits are invariant planes.

This result, established by Khachaturyan and Shatalov[15] from equation (II-A-7), completes the contact between the elastic and crystallographic theories of the martensite habits and may also explain the "tweed" microstructures observed in the early stages of the phase decomposition in several systems[39].

The Khachaturyan development of the macroscopic elastic theory

used above involves the solution of the elastic equilibrium equations in reciprocal space. The same results are, of course, determinable from real space formulations of the problem along the lines proposed by Eshelby[17]. While the mathematics are more formidable in the real space formulation and the physical content of the equations is less transparent, significant recent results have been obtained. Shibata and Ono[16] used the Eshelby formulation to compute the preferred habit plane of martensitic inclusions by varying the shape and orientation of ellipsoidal inclusions to identify minimum energy configurations. Lee, Aaronson, and Barnett[40] generalized the Eshelby analysis to treat ellipsoidal inclusion in anisotropic media. Lee[41] has recently shown how differences between the elastic constants of the matrix and the inclusion may be incorporated into the treatment of ellipsoidal inclusions.

B. The Microscopic Elastic Theory

The macroscopic elastic theories described in the previous section have the common assumption that the coherent inclusions are large compared to the lattice parameter. If the particle size is more nearly equal to the lattice parameter an alternate microscopic formulation may be used.

The microscopic or "crystal lattice statics" model is also well developed. Its history apparently begins with the work of Matsubara[42] who modified the lattice dynamics of Born and Huang[43] to describe the static equilibrium displacements around a point defect (hence the term "lattice statics"). Matsubara's work initiated a series of theoretical investigations into strains associated with isolated point defects. The theory was developed (in several cases independently) and extended by Kanzaki[44], Hardy[45,46], Tewordt[47], Khachaturyan[34-38], Ho and Benedek[48,49], Siems[50], and others.

A second class of problems for which the lattice statics model has often been used concerns the equilibrium lattice distortion caused by crystal dislocations. Relevant work includes that of Maradudin[51], Celli[52], Gallotto and Omini[53], Brailsford[54,55], Boyer and Hardy[56] and Easterling[57]. Hsei and Thomson[58] have used similar models in the analysis of creep and crack growth problems.

The extension of point defect theories to treat crystals containing distributions of defects, for example, metallic solid solutions, is an obvious direction for theoretical research. The associated elastic problem is, however, difficult. Initial progress was made by Friedel[59] and by Eshelby[60] who used a semi-continuum treatment to compute the

elastic energy of an isotropic solid solution in which the solute atoms are modeled as misfitting spheres (center of dilatation) with a random distribution. A similar model was later used by Cahn[61] to assess the influence of the elastic interaction on spinodal decomposition in metals.

The assumption of quasi-continuum particles in an isotropic medium greatly simplifies the mathematical complexity of the solid solution model, but at some cost to the physics. The principal physical shortcomings are two. First, the elastic interaction between centers of dilatation in an infinite, isotropic medium is identically zero. In the Friedel-Eshelby model, solute atoms interact only through an image-force effect due to the finite dimensions of the crystal. Even when the solute atoms are allowed to have elastic moduli different from those of the matrix, the direct interaction is weak (of order r^{-6}). It is known, however, that elastic anisotropy, as found in all real metals, will lead to a direct interaction between particles of order r^{-3} which is, moreover, strongly direction-dependent. Second, the derivation of the Friedel-Eshelby model, which proceeds directly from the macroscopic limit, leaves the correspondence between the model and the microscopic physics of the crystal lattice somewhat unclear.

Apprarently the first truly microscopic elastic treatment of a solid solution was constructed by Khachaturyan[34] who formulated a model for the energy of an interstitial solid solution. The result was used by Khachaturyan and Shatalov[35] to predict the crystal structure of ordered interstitial superlattices in tantalum, and has since been widely applied in the theoretical analysis of ordering in solid solutions[38]. These derivations were subsequently repeated by Cook

and Fontaine[62].

In the present work we shall employ a model of the martensite transformation which is essentially a quasi-continuum model in the tradition of Friedel and Eshelby (but without the strong assumptions of elastic isotropy). It is, however, possible to obtain this model from a fundamental starting point in the lattice statics model. The formulation and derivation of the model is presented in the balance of this section. The derivation is given in some detail for three reasons: to demonstrate the contact between the lattice static and quasi-continuum treatments, to clarify the nature of the assumptions involved, and to provide a self-contained derivation which is free of the (sometimes real, sometimes apparent) inconsistencies between the earlier treatments.

The formulation used here is based on the Khachaturyan model of the interstitial solid solution[34].

(1) Model of a Multi-component Substitutional Solid Solution.

Let a multi-component solution be created by introducing elastic defects, which may be either solute atoms or inclusions of a more general type, onto the sites of a solvent host lattice. We shall make three general assumptions:

(a) An elastic defect of type p may be characterized by the linear elastic strain $\varepsilon^{o}_{ij}(p)$, whose negative is the strain required to deform it from a fully relaxed state until it fits precisely into the host lattice. The strain $\varepsilon^{o}_{ij}(p)$ is a measure of the "lattice mismatch" between the solute and solvent species.

The definition of $\varepsilon^{o}_{ij}(p)$ of course requires a clear specification of the structure of the relaxed reference state to which the solute is

referred. When the solute preferentially forms a crystal having the same crystal structure as the solvent, or when the solute is an element of new phase whose crystal structure is specified, then the appropriate reference structure is clear. On the other hand, when the solute preferentially forms a crystal having an equilibrium structure different from that of the solvent the appropriate reference structure is not obvious and should be chosen so as to minimize the free energy of solution. Since the elastic energy associated with deformation is large and increases monotonically with the magnitude of the deformation, the free energy of solution will usually be minimized if the reference structure used in the definition of $\varepsilon^{o}_{ij}(p)$ is that stable or metastable structure of the pth solute which is geometrically closest to the structure of the solvent. The solution may then be made through a quasi-chemical cycle involving a structural transformation (if necessary) which brings the solute from the equilibrium state to its metastable structure closest to that of the solvent followed by a small elastic distortion to establish a coincident lattice. The second step defines the elastic strain $\varepsilon^{o}_{ij}(p)$.

If the reference structure for the pth elastic defect is identical to that of the host crystal, then the reference strain $\varepsilon^{o}_{ij}(p)$ is a simple dilatation (homogeneous expansion or contraction). In this case each solute species is represented by only one elastic defect. However, if the reference structure of the defect differs from that of the host lattice, then the reference strain contains shear as well as dilatational components and a single solute species may give rise to several distinct elastic defects, which differ in the orientation of the principal axes of the reference strain with respect to the axes of the host

crystal. For example, the simplest tetragonal defect in a cubic crystal may be present in any of three distinct variants, which differ in the orientation of the tetragonal axis.

(b) We shall assume that the difference in the Born-von Karman constants, and hence the elastic constants, between the solute and the solvent is sufficiently small that it may be ignored.

The assumption of equal elastic constants is a strong one, but provides a major formal simplification of the model and insures its mathematical tractability. The study of the consequences of differences in the elastic constants has not progressed to the point where the reasonableness of this assumption can be quantitatively assessed, but available prior work[16,17] based on continuum calculations does suggest that the "modulus defect" may often be safely ignored.

(c) We shall assume that the free energy of the solution is well represented by an expansion to terms in the second order in the composition, elastic displacement, and their cross products (the harmonic approximation). Higher order terms will be neglected.

The harmonic approximation not only simplifies the computation but also has the advantage of preserving a simple superposition principle within the model in which, for example, the elastic strain at a point in the solution may be written as a simple sum of strains associated with each of the elementary defects. It is this superposition which permits us to extract a treatment of elastic inclusions of finite size by simply modeling these as agglomerations of elementary defects.

The distribution of defects of type p over the lattice may be described by the function

$$C_p(\underset{\sim}{r}) = \begin{cases} 1 \text{ for atom of type p at } \underset{\sim}{r} \\ 0 \text{ otherwise} \end{cases} \qquad \text{(II-B-1)}$$

The atomic fraction of p is

$$\overline{C}_p = \frac{1}{N}\sum_{\underset{\sim}{r}} C_p(\underset{\sim}{r}) = \frac{N_p}{N} \qquad \text{(II-B-2)}$$

where N_p is the number of atoms of type p, N is the total number of lattice sites, and the summation is over the lattice. If more than one type of solute is present then clearly

$$C_p(\underset{\sim}{r})\ C_q(\underset{\sim}{r}) = \delta_{pq} C_p(\underset{\sim}{r}) \qquad \text{(II-B-3)}$$

where δ_{pq} is the Kronecker symbol.

The introduction of solute atoms into the host matrix will cause some distortion of the matrix if any of the $\varepsilon^o_{ij}(p)$ are non-zero. Distrotions of the lattice, due either to solute atoms or to external loading, will be described by the vector displacement function

$$\underset{\sim}{u}(\underset{\sim}{r}) = \underset{\sim}{r}' - \underset{\sim}{r} \qquad \text{(II-B-4)}$$

where $\underset{\sim}{r}'$ is the position of the lattice point in the distorted state and $\underset{\sim}{r}$ is its poition in the pure, stress-free solvent matrix.

(2) The Elastic Hamiltonian

Let a distribution $C_p(\underset{\sim}{r})$ of defects of type p ($p = 1, \ldots.\nu$) be introduced into the host lattice. Let the lattice be spatially homo-

geneous and elastic and let its states of strain be described by the displacement field $u_i(\underset{\sim}{r})$ defined in eq. II-B-4. Treating the energy, E, as a continuous functional of the displacement field, $u_i(\underset{\sim}{r})$ and of the concentration fields, $C_p(\underset{\sim}{r})$, then the energy is, to second order,

$$E\left\{c(\underset{\sim}{r}),\ u_i(\underset{\sim}{r})\right\} = E_o + \sum_p \sum_{\underset{\sim}{r}} E_c^p\, C_p(\underset{\sim}{r}) - \sum_{\underset{\sim}{r}} (E_{u_i})\, u_i(\underset{\sim}{r})$$

$$+ \frac{1}{2} \sum_p \sum_{\underset{\sim}{r}\underset{\sim}{r}'} E_{cc}^{pq}(\underset{\sim}{r} - \underset{\sim}{r}')\, C_p(\underset{\sim}{r})\, C_q(\underset{\sim}{r}') \qquad \text{(II-B-5)}$$

$$+ \frac{1}{2} \sum_p \sum_{\underset{\sim}{r}\underset{\sim}{r}'} f_i^p(\underset{\sim}{r} - \underset{\sim}{r}')\, C_p(\underset{\sim}{r})\, u_i(\underset{\sim}{r}')$$

$$+ \frac{1}{2} \sum_{\underset{\sim}{r}\underset{\sim}{r}'} A_{ij}(\underset{\sim}{r} - \underset{\sim}{r}')\, u_i(\underset{\sim}{r})\, u_j(\underset{\sim}{r}')$$

the symbol

$$E_\phi = [\delta E/\delta\phi(\underset{\sim}{r})]_o \qquad \text{(II-B-6)}$$

and

$$E_{\phi\psi}(\underset{\sim}{r} - \underset{\sim}{r}') = [\delta^2 E/\delta\phi(\underset{\sim}{r})\delta\phi(\underset{\sim}{r}')]_o \qquad \text{(II-B-7)}$$

where the variational derivatives are taken in the reference state $C_p(\underset{\sim}{r}) = 0$ $(p = 1, \ldots \nu)$ and $u_i(\underset{\sim}{r}) = 0$.
Mechanical equilibrium in the reference state requires that the vector

$$E_{\underset{\sim}{u}} = 0, \qquad \text{(II-B-8)}$$

since $\underset{\sim}{u}$ may have either sign. The remaining coefficients may be evaluated by using an equivalent cycle to create the final state, roughly

along the lines suggested by Eshelby[18].

Let the solid solution be created from the pure one-component solvent in a cycle of six operations, as diagrammed in Figure 1:

Step (1): Taking the pure solvent crystal, isolate clusters of which the pth contains N_p solvent atoms, and cut each cluster out of the solvent lattice. If the solvent and each of the clusters is large enough for surface effects to be ignored, the energy of the assembly is not changed in the process.

Step (2): For each atom of the pth cluster substitute an atom of the pth solute, and let the transformed lattice relax to its stress-free shape. This transmutation will involve the energy change

$$\Delta\phi_2 = \sum_{p=1}^{\nu} F_{ch}(p) = N \sum_{p=1}^{\nu} \overline{C}_p \; \Delta\mu_p^b \qquad \text{(II-B-9)}$$

where $\Delta\mu_p^b$ is the chemical energy difference per atom between the solvent and the pth solute in its reference crystal structure. The associated free expansion of the pth cluster involves no energy change since the cluster is stress-free. It is described by the strain tensor $\varepsilon_{ij}^o(p)$, whose definition is discussed in the previous subsection.

Step (3): Let surface tractions be applied to each cluster to restore it to the shape it had before the transmutation occurred. The restoration of shape requires the strain $\varepsilon_{ij} = -\varepsilon_{ij}^o(p)$. Since each cluster is macroscopic, the deformation may be described by continuum elasticity. The internal stress induced by the surface traction is

$$\sigma_{ij} = \lambda_{ijk\ell}(-\varepsilon_{k\ell}^o(p)). \qquad \text{(II-B-10)}$$

Since the final homogeneous strain within the pth particle is

$$\varepsilon_{ij} = -\varepsilon_{ij}^o(p), \qquad \text{(II-B-11)}$$

the change in mechanical energy is

$$\phi_{el}^{self} = \frac{1}{2} V_p \lambda_{ijk\ell} \varepsilon_{ij}^{o}(p) \varepsilon_{k\ell}^{o}(p)$$

$$= \frac{1}{2} N\overline{C}_p v \lambda_{ijk\ell} \varepsilon_{ij}^{o}(p) \varepsilon_{k\ell}^{o}(p) \qquad \text{(II-B-12)}$$

where v is the atomic volume. The total energy change for the assembly is

$$\Delta\phi_3 = \sum_p \phi_{el}^{self} = \frac{N}{2} \sum_{p=1}^{\nu} v\overline{C}_p \lambda_{ijk\ell} \varepsilon_{ij}^{o}(p) \varepsilon_{k\ell}^{o}(p) \qquad \text{(II-B-13)}$$

<u>Step (4):</u> Let the clusters (p=1, ...ν) be reintroduced into the solvent crystal. Since each cluster just fits into the space from which it was removed, there is no free energy change in this process.

<u>Step (5):</u> Now, let the solute be dispersed through the host lattice at constant shape to create the solute distribution appropriate to the solid solution. Since each atomic defect is undistorted $\underset{\sim}{u}(\underset{\sim}{r})$ remains equal to zero during this step and no strain energy is developed. The energy change is chemical, and is the chemical free energy of mixing. It has two contributions: (1) a free energy change ($\Delta\mu_p^s$) per atomic defect on dissolution, which is associated with the replacement of the homogeneous environment of the defect by an environment of host atoms (if the defect were an element of new phase with bulk properties this free energy would be simply the chemical contribution to the surface free energy of the defect particle, a point of view we shall return to in the next section); (2) a configurational free energy change due to the mutual chemical interaction of solute defects. To second order in the solute interaction the resulting free energy change is

$$\Delta\phi_5 = G_{mix}^{ch} = N \sum_p \Delta\mu_p^s \overline{C}_p + \frac{1}{2} \sum_{pq} \sum_{\underset{\sim}{r}\underset{\sim}{r}'} V_{pq}^{ch}(\underset{\sim}{r} - \underset{\sim}{r}')\, C_p(\underset{\sim}{r}) C_q(\underset{\sim}{r}') \qquad \text{(II-B-14)}$$

Since the final state is taken to be a specific distribution of defects

there is no change in the configurational entropy; both the initial and final configurations are fixed to within an interchange of like particles.

Step (6): Finally, let the distributed atoms relax, introducing an equilibrium elastic strain into the lattice. In this relaxation, each solute atom will function as a center of force which acts to displace the lattice about it. The lattice displacement is opposed by the elastic resistance of the lattice. The associated energy may therefore be written

$$\Delta\Phi_6 = \Phi^{relax} = -\sum_{p=1}^{\nu} \sum_{\underset{\sim}{r}\underset{\sim}{r}'} \underset{\sim}{f}^p(\underset{\sim}{r} - \underset{\sim}{r}')\, u(\underset{\sim}{r}')\, C_p(\underset{\sim}{r})$$

$$+ 1/2 \sum_{\underset{\sim}{r}\underset{\sim}{r}'} A_{ij}(\underset{\sim}{r} - \underset{\sim}{r}')\, u_i(\underset{\sim}{r}')\, u_j(\underset{\sim}{r}) \qquad \text{(II-B-15)}$$

which corresponds in form to the last two terms of eq. II-B-6 if $A_{ij}(\underset{\sim}{r} - \underset{\sim}{r}')$ is the Born-von Karman tensor (dynamical matrix) of the host lattice[43]. The $\underset{\sim}{f}^p(\underset{\sim}{r} - \underset{\sim}{r}')$ are "Kanzaki forces"[44] which act from a solute atom of type p at location $\underset{\sim}{r}$ on an atom at site $\underset{\sim}{r}'$. Since the elastic relaxation is spontaneous, it follows that

$$\Phi^{relax} \leq 0 \qquad \text{(II-B-16)}$$

The physical effect of the elastic relaxation is to remove part of the energy of elastic distortion introduced when the solute species were deformed to fit properly into the host lattice.

Summing the free energy contributions $\Delta\Phi_1$ to $\Delta\Phi_6$ gives the total energy in an equation formally identical to equation (II-B-5)

$$\Delta E = E(\{C_p(\underset{\sim}{r}),\ u_i(\underset{\sim}{r})\}) - E_0$$

$$= \Delta\phi_2 + \Delta\phi_3 + \Delta\phi_5 + \Delta\phi_6$$

$$= N \sum_p \overline{C}_p \left[\Delta\mu_p^b + \Delta\mu_p^s + \frac{v}{2}\lambda_{ijk\ell}\varepsilon_{ij}^o(p)\varepsilon_{k\ell}^o(p)\right]$$

$$+ \frac{1}{2}\sum_{pq}\sum_{\underset{\sim}{r}\underset{\sim}{r}'} V_{ch}^{pq}(\underset{\sim}{r} - \underset{\sim}{r}')\ C_p(\underset{\sim}{r})\ C_q(\underset{\sim}{r}')$$

$$- \sum_p \sum_{\underset{\sim}{r}\underset{\sim}{r}'} \underset{\sim}{f}^p(\underset{\sim}{r} - \underset{\sim}{r}')\ \underset{\sim}{u}(\underset{\sim}{r}')\ C_p(\underset{\sim}{r}) \qquad \text{(II-B-17)}$$

$$+ \frac{1}{2}\sum_{\underset{\sim}{r}\underset{\sim}{r}'} A_{ij}(\underset{\sim}{r} - \underset{\sim}{r}')\ u_i(\underset{\sim}{r})\ u_j(\underset{\sim}{r}')$$

The term linear in $\overline{C}_p$ represents the self-energy (chemical plus elastic) of the solute atoms, the term quadratic in $C_p(\underset{\sim}{r})$ contains the chemical energy of mixing, and the last two terms contain the elastic relaxation energy and also govern the response of the solution to elastic displacement due to external fields or to lattice vibration (in the harmonic) approximation). In a simpler notation:

$$\Delta E = \Delta\phi_{chem} + \Delta\phi_{el} \qquad \text{(II-B-18)}$$

where

$$\Delta\phi_{chem} = N \sum_p \overline{C}_p \Delta\mu_p + \frac{1}{2}\sum_{pq}\sum_{\underset{\sim}{r}\underset{\sim}{r}'} V_{ch}^{pq}(\underset{\sim}{r} - \underset{\sim}{r}')\ C_p(\underset{\sim}{r})\ C_q(\underset{\sim}{r}') \qquad \text{(II-B-19)}$$

is the change of chemical free energy, where $\Delta\mu_p$ is the sum of $\Delta\mu_p^b$ and $\Delta\mu_p^s$ and

$$\Delta\phi_{el} = N \sum_p \overline{C}_p \frac{v}{2}\lambda_{ijk\ell}\varepsilon_{ij}^o(p)\ \varepsilon_{k\ell}^o(p) - \sum_p \sum_{\underset{\sim}{r}\underset{\sim}{r}'} f^p(\underset{\sim}{r} - \underset{\sim}{r}')\ u(\underset{\sim}{r})\ C_p(\underset{\sim}{r})$$

$$+ \frac{1}{2}\sum_{\underset{\sim}{r}\underset{\sim}{r}'} A_{ij}(\underset{\sim}{r} - \underset{\sim}{r}')\ u_i(\underset{\sim}{r})\ u_j(\underset{\sim}{r}') \qquad \text{(II-B-20)}$$

is the elastic energy change.

The coefficients appearing in equation II-B-17 are, of course,

restricted by the symmetry of the crystal in its solute and deformation-free state, and are further restricted by the requirement that ΔE be invariant to rigid body displacements. Invariance to a rigid body translation specified by

$$\underset{\sim}{u}(\underset{\sim}{r}) = \underset{\sim}{a} \tag{II-B-21}$$

where $\underset{\sim}{a}$ is a constant vector, gives the constraints:

$$\sum_{\underset{\sim}{r}'} \underset{\sim}{f}^{p}(\underset{\sim}{r} - \underset{\sim}{r}') = 0 \tag{II-B-22}$$

and

$$\sum_{\underset{\sim}{r}\underset{\sim}{r}'} A_{ij}(\underset{\sim}{r} - \underset{\sim}{r}') = 0 \tag{II-B-23}$$

Invariance to a rigid body rotation, specified by the displacement

$$u_i(\underset{\sim}{r}) = \omega_{ij} r_j \tag{II-B-24}$$

where ω_{ij} are constants, gives the additional constraints:

$$\sum_{\underset{\sim}{r}'} r'_j \, f_i(\underset{\sim}{r} - \underset{\sim}{r}') = 0 \tag{II-B-25}$$

and

$$\sum_{\underset{\sim}{r}\underset{\sim}{r}'} A_{ij}(\underset{\sim}{r} - \underset{\sim}{r}') \, r_\ell \, r'_m = 0 \tag{II-B-26}$$

If the host crystal is symmetric to inversion, as it is in virtually all cases of current interest to us, then

$$\underset{\sim}{f}^{p}(\underset{\sim}{r} - \underset{\sim}{r}') = -\underset{\sim}{f}^{p}(\underset{\sim}{r} - \underset{\sim}{r}') \tag{II-B-27}$$

and

$$A_{ij}(\underset{\sim}{r} - \underset{\sim}{r}') = A_{ij}(\underset{\sim}{r}' - \underset{\sim}{r}) \tag{II-B-28}$$

In much of the following we shall ignore the chemical contribution to the energy and be concerned with the evaluation of the elastic contribution to eq. (II-B-17), which is

$$\Delta\Phi_{el} = N \sum_p \overline{C}_p \frac{1}{2} v\lambda_{ijk\ell} \varepsilon^o_{ij}(p) \varepsilon^o_{k\ell}(p) \qquad \text{(II-B-29)}$$

$$- \sum_p \sum_{\underset{\sim}{r}\underset{\sim}{r}'} f^p(\underset{\sim}{r} - \underset{\sim}{r}') \; \mu(\underset{\sim}{r}') C_p(\underset{\sim}{r})$$

$$+ \frac{1}{2} \sum_{\underset{\sim}{r}\underset{\sim}{r}'} A_{ij}(\underset{\sim}{r} - \underset{\sim}{r}') \; u_i(\underset{\sim}{r}) u_j(\underset{\sim}{r}')$$

(3) The Static Equilibrium Displacement:

The computation of the equilibrium lattice displacement field within the solid solution is not only important in its own right but, as we shall see, also permits a substantial simplification of the expression for the elastic energy.

We begin by writing the static displacement field $u_i(\underset{\sim}{r})$ as a sum of two terms:

$$u_i(\underset{\sim}{r}) = \varepsilon_{ij} r_j + v_i(\underset{\sim}{r}) \qquad \text{(II-B-30)}$$

In this decomposition ε_{ij} is a uniform, macroscopic strain that has, in general, two sources: the net deformation of the crystal due to the solute lattice strain and the elastic deformation due to external forces. The field $v_i(r)$ is the internal displacement, which, if it is to have no macroscopic consequence, must be chosen so that it vanishes over the surface of the body. The concentration field may also be decomposed into its mean and variation:

$$C_p(\underset{\sim}{r}) = \overline{C}_p + \Delta C_p(\underset{\sim}{r}) \qquad \text{(II-B-31)}$$

With these definitions, the elastic energy (eq. II-B-29) may be rewritten:

$$\Delta\Phi_{el} = \Phi^o_{el} - N \, \varepsilon_{ij} \sum_p \Lambda_{ij}(p) \overline{C}_p + \frac{N}{2} \Lambda_{ijk\ell} \varepsilon_{ij} \varepsilon_{k\ell}$$

$$- \sum_p \sum_{\underset{\sim}{r}\underset{\sim}{r}'} f^p_i(\underset{\sim}{r} - \underset{\sim}{r}') \; v_i(\underset{\sim}{r}') \; \Delta C_p(\underset{\sim}{r}) \qquad \text{(II-B-32)}$$

$$+ \frac{1}{2} \sum_{\underset{\sim}{r}\underset{\sim}{r}'} A_{ij}(\underset{\sim}{r} - \underset{\sim}{r}') \, v_i(\underset{\sim}{r}) v_j(\underset{\sim}{r}')$$

Where Φ^{o}_{el} is the elastic self energy defined in equation (II-B-13), and is independent of the elastic displacement. The tensors $\Lambda_{ij}(p)$ and $\Lambda_{ij\ell m}$ are given by the summations:

$$\Lambda_{ij}(p) = 1/2 \sum_{\underset{\sim}{r}} [f^{p}_{i}(\underset{\sim}{r})\ r_j + f^{p}_{j}(\underset{\sim}{r})\ r_i] \qquad \text{(II-B-33)}$$

$$\Lambda_{ij\ell m} = 1/4 \sum_{\underset{\sim}{r}} [A_{ij}(\underset{\sim}{r})\ r_\ell r_m + A_{\ell m}(\underset{\sim}{r})\ r_i r_j + A_{i\ell}(\underset{\sim}{r}) r_j r_m + A_{jm}(\underset{\sim}{r})\ r_i r_\ell] \qquad \text{(II-B-34)}$$

(a) The Uniform Relaxation Strain

The change in the internal energy due to imposition of an external stress is due to those terms in equation (II-B-32) which depend on the homogeneous strain ε_{ij} since the internal displacement $v_i(r)$ vanishes on the boundary. By the usual relations of elasticity, the macroscopic elastic stress is related to the homogeneous strain by

$$\sigma_{ij} = \frac{\partial}{\partial \varepsilon_{ij}} (\Delta\Phi_{el}/V) \qquad \text{(II-B-35)}$$

from which it follows that

$$\sigma_{ij} = - \sum_{p} \frac{\Lambda_{ij}(p)}{v} \bar{C}_p + \frac{1}{v} \Lambda_{ijk\ell}\varepsilon_{k\ell} \qquad \text{(II-B-36)}$$

where v is the atomic volume (V/N). Defining the tensor $\bar{\varepsilon}_{ij}$ by the relation

$$\Lambda_{ijk\ell}\bar{\varepsilon}_{k\ell} = \sum_{p} \Lambda_{ij}(p)\ \bar{C}_p \qquad \text{(II-B-37)}$$

we have

$$\sigma_{ij} = \frac{1}{v} \Lambda_{ijk\ell}(\varepsilon_{k\ell} - \bar{\varepsilon}_{k\ell}) \qquad \text{(II-B-38)}$$

Comparison with Hook's Law

$$\sigma_{ij} = \lambda_{ijk\ell}\varepsilon^{el}_{k\ell} \qquad \text{(II-B-39)}$$

gives the identities

$$\lambda_{ijk\ell} = \frac{1}{v} \Lambda_{ijk\ell} \qquad \text{(II-B-40)}$$

and

$$\varepsilon^{el}_{k\ell} = (\varepsilon_{k\ell} - \bar{\varepsilon}_{k\ell}) \qquad \text{(II-B-41)}$$

where $\varepsilon^{el}_{k\ell}$ is that part of the elastic strain due to the externally imposed stress σ_{ij}. In the stress-free state $\sigma_{ij} = 0$ and $\varepsilon^{el}_{k\ell} = 0$; hence

$$\varepsilon_{k\ell} = \bar{\varepsilon}_{k\ell} \quad (\sigma_{ij} = 0) \qquad \text{(II-B-42)}$$

is the uniform relaxation strain introduced by alloying the crystal.

The crystal deformation on alloying may be expressed in terms of the solute content. Setting $\sigma_{ij} = 0$ and $\varepsilon_{ij} = \bar{\varepsilon}_{ij}$ in equation (II-B-36) gives

$$\lambda_{ijk\ell}\bar{\varepsilon}_{k\ell} = \sum_p \frac{\Lambda_{ij}(p)}{v} \bar{C}_p \qquad \text{(II-B-43)}$$

which may be solved for the $\bar{\varepsilon}_{ij}$:

$$\bar{\varepsilon}_{ij} = \sum_p \left(\frac{1}{v}\right) S_{ijk\ell}\Lambda_{k\ell}(p)\, \bar{C}_p \qquad \text{(II-B-44)}$$

where $S_{ijk\ell}$ is the elastic compliance tensor, the tensor inverse to $\lambda_{ijk\ell}$.

Equation (II-B-44) shows that Vegard's Law is obeyed with respect to each of the solute species, as is epxected since the model is second-order. The Vegard's Law coefficient may be estimated by making an extrapolation to the limit $\bar{C}_p = 1$. In this case

$$\bar{\varepsilon}_{ij} = \varepsilon^{o}_{ij}(p) \qquad (\bar{C}_p = 1) \qquad \text{(II-B-45)}$$

and we are led to the simple result

$$\bar{\varepsilon}_{ij} = \sum_p \varepsilon^{o}_{ij}(p)\, \bar{C}_p. \qquad \text{(II-B-46)}$$

The value of $\Lambda_{ij}(p)$ which is consistent with equation (II-B-45) is, from equation (II-B-43),

$$\Lambda_{ij}(p)/v = \sigma^{o}_{ij}(p) = \lambda_{ijk\ell}\varepsilon^{o}_{ij}(p) \qquad \text{(II-B-47)}$$

The stress $\sigma^{o}_{ij}(p)$ is a material constant, the "transformation stress" and is simply the negative of the elastic stress required to reverse the strain caused by the replacement of the solvent by the solute species p.

With the substitution of the uniform relaxation strain, $\bar{\varepsilon}_{ij}$, the elastic energy of the crystal in the absence of external stress may be written in the simpler form:

$$\Delta\Phi_{el} = \Phi^{o}_{el} - \frac{Nv}{2}\sum_{pq}\lambda_{ijk\ell}\varepsilon^{o}_{ij}(p)\ \varepsilon^{o}_{k\ell}(q)\ \bar{C}_p\ \bar{C}_q$$

$$- \sum_{p}\sum_{\underset{\sim}{r}\underset{\sim}{r}'} f^{p}_{i}(\underset{\sim}{r} - \underset{\sim}{r}')\ v_i(\underset{\sim}{r}')\ \Delta C_p(\underset{\sim}{r})$$

$$+ 1/2 \sum_{\underset{\sim}{r}\underset{\sim}{r}'} A_{ij}(\underset{\sim}{r} - \underset{\sim}{r}')\ v_i(\underset{\sim}{r})\ v_j(\underset{\sim}{r}') \qquad \text{(II-B-48)}$$

The presence of an external stress, σ_{ij}, may be simply accounted for by adding the term

$$\Delta E_{el} = V\ \sigma_{ij}\ \Delta\varepsilon_{ij} \qquad \text{(II-B-49)}$$

where

$$\Delta\varepsilon_{ij} = \varepsilon_{ij} - \bar{\varepsilon}_{ij} \qquad \text{(II-B-50)}$$

is the elastic strain measured with respect to the relaxed state.

(b) The Internal Strain.

The equilibrium local displacement field $\underset{\sim}{v}(\underset{\sim}{r})$ is found by requiring that the elastic energy (ΔE_{el} in Equation (II-B-58) be stable with respect to variations of the local displacement:

$$\delta\Delta E_{el}/\delta\underset{\sim}{v}(\underset{\sim}{r}) = 0 \qquad \text{(II-B-51)}$$

The necessary condition is

$$\sum_{\underset{\sim}{r}'} A_{ij}(\underset{\sim}{r} - \underset{\sim}{r}')\ v_j(\underset{\sim}{r}') = \sum_{p\ \underset{\sim}{r}'} f_i^p\ (\underset{\sim}{r}' - \underset{\sim}{r})\ \Delta C_p(\underset{\sim}{r}') \qquad \text{(II-B-52)}$$

Since the local displacement $\underset{\sim}{v}(\underset{\sim}{r})$ vanishes on the boundary of the body (by its definition), we may employ cyclic boundary conditions for the crystal in its homogeneously strained state. Taking the Fourier transform of both sides of equation (II-B-52) then gives

$$\tilde{A}_{ij}(\underset{\sim}{k})\ \tilde{v}_j(\underset{\sim}{k}) = \sum_{p=1}^{\nu} \tilde{F}_i^p\ (\underset{\sim}{k})\ \Delta\tilde{C}_p(\underset{\sim}{k}) \qquad \text{(II-B-53)}$$

where

$$\tilde{A}_{ij}(\underset{\sim}{k}) = \sum_{\underset{\sim}{r}} A_{ij}(\underset{\sim}{r})\ e^{-i\underset{\sim}{k}\cdot\underset{\sim}{r}} \qquad \text{(II-B-54)}$$

is the dynamical matrix,

$$\tilde{\underset{\sim}{F}}^p(\underset{\sim}{k}) = \sum_{\underset{\sim}{r}} \underset{\sim}{f}^p(\underset{\sim}{r})\ e^{-i\underset{\sim}{k}\cdot\underset{\sim}{r}} \qquad \text{(II-B-55)}$$

and

$$\Delta\tilde{C}_p(\underset{\sim}{k}) = \sum_{\underset{\sim}{r}} \Delta\tilde{C}_p(\underset{\sim}{r})\ e^{-i\underset{\sim}{k}\cdot\underset{\sim}{r}} \qquad \text{(II-B-56)}$$

The solution of II-B-53 for the Fourier component $v_i(\underset{\sim}{k})$ is

$$\tilde{v}_i(\underset{\sim}{k}) = G_{ij}(\underset{\sim}{k}) \sum_{p=1}^{\nu} F_j^p(\underset{\sim}{k})\ \Delta\tilde{C}_p(\underset{\sim}{k}) \qquad \text{(II-B-57)}$$

where G_{ij} is the Green's tensor which is the inverse of the dynamical matrix $\tilde{A}$:

$$G_{ij}(\underset{\sim}{k})\ \tilde{A}_{j\ell}(\underset{\sim}{k}) = \delta_{i\ell}.$$

The Hermitian tensor $G_{ij}(k)$ can be written in terms of eigentensors, $\underset{\sim}{\varepsilon}_s(\underset{\sim}{k})$, and eigenvalues, $m\omega_s^2(\underset{\sim}{k})$ of the dynamical matrix $A_{ij}(k)$. These are the solutions to the equation

$$\tilde{A}_{ij}(\underset{\sim}{k})\ \varepsilon_s^j(\underset{\sim}{k}) = m\omega_s^2(\underset{\sim}{k})\ \varepsilon_s^i(\underset{\sim}{k}) \qquad \text{(II-B-58)}$$

where m is the mass of the host atom, ω_s is the vibration frequency of

the branch s, and $\underset{\sim}{k}$ is a wave vector. The Green's tensor $G_{ij}(k)$ may then be written

$$G_{ij}(\underset{\sim}{k}) = \sum_{s=1}^{3} \frac{\varepsilon_s^i(\underset{\sim}{k})\ \varepsilon_s^j(\underset{\sim}{k})}{m\omega_s^2(\underset{\sim}{k})} \tag{II-B-59}$$

Substituting II-B-59 into (II-B-57) then gives

$$\underset{\sim}{\tilde{\nu}}(k) = \sum_{p=1}^{\nu} \sum_{s=1}^{3} \frac{\underset{\sim}{\varepsilon}_s(\underset{\sim}{k})\ (\underset{\sim}{\varepsilon}_s(\underset{\sim}{k})\underset{\sim}{\tilde{F}}^p(\underset{\sim}{k}))}{m\omega_s^2(\underset{\sim}{k})}\ \Delta\tilde{C}_p(\underset{\sim}{k}) \tag{II-B-60}$$

Using the solutions (II-B-54) for the internal displacement field, the elastic relaxation energy becomes

$$\begin{aligned}
\Phi_{el}^{relax} &= -\frac{N}{2}\sum_{pq} v\lambda_{ijk\ell}\varepsilon_{ij}^{o}(p)\ \varepsilon_{k\ell}^{o}(q)\ \bar{C}_p\bar{C}_q \\
&\quad - \frac{1}{2N}\sum_{pq}\sum_{\underset{\sim}{k}} (F_i^p(\underset{\sim}{k})\ G_{ij}(\underset{\sim}{k})\ F_j^{q*}(\underset{\sim}{k}))\ \Delta\tilde{C}_p(\underset{\sim}{k})\ \Delta\tilde{C}_p^*(\underset{\sim}{k}) \\
&= -\frac{N}{2}\sum_{pq} v\lambda_{ijk\ell}\varepsilon_{ij}^{o}(p)\ \varepsilon_{k\ell}^{o}(q)\ \bar{C}_p\bar{C}_q \\
&\quad - \frac{1}{2N}\sum_{pq}\sum_{\underset{\sim}{k}}\sum_{s} \frac{(\underset{\sim}{\varepsilon}_s(\underset{\sim}{k})\underset{\sim}{\tilde{F}}^p(\underset{\sim}{k}))\ (\underset{\sim}{\varepsilon}_s(\underset{\sim}{k})\underset{\sim}{\tilde{F}}^q(\underset{\sim}{k}))^*}{m\omega_s^2(\underset{\sim}{k})}\ \Delta\tilde{C}_p(\underset{\sim}{k})\ \Delta\tilde{C}_p^*(\underset{\sim}{k})
\end{aligned}$$

and hence

$$\begin{aligned}
\Delta\Phi_{el} &= \frac{N}{2}\sum_{p}(v\lambda_{ijk\ell}\varepsilon_{kj}^{o}(p)\varepsilon_{k\ell}^{o}(p))\ \bar{C}_p \\
&\quad - \frac{N}{2}\sum_{pq}(v\lambda_{ijk\ell}\varepsilon_{ij}^{o}(p)\ \varepsilon_{k\ell}^{o}(q))\ \bar{C}_p\bar{C}_q \\
&\quad - \frac{1}{2N}\sum_{pq}\sum_{\underset{\sim}{k}}(\tilde{F}_i(\underset{\sim}{k})G_{ij}(\underset{\sim}{k})\ \tilde{F}_j^{q*}(\underset{\sim}{k}))\ \Delta\tilde{C}_p(\underset{\sim}{k})\ \Delta\tilde{C}_q^*(\underset{\sim}{k})
\end{aligned} \tag{II-B-62}$$

Eq. (II-B-62) is the total elastic energy due to alloying an unconstrained crystal; the relaxation of the elastic energy due to the total volume expansion during the transformation process is taken into account.

(4) Separation of Physically Distinct Contributions to the Elastic Energy.

Physically, the elastic contribution to the free energy of the crystal can be divided into three parts: (a) the elastic self energy, which is a simple sum of one-particle elastic energies and is equal to the energy which would be observed if the particles did not interact, for example, if they were present in infinite dilution; (b) a configuration - independent pairwise interaction energy whose magnitude depends only on the type and the total concentration of the solute atoms present; this interaction is indirect and has its source in the elastic image forces which arise from relaxation of the unconstrained crystal boundary; (c) a configuration - dependent pairwise interaction energy which results from the direct elastic interaction of the defects. The correct separation of these physically different contributions to the elastic energy can be important. For example, in treating the effect of elastic energy on the decomposition of a binary alloy, one needs to consider only the direct pairwise interaction since the self energy and image force contributions are unchanged by the reconfiguration of a fixed number of solute atoms. In treating the elastic energy contribution to the free energy of an elastically isotropic binary solution, it may be easily shown that the direct pairwise interaction vanishes, so that only the self-energy and image-force contributions need to be taken into account.

Equation II-B-62 does not, in fact separate the elastic energy into physically distinct terms; parts of both the self energy and the "image force" contributions are buried in the third term on the right hand side. To complete the separation we rewrite this term in the form:

$$\frac{1}{2N}\sum_{pq}\sum_{\underset{\sim}{k}}(\tilde{F}^{p}_{i}(\underset{\sim}{k})\ G_{ij}(\underset{\sim}{k})\ \tilde{F}^{q*}_{j}(\underset{\sim}{k}))\ \Delta\tilde{C}_{p}(\underset{\sim}{k})\ \Delta\tilde{C}_{q}(\underset{\sim}{k})$$

$$= \frac{1}{2N}\sum_{pq}\sum_{\underset{\sim}{k}}(\tilde{F}^{p}_{i}(\underset{\sim}{k})\ G_{ij}(\underset{\sim}{k})\ F^{q*}_{j}(\underset{\sim}{k}) - Q_{pq})\ \Delta\tilde{C}_{p}(\underset{\sim}{k})\ \Delta\tilde{C}_{q}(\underset{\sim}{k})$$

$$+ \frac{1}{2}\sum_{pq} Q_{pq}\sum_{\underset{\sim}{k}}\Delta\tilde{C}_{p}(\underset{\sim}{k})\ \Delta\tilde{C}^{*}_{q}(\underset{\sim}{k}) \qquad \text{(II-B-63)}$$

where

$$Q_{pq} = \langle\tilde{F}^{p}_{i}(\underset{\sim}{k})\ G_{ij}(\underset{\sim}{k})\ \tilde{F}^{q*}_{j}(\underset{\sim}{k})\rangle \qquad \text{(II-B-64)}$$

is an average over th first Brillouin zone. Using the identities

$$\frac{1}{N}\sum_{\underset{\sim}{k}}\Delta\tilde{C}_{p}(\underset{\sim}{k})\ \Delta\tilde{C}_{q}(\underset{\sim}{k}) = N\delta_{pq}\overline{C}_{p} - N\ \overline{C}_{p}\overline{C}_{q} \qquad \text{(II-B-65)}$$

and using (II-B-3) we have

$$\frac{1}{2}\sum_{pq}\sum_{\underset{\sim}{k}}(\tilde{F}^{p}_{i}(\underset{\sim}{k})\ G_{ij}(\underset{\sim}{k})\ \tilde{F}^{q*}_{j}(\underset{\sim}{k}))\Delta\tilde{C}_{p}(\underset{\sim}{k})\ \Delta\tilde{C}^{*}_{q}(\underset{\sim}{k})$$

$$= \frac{1}{2}N\sum_{pq}\sum_{\underset{\sim}{k}}(\tilde{F}^{p}_{i}(\underset{\sim}{k})\ G_{ij}(\underset{\sim}{k})\ \tilde{F}^{*q}_{j}(\underset{\sim}{k}) - Q_{pq})\ \Delta\tilde{C}_{p}(\underset{\sim}{k})\ \Delta\tilde{C}^{*}_{q}(\underset{\sim}{k})$$

$$+ \frac{N}{2}\sum_{p}Q_{pp}\overline{C}_{p} - \frac{N}{2}\sum_{pq}Q_{pq}\overline{C}_{p}\overline{C}_{q} \qquad \text{(II-B-66)}$$

Substituting equation II-B-66 into II-B-62 and gathering like terms yields

$$\Delta\Phi_{el} = \frac{N}{2}\sum_{p}(v\lambda_{ijk\ell}\varepsilon^{o}_{ij}(p)\ \varepsilon^{o}_{k\ell}(p) - Q_{pp})\ \overline{C}_{p}$$

$$+ \frac{N}{2}\sum_{pq}(-v\lambda_{ijk\ell}\varepsilon^{o}_{ij}(p)\ \varepsilon^{o}_{k\ell}(q) + Q_{pp})\ \overline{C}_{p}\overline{C}_{q} \qquad \text{(II-B-67)}$$

$$+ \frac{1}{2N}\sum_{pq}\sum_{\underset{\sim}{k}}(-\tilde{F}^{p}_{i}(\underset{\sim}{k})\ G_{ij}(\underset{\sim}{k})\ \tilde{F}^{q*}_{j}(\underset{\sim}{k}) + Q_{pq})\ \Delta\tilde{C}_{p}(\underset{\sim}{k})\ \Delta\tilde{C}^{*}_{q}(\underset{\sim}{k})$$

The contributions to eq. II-B-67 are separated into three terms,

The first one is a self energy, which is linear in the $\overline{C}_p$, the second is an indirect binary interaction, or image force term, which depends on the cross-products $\overline{C}_p\overline{C}_q$, and the third is a configurationally-dependent pairwise interaction which depends on the products of the Fourier components $\Delta\tilde{C}_p(\underset{\sim}{k})\ \Delta C_q^*(\underset{\sim}{k})$.

(5) Real-Space Form of the Elastic Hamiltonian.

One final modification of the elastic energy expression is useful. If the elastic energy expression is back-Fourier transformed to real space, it should yield an expression of the form

$$\Delta\Phi_{el} = \sum_{\underset{\sim}{r}} \sum_p E_p^o\ C_p(\underset{\sim}{r}) + \frac{1}{2} \sum_{\underset{\sim}{r}\underset{\sim}{r}'} \sum_{pq} \omega_{pq}(\underset{\sim}{r} - \underset{\sim}{r}')\ C_p(\underset{\sim}{r})\ C_q(\underset{\sim}{r}') \qquad \text{(II-B-68)}$$

where $\omega_{pq}(\underset{\sim}{r} - \underset{\sim}{r}')$ is the two-particle elastic interaction in real space. To rephrase eq. II-B-67 in a form in which the reverse transformation to eq. II-B-68 is obvious, we use the identity

$$\tilde{C}_p(\underset{\sim}{k}) = \sum_{\underset{\sim}{r}} C_p(\underset{\sim}{r}) e^{-i\underset{\sim}{k}\cdot\underset{\sim}{r}} \qquad \text{(II-B-69)}$$

from which it follows that

$$C_p(\underset{\sim}{k}) = \begin{cases} N\ \overline{C}_p & \text{if } \underset{\sim}{k} = 0 \\ 0 & \text{if } \underset{\sim}{k} \neq 0 \end{cases} \qquad \text{(II-B-70)}$$

and that

$$\Delta\tilde{C}_p(\underset{\sim}{k}) = \sum_{\underset{\sim}{r}} (C_p(\underset{\sim}{r}) - \overline{C}_p) e^{-i\underset{\sim}{k}\cdot\underset{\sim}{r}}$$

$$\Delta\tilde{C}_p(\underset{\sim}{k}) = \begin{cases} 0 & \text{if } \underset{\sim}{k} = 0 \\ \tilde{C}_p(\underset{\sim}{k}) & \text{if } \underset{\sim}{k} \neq 0 \end{cases} \qquad \text{(II-B-71)}$$

With these identities we have

$$\Delta\Phi_{el} = N \sum_p \Phi_{self}^{el}(p)\ \overline{C}_p + \frac{N}{2} \sum_{pq} V_{pq}^o\ \overline{C}_p\overline{C}_q$$

$$+ \frac{1}{2N} \sum_{pq} \sum_{\underset{\sim}{k}}{}' V_{pq}^{el}(\underset{\sim}{k})\ \tilde{C}_p(\underset{\sim}{k})\ \tilde{C}_q^*(\underset{\sim}{k}) \qquad \text{(II-B-72)}$$

where

$$\Phi^{el}_{self}(p) = \frac{1}{2}(v\lambda_{ijk\ell}\varepsilon^{o}_{ij}(p)\ \varepsilon^{o}_{k\ell}(p) - Q_{pp}) \tag{II-B-73}$$

$$V^{o}_{pq} = -(v\lambda_{ijk\ell}\varepsilon^{o}_{ij}(p)\ \varepsilon^{o}_{k\ell}(q) - Q_{pq}) \tag{II-B-74}$$

and

$$V^{el}_{pq}(\underset{\sim}{k}) = -\ \tilde{F}^{p}_{i}(\underset{\sim}{k})\ G_{ij}(\underset{\sim}{k})\ \tilde{F}^{q\,*}_{j}(\underset{\sim}{k}) + Q_{pq}$$

$$= -\sum_{s}{}' \frac{(\underset{\sim}{\varepsilon}_{s}(\underset{\sim}{k}) \cdot \tilde{\underset{\sim}{F}}^{p}(\underset{\sim}{k}))\ (\underset{\sim}{\varepsilon}_{s}(\underset{\sim}{k}) \cdot \tilde{\underset{\sim}{F}}^{q}(\underset{\sim}{k}))^{*}}{m\omega^{2}_{s}(\underset{\sim}{k})} + Q_{pq} \tag{II-B-75}$$

The prime on the summation in the third term on the right hand side of II-B-72 indicates that the summation is not to include the term $\underset{\sim}{k} = 0$ which is a branch point of $V^{el}_{pq}(\underset{\sim}{k})$ (eq. II-B-75). If, however, we define the potential

$$\hat{V}^{el}_{pq}(\underset{\sim}{k}) = \begin{cases} V^{o}_{pq} & \underset{\sim}{k} = 0 \\ V^{el}_{pq}(\underset{\sim}{k}) & \underset{\sim}{k} \neq 0 \end{cases} \tag{II-B-76}$$

then, using (II-B-70), $\Delta\Phi_{el}$ may be written

$$\Delta\Phi_{el} = \frac{N}{2}\sum_{p} \Phi^{el}_{self}(p)\ \overline{C}_{p}$$

$$+ \frac{1}{2N}\sum_{pq}\sum_{\underset{\sim}{k}} \hat{V}^{el}_{pq}(\underset{\sim}{k})\ \tilde{C}_{p}(\underset{\sim}{k})\ \tilde{C}_{q}(\underset{\sim}{k}). \tag{II-B-77}$$

The Fourier inverse of eq. (II-B-77) has the form of eq. II-B-68 with

$$E^{o}_{p} = N\ \Phi^{el}_{self}(p)\ \overline{C}_{p} \tag{II-B-78}$$

and

$$\omega_{pq}(r - r') = \frac{1}{N}\sum_{\underset{\sim}{k}} \hat{V}^{el}_{pq}(\underset{\sim}{k})\ e^{i\underset{\sim}{k}\cdot(\underset{\sim}{r} - \underset{\sim}{r}')} \tag{II-B-79}$$

The two-particle interaction in real space is hence just the Fourier transform of the function $\hat{V}^{el}_{pq}(\underset{\sim}{k})$, which has been so defined that its $\underset{\sim}{k} = 0$ value gives the indirect, or image force interaction between

species, and its values at $\underset{\sim}{k} \neq 0$ give the direct elastic interaction. One may easily show that the real space interaction of a particle with itself, $\omega_{pq}(0)$, vanishes (at least to within terms of order $\frac{1}{N}$) as it should.

Equation II-B-77, or its equivalent real-space form, equation II-B-68, gives the total elastic energy in the lattice statics model. The equation provides a solvable expression for the elastic energy of an arbitrary distribution of substitutional defects of arbitrary types under the dual assumptions that non-uniformity in the elastic constants and anharmonic effects may be ignored. The equation has an appealing physical form in the sense that the elastic energy is expressed as a sum of an elastic self energy and a two-particle interaction term. The latter is, in turn, easily separated into its two physical components: a configurationally-independent "image force" interaction, which is given by the value of $\hat{V}^{el}_{pq}(\underset{\sim}{k})$ at $\underset{\sim}{k} = 0$, and a direct interaction, which is sensitive to the precise configuration of defects, and which is responsible for the Fourier components of the interaction potential $\hat{V}^{el}_{pq}(\underset{\sim}{k})$ for $\underset{\sim}{k} \neq 0$.

The lattice statics model is, however, difficult to use in actual calculations since the evaluation of the interaction potentials $\hat{V}^{el}_{pq}(\underset{\sim}{k})$ or $\omega_{pq}(\underset{\sim}{r} - \underset{\sim}{r}')$ requires a knowledge of the full phonon spectrum of the matrix, which is rarely known. The evaluation of the interaction terms can be greatly simplified through the introduction of a long wavelength approximation in the spirit of the Debye model of lattice vibrations.

(6) The Total Free Energy and the Thermoelastic Potential

Returning to equation (II-B-18), the total free energy of the crystal containing a distribution of interaction defects is

$$\Delta E = \Delta\Phi_{chem} + \Delta\Phi_{el} \qquad \text{(II-B-18)}$$

where

$$\Delta\Phi_{chem} = N \sum_p \bar{C}_p \, \Delta\mu_p + \frac{1}{2} \sum_{pq} \sum_{\underset{\sim}{r}\underset{\sim}{r}'} V^{ch}_{pq}(\underset{\sim}{r} - \underset{\sim}{r}') \, C_p(\underset{\sim}{r}) \, C_q(\underset{\sim}{r}') \tag{II-B-19}$$

and

$$\Delta\Phi_{el} = N \sum_p \Phi^{el}_{self}(p) \, \bar{C}_p + \frac{1}{2} \sum_{pq} \sum_{\underset{\sim}{r}\underset{\sim}{r}'} \omega_{pq}(\underset{\sim}{r} - \underset{\sim}{r}') \, C_p(\underset{\sim}{r}) \, C_q(\underset{\sim}{r}') \tag{II-B-20}$$

where the elastic interaction parameters are evaluated as described above. The total energy may also be written as the equivalent lattice sum:

$$\begin{aligned} \Delta E &= \Delta E \left(\{C_q(\underset{\sim}{r})\}\right) \\ &= \sum_{\underset{\sim}{r}} \sum_p \left[\Delta\mu_p + \Phi^{el}_{self}(p)\right] C_p(\underset{\sim}{r}) \\ &\quad + \frac{1}{2} \sum_{\underset{\sim}{r}\underset{\sim}{r}'} \sum_{pq} \left[V^{ch}_{pq}(\underset{\sim}{r} - \underset{\sim}{r}') + \omega_{pq}(\underset{\sim}{r} - \underset{\sim}{r}')\right] C_p(\underset{\sim}{r}) \, C_q(\underset{\sim}{r}') \end{aligned} \tag{II-B-80}$$

It is useful to define a "thermoelastic potential", $\phi_p(\underset{\sim}{r}, \{C_q(\underset{\sim}{r}')\})$, which is equal to the free energy change on introducing a defect of type p at position $\underset{\sim}{r}$ in a body containing defects distributed according to the distribution functions $C_q(\underset{\sim}{r}')$ $(q = 1, \ldots . \nu)$. The introduction of the extra defect $(p, \underset{\sim}{r})$ corresponds to the change of the distribution functions

$$C_q(\underset{\sim}{r}') \rightarrow \left\{C_q(\underset{\sim}{r}') + \delta_{qp}\delta_{\underset{\sim}{r}\underset{\sim}{r}'}\right\}$$

From equation II-B-8

$$\begin{aligned} \phi_p(\underset{\sim}{r}, \{C_q(\underset{\sim}{r}')\} &= \Delta E \left(\left\{C_q(\underset{\sim}{r}') + \delta_{pq}\delta_{\underset{\sim}{r}\underset{\sim}{r}'}\right\}\right) - \Delta E \left(\left\{C_q(\underset{\sim}{r}')\right\}\right) \\ &= \phi^o_p + \phi'_p(\underset{\sim}{r}, \left\{C_q(\underset{\sim}{r}')\right\}) \end{aligned} \tag{II-B-81}$$

where

$$\phi^o_p = \Delta\mu_p + \Phi^{el}_{self}(p) + \omega_{pp}(0) \tag{II-B-82}$$

and the "partial thermoelastic potential"

$$\phi_p^{'}(\underset{\sim}{r}, \{(C_q(\underset{\sim}{r}')\}) = \sum_{\underset{\sim}{r}'} \sum_q [V_{pq}^{ch}(\underset{\sim}{r} - \underset{\sim}{r}') + \omega_{pq}(\underset{\sim}{r} - \underset{\sim}{r}')] \, C_q(\underset{\sim}{r}')$$

$$= \sum_{\underset{\sim}{r}'} \sum_q \phi_{pq}(\underset{\sim}{r} - \underset{\sim}{r}') \, C_q(\underset{\sim}{r}') \qquad \text{(II-B-83)}$$

The thermoelastic potential governs the free energy change during defect additions.

It follows from the preceding paragraphs that the creation of a solution of defects through the successive addition of elementary defects which are selected according to an energy criterion may be treated by computing the thermoelastic potentials for all possible events in an initial state and updating these by simple addition as individual events are selected and allowed to occur. This method of analysis is particularly well suited for use in a digital computer.

The thermoelastic potential also governs the energy change on redistributing defects within the body. If a defect of type p at $\underset{\sim}{r}_o$ is repositioned to $\underset{\sim}{r}_1$, the process may be represented by deleting the defect $(p,\underset{\sim}{r}_o)$ and adding a defect $(p,\underset{\sim}{r}_1)$. The associated free energy change is a simple difference between partial thermoelastic potentials:

$$\Delta F[(p,\underset{\sim}{r}_o) \rightarrow (p,\underset{\sim}{r}_1)] = \phi_p^{'}(\underset{\sim}{r}_1, \{C_q(\underset{\sim}{r}')\}) - \phi_p^{'}(\underset{\sim}{r}_o \{C_q(\underset{\sim}{r}')\}) \qquad \text{(II-B-84)}$$

where the symbol $\{C_q(\underset{\sim}{r}')\}$ has the meaning, as in eq. II-B-83, of the distribution of defects less that under consideration. The transition $(p,\underset{\sim}{r}_o) \rightarrow (p,\underset{\sim}{r}_1)$ change the thermoelastic potentials for other events $(p',\underset{\sim}{r})$ by the simple addition:

$$\phi_{p'}^{'}(\underset{\sim}{r}, \{C_q(\underset{\sim}{r}') + \delta_{qp} \, \delta_{\underset{\sim}{r}'\underset{\sim}{r}_1} - \delta_{qp} \delta_{\underset{\sim}{r}'\underset{\sim}{r}_o}\})$$

$$= \phi_{p'}^{'}(\underset{\sim}{r}, \{C_q(\underset{\sim}{r}')\}) + \phi_{p'p}(\underset{\sim}{r} - \underset{\sim}{r}_1) - \phi_{p'p}(\underset{\sim}{r} - \underset{\sim}{r}_o) \qquad \text{(II-B-85)}$$

where the function $\phi_{p'p}(\underset{\sim}{r} - \underset{\sim}{r}')$ is defined in equation II-B-83. Equations II-B-81 to II-B-85 are particularly useful for analysis of diffusional processes in a digital computer.

C. The Long-Wavelength Approximation

The governing equation of the lattice statics model may be considerably simplified by introducing the long-wavelength approximation, which essentially involves replacing the dynamical properties of the matrix by those of an equivalent elastic continuum. The simplification comes principally in the evaluation of the term

$$V^{el}_{pq}(\underset{\sim}{k}) = - \tilde{F}^{p}_{j}(\underset{\sim}{k}) \cdot G_{ij}(\underset{\sim}{k}) \cdot \tilde{F}^{q*}_{i}(\underset{\sim}{k}) \qquad \text{(II-C-1)}$$

Consider first the force $\tilde{F}^{p}_{j}(\underset{\sim}{k})$. By its definition

$$\tilde{F}^{p}_{j}(\underset{\sim}{k}) = \sum_{\underset{\sim}{r}} f^{p}_{j}(\underset{\sim}{r}) e^{-i\underset{\sim}{k} \cdot \underset{\sim}{r}} \qquad \text{(II-C-2)}$$

In the limit of small $\underset{\sim}{k}$ (long wavelength)

$$\begin{aligned} \tilde{F}^{p}_{j}(\underset{\sim}{k}) &\sim \sum_{\underset{\sim}{r}} f^{p}_{j}(\underset{\sim}{r}) \; (1 - i\underset{\sim}{k} \cdot \underset{\sim}{r} + \ldots) \\ &= \sum_{\underset{\sim}{r}} f^{p}_{j}(\underset{\sim}{r}) - ik_{\ell} \sum_{\underset{\sim}{r}} f^{p}_{j}(\underset{\sim}{r}) \; r_{\ell} \end{aligned} \qquad \text{(II-C-3)}$$

where the summation convention is assumed for the subscript ℓ. The first term on the right in II-C-3 is automatically zero from the condition that the energy be invariant to rigid displacements (eq. II-B-22). The second may be simplified by adding and subtracting symmetrizing terms:

$$\begin{aligned} \sum_{\underset{\sim}{r}} f^{p}_{j}(\underset{\sim}{r}) \; r_{\ell} &= \frac{1}{2} \sum_{\underset{\sim}{r}} \left[f^{p}_{j}(\underset{\sim}{r}) \; r_{\ell} + f^{p}_{\ell}(\underset{\sim}{r}) \; r_{j} \right] \\ &\quad + \frac{1}{2} \sum_{\underset{\sim}{r}} \left[f^{p}_{j}(\underset{\sim}{r}) \; r_{\ell} - f^{p}_{\ell}(\underset{\sim}{r}) \; r_{j} \right] \end{aligned} \qquad \text{(II-C-4)}$$

The second term on the right in (II-C-4) vanishes by the condition that the energy is invariant to rigid rotations. The first term was evaluated in eq. (II-B-47) and gives

$$\sum_{\underset{\sim}{r}} f^{p}_{j}(\underset{\sim}{r}) \; r_{\ell} = v \; \sigma^{o}_{j\ell}(0), \qquad \text{(II-C-5)}$$

where $\sigma^{o}_{j\ell}(p)$ is the transformation stress for a particle of type p. It follows that in the long-wavelength approximation

$$\tilde{F}^{p}_{j}(\underset{\sim}{k}) = -ik_{\ell}\ v\ \sigma^{o}_{j\ell}(p) \qquad \text{(II-C-6)}$$

The Green's function, $G_{ij}(k)$ was defined in equation II-B-59 to be the inverse of the dynamical matrix, $A_{ij}(k)$. The long-wavelength form of the dynamical matrix is well known[13] and is

$$\begin{aligned} A_{ij}(\underset{\sim}{k}) &= v\lambda_{ijk\ell j}k_k k_\ell \\ &= |k|^2 v\,\lambda_{ik\ell j}e_k e_\ell \\ &= |k|^2 v\ \Omega^{-1}_{ij}(\underset{\sim}{e}) \end{aligned} \qquad \text{(II-C-7)}$$

where $\underset{\sim}{e}$ is a unit vector in the direction of $\underset{\sim}{k}$ and the equation defines the inverse matrix Ω^{-1}_{ij}. It follows that the long-wavelength form of the Green's function is

$$G_{ij}(\underset{\sim}{k}) = \frac{1}{v|\underset{\sim}{k}|^2}\,\Omega_{ij}(\underset{\sim}{e}) \qquad \text{(II-C-8)}$$

Using equations (II-C-6) and (II-C-8), it then follows that

$$V^{el}_{pq}(\underset{\sim}{k}) = -ve_i\sigma^{o}_{ij}(p)\ \Omega_{j\ell}(\underset{\sim}{e})\ \sigma^{o}_{\ell m}(q)e_m + Q_{pq} \qquad \text{(II-C-9)}$$

for $k \neq 0$, where

$$\begin{aligned} Q_{pq} &= \langle e_i\sigma^{o}_{ij}(p)\ \Omega_{j\ell}(e)\ \sigma^{o}_{\ell m}(q)\ e_m\rangle\ v \\ &= \frac{v}{N}\sum_{k}{}'\ e_i\sigma^{o}_{ij}(p)\ \Omega_{j\ell}(\underset{\sim}{e})\ \sigma^{o}_{\ell m}(q)\ e_m \end{aligned} \qquad \text{(II-C-10)}$$

The term $\underset{\sim}{k} = 0$ is eliminated from the summation, since $\underset{\sim}{e}$ and hence $\Omega(\underset{\sim}{e})$ are undefined there.

Equation II-C-9 presents the Fourier component of the two-body elas-

tic interaction as a product of terms which can be computed from the elastic constants, $\lambda_{ij\ell m}$, and the transformation strain $\varepsilon^{o}_{ij}(p)$. Since the image force interaction, $V^{el}_{pq}(0)$ depends on the same quantities, the elastic energy of an arbitrary distribution of substitutional species can readily be computed in the long-wavelength approximation.

The long-wavelength approximation is valid when the substitutional defects are aggregated into macroscopic inclusions whose dimensions are large compared to the lattice spacing. When this condition is not strictly satisfied, as in the model of the martensite transformation presented in the following section, the long-wavelength approximation is used in the spirit of the Debye model: to allow a simple, tractable analysis of a more complex situation.

D. Limit Transition to the Continuum Theory of Macroscopic Elastic Inclusions.

The model of the martensite transformation that is developed and used in the following section is a semi-continuum model. It will employ the real space form of the lattice statics equation for the elastic energy as presented in equation II-B-68, but will assume a binary interaction, $\omega_{pq}(r - r')$, which is obtained through the long-wavelength approximation. The equations needed for this model were derived in subsections II-B and II-C. For the sake of completeness, however, and to demonstrate the internal cohesiveness of the theory of elastic defects as developed here, we shall conclude this section by deriving the form of the elastic Hamiltonian in its full continuum limit. The resulting equation will be seen to be identical to that derived by Khachaturyan and Shatalov[14] (equation II-A-7) from a starting point in continuum elasticity.

The reduction to the case of macroscopic elastic inclusions in the continuum limit involves three steps: (1) The inclusions are assumed to be large compared to the lattice spacing. (2) The summations appearing in the expression for the elastic energy are replaced by asymptotically equivalent integrations. (3) The interaction potentials are evaluated in the long-wavelength limit.

Consider a body which contains a distribution of coherent inclusions which are individually large compared to the lattice parameter. To maintain contact with the lattice statics model, we may imagine these inclusions to be formed by agglomerating individual point defects. For simplicity let each inclusion be composed of a single type (p) of defect.

The distribution of inclusions of type p is described by the

function

$$\theta_p(\underset{\sim}{r}) = \begin{cases} 1 \text{ for r inside an inclusion of type p} \\ 0 \text{ otherwise} \end{cases} \qquad \text{(II-D-1)}$$

Then clearly

$$C_p(\underset{\sim}{r}) = \theta_p(\underset{\sim}{r}) \qquad \text{(II-D-2)}$$

The Fourier transform of the distribution function is

$$\tilde{C}_p(\underset{\sim}{k}) = \sum_{\underset{\sim}{r}} C_p(\underset{\sim}{r}) e^{-i\underset{\sim}{k} \cdot \underset{\sim}{r}} \qquad \text{(II-D-3)}$$

When the inclusions are macroscopic in the sense that their characteristic linear dimension, ℓ, satisfies the constraint $a/\ell << 1$ then the summation in equation (II-D-3) may be replaced by the integration

$$\tilde{C}_p(\underset{\sim}{k}) \approx \frac{1}{v} \int_{-\infty}^{\infty} d^3\underset{\sim}{r}\, e^{-i\underset{\sim}{k} \cdot \underset{\sim}{r}}\, \theta_p(r) = \frac{1}{v} \tilde{\theta}_p(\underset{\sim}{k}), \qquad \text{(II-D-4)}$$

where v is the volume of the unit cell.

To find the elastic energy of the distribution of inclusions in the continuum limit, it is simplest to return to equation II-B-62, which may be written:

$$\Delta E_{el} = \frac{N}{2} \sum_{pq} v\lambda_{ijk\ell} \varepsilon^o_{ij}(p)\, \varepsilon^o_{k\ell}(q)\, (\bar{C}_p \delta_{pq} - \bar{C}_p \bar{C}_q)$$

$$- \frac{1}{2N} \sum_{pq} \sum_{\underset{\sim}{k}} \tilde{F}^p_i(\underset{\sim}{k})\, G_{ij}(\underset{\sim}{k})\, \tilde{F}^{q*}_j(\underset{\sim}{k})\, \Delta\tilde{C}_p(\underset{\sim}{k})\, \Delta\tilde{C}^*_q(\underset{\sim}{k}) \qquad \text{(II-D-5)}$$

or

$$\Delta E_{el} = \frac{1}{2N} \sum_{pq} \sum_{\underset{\sim}{k}}{}' \; v\lambda_{ijk\ell} \varepsilon^o_{ij}(p)\, \varepsilon^o_{k\ell(q)}$$

$$- \tilde{F}^p_i(\underset{\sim}{k})\, G_{ij}(\underset{\sim}{k})\, \tilde{F}^{q*}_j(\underset{\sim}{k})\, \tilde{C}_p(\underset{\sim}{k})\, \tilde{C}^*_p(\underset{\sim}{k}) \qquad \text{(II-D-6)}$$

where the identities (II-B-64) and (II-B-66) have been used, and the prime on the summation over $\underset{\sim}{k}$ indicates deletion of the $\underset{\sim}{k} = 0$ term.

With the definition

$$B_{pq}(\underset{\sim}{k}) = \lambda_{ijk\ell}\ \varepsilon^{o}_{ij}(p)\ \varepsilon^{o}_{k\ell}(q)$$

$$- \left(\frac{1}{v}\right) \tilde{F}^{p}_{i}(\underset{\sim}{k})\ G_{ij}(\underset{\sim}{k})\ \tilde{F}^{*q}_{j}(\underset{\sim}{k}) \qquad \text{(II-D-7)}$$

and the use of equation (II-D-4),

$$\Delta E_{el} = \left(\frac{1}{2Nv}\right) \sum_{pq} \sum_{\underset{\sim}{k}}{}' B_{pq}(\underset{\sim}{k})\ \tilde{\theta}_{p}(\underset{\sim}{k})\ \tilde{\theta}^{*}_{q}(\underset{\sim}{k}). \qquad \text{(II-D-8)}$$

The summation on the right hand side of equation II-D-8 is taken over the N points of the first unit cell of the crystal (excluding the point $\underset{\sim}{k} = 0$). Each of these points occupies a volume in k-space equal to $(2\pi)^3/V$, where $V = Nv$ is the total volume of the crystal. Taking the limit of large crystal size under the condition that the inclusion size is small compared to that of the crystal ($\ell/V^{1/3} << 1$) the summation in equation (II-D-8) may be replaced by the integration

$$\frac{1}{2Nv} \sum_{\underset{\sim}{k}}{}' B_{pq}(\underset{\sim}{k})\ \tilde{\theta}_{p}(\underset{\sim}{k})\ \tilde{\theta}^{*}_{q}(\underset{\sim}{k}) = \frac{1}{2} \int' \frac{d^3k}{(2\pi)^3}\ B_{pq}(\underset{\sim}{k})\ \tilde{\theta}_{p}(\underset{\sim}{k})\ \tilde{\theta}^{*}_{q}(\underset{\sim}{k}) \qquad \text{(II-D-9)}$$

where the integral is taken over the first Brillouin Zone of the crystal and where the prime on the integral has the meaning that a volume $(2\pi)^3/V$ about $k = 0$ is to be excluded from the integration. When V is large this exclusion defines the "principal value" of the integral. Using equation II-D-9 the elastic energy is

$$\Delta E_{el} = \frac{1}{2} \sum_{pq} \int' \frac{d^3k}{(2\pi)^3}\ B_{pq}(\underset{\sim}{k})\ \tilde{\theta}_{p}(\underset{\sim}{k})\ \tilde{\theta}^{*}_{q}(\underset{\sim}{k}) \qquad \text{(II-D-10)}$$

To complete the identification of equation (II-B-10) with the Khachaturyan-Shatalov equation (equation II-A-7) we note that the shape function $\tilde{\theta}_{p}(\underset{\sim}{k})$ of an inclusion of volume $V_p (<< V)$ will have significant

magnitude over a volume of approximately $(\Delta k)^3 \approx (2\pi)^3/V_p$ about $\underset{\sim}{k} = 0$. If V_p is large Δk is small, and we are usually justified in replacing $B_{pq}(\underset{\sim}{k})$ by its long-wavelength form. Using equations II-D-7, II-C-6, and II-C-8, we have

$$\begin{aligned} B_{pq}(\underset{\sim}{k}) &= B_{pq}(\underset{\sim}{e}) \\ &= \lambda_{ijk\ell}\varepsilon^{o}_{ij}(p)\ \varepsilon^{o}_{k\ell}(q) \\ &\quad - e_i\sigma^{o}_{ij}(p)\ \Omega_{j\ell}(\underset{\sim}{e})\ \sigma^{o}_{\ell m}(q)\ e_m. \end{aligned} \qquad \text{(II-D-11)}$$

Substitution of the expression for $B_{pq}(\underset{\sim}{e})$ given in II-D-11 into II-D-10 makes this equation identical with the Khatchaturyan-Shatalov solution (eq. II-A-7) for the elastic energy of a distribution of coherent inclusions in an elastic continuum.

III. THE MARTENSITE TRANSFORMATION.

As described in the introduction the martensite transformation is a diffusionless transformation which accomplishes a change in crystal structure. Since, at least in the initial stages of the transformation, the particles of the new phase are coherently connected to the parent matrix, the problem of elastic accomodation necessarily plays a major role in the thermodynamics of the transformation.

The need to accomodate elastic distortions significantly influences both the nucleation of the martensite phase and the kinetics and morphology of its subsequent development. In the case of alloy steels (and of many of the other systems that are known to undergo martensitic transformations) elastic strain affects nucleation in two rather different ways. First, the relevant theoretical studies argue that the strain energy associated with a coherent, single variant martensite particle is so large that it is not possible for the transformation to nucleate spontaneously in a perfect crystal. It is now commonly thought that the martensite transformation nucleates heterogeneously and that its initiation is catalyzed by the presence of crystal lattice defects whose own strain fields may partly compensate for the strain associated with the formation of the martensite particle. Second, the nature of the martensite transformation is such that a single nucleation process is generally insufficient to permit the transformation to proceed to completion. The repeated nucleation of individual martensite plates is necessary. The strain energy associated with the martensite transformation may also be important in promoting this secondary nucleation, by catalyzing nucleation in those places and orientations which serve to relieve the internal elastic field.

The influence of elastic strain on the growth and morphology of martensite plates is conditioned by the fact that the martensite particle may form in any one of several crystallographic variants, each of which exhibits the preferred crystallographic relation with the parent matrix. For example, the FCC → BCC martensite transformation provides three distinct crystal lattice rearrangements. These differ in the orientation of the tetragonal axis of the Bain distortion, which may lie along any one of the three cubic axes of the parent phase. A similar situation occurs whenever the transformation is of the crystallographic type cubic → tetragonal (fig. 2).

The existence of several distinct orientational variants of the product phase provides a configurational freedom which may be used to reduce the elastic energy. The martensite particle is free to grow as a composite particle of two or more variants which are so configured as to provide a mutual relaxation of elastic strain. In the case of the FCC → BCC transformation, the martensite particle tends to grow as a thin plate which consists of periodically alternating layers of the tetragonal phase with different directions of the tetragonal axis (Fig. 3). If the relative fractions of the two variants within this plate are properly chosen, and if the plate is given an appropriate habit in the parent matrix, then the bulk elastic energy may be made very small. This result is the implicit theoretical basis for the crystallographic theories of the habit plane of martensitic particles[10].

Given the prominence of elastic effects in the nucleation, growth, and morphology of martensite, it seems reasonable to suppose that many of the other interesting and unique features of the martensite transformation will have their source in the need to accomodate elastic strain

as the transformation proceeds. Tractable models of the development of the martensite transformation which include the predominant elastic effects should hence prove particularly fruitful in new theoretical insight. Such a model can be drawn directly from the elastic theory developed in the preceding section. Since this theory permits one to calculate the elastic energy of an arbitrary distribution of elastic inclusions, it may be used to compute the elastic energy of a progressing martensitic transformation in any hypothetical intermediate stage, and to identify the incremental transformation steps which are most favorable with respect to the elastic energy. While such a model is not likely to be tractable analytically, the form of the equations is such that they can be quite easily phrased for solution in a computer, leading to a developmental model of the martensitic transformation.

A simple elastic model of the developing martensite transformation is formulated in the balance of this section. It is obtained through a straightforward adaptation of the lattice-statics model presented in the preceding section, with minor modifications to show how the possibly finite size of the elementary martensite particles and their surface and twin-boundary energies may be taken into account.

A. The Description of Martensite in Terms of Elementary Particles

The simulation of the martensite transformation requires the introduction of a minimal element of martensite phase, which we shall call the elementary martensite particle (EMP). The distribution of martensite within a crystal will then be represented by a suitable combination of EMP. In the linear approximation which we shall use the elastic strain within the crystal is simply the sum of the strains associated with each of the EMP; the elastic energy is the sum of their self-energies plus the energy associated with their mutual interaction.

The smaller the EMP the more accurately an arbitrary distribution of the martensite phase can be modeled. However, it should be recognized that there is a physical lower boundary on the size of an EMP which can be reasonably assumed to exist in isolation. This boundary is set by the need for the EMP to have the crystallographic identity of the martensite phase; if the particle is too small, surface tension will dominate and destroy the internal atomic arrangement. The linear size of the particle must at least exceed the correlation length required for a coherent transition from the parent lattice to that of the martensite, essentially the thickness of the martensite parent-interface.

A rough estimate of the correlation length (R_c) may be found by equating the surface energy of a particle of radius R_c to the heat released on forming it[1]:

$$\gamma 4\pi R_c^{\ 2} \sim \frac{4\pi}{3} R_c^{\ 3} Q, \qquad \text{(III-A-1)}$$

According to the evaluation[1,62] for iron based martensite, the surface energy is about 1.2×10^{-5} kcal/cm^2 and the heat release is about 240 kcal/cm^3 which gives

$$R_c \sim 3\gamma/Q \sim 15\ \text{Å} \qquad \text{(III-A-2)}$$

This evaluation suggests a minimum particle size of ∿8-27 unit cells of the martensite phase. (2 ∿ 3 crystal lattice parameters).

To describe the martensite distribution in terms of a distribution of finite EMP, we refer the parent crystal to a superlattice of cells, each of which is of the size of an EMP. If there are ν variants of the martensite, we must assume ν kinds of EMP. Each of these is distinguished by its orientation and by its transformation strain, $\varepsilon^o_{ij}(p)$ ($p = 1, \ldots \nu$), where the $\varepsilon^o_{ij}(p)$ differ only through a rotation with respect to axes fixed in the parent phase. The martensite distribution is then reproduced by placing EMP of the correct variant at the appropriate sites of the superlattice.

The spatial distribution of the martensite phase is described mathematically by the function

$$\zeta_p(\underset{\sim}{R}) = \begin{cases} 1 \text{ for an EMP of type p at } \underset{\sim}{R} \\ 0 \text{ otherwise} \end{cases} \qquad \text{(III-A-3)}$$

where $\underset{\sim}{R}$ is a translation vector of the superlattice. This description is illustrated in two-dimensions in Fig. 4, in which both the fine grid of the parent crystal lattice and the coarse grid of the superlattice are displayed. Since only one martensite particle may occupy a given cell of the superlattice, the $\zeta_p(\underset{\sim}{R})$ satisfies the identity

$$\zeta(\underset{\sim}{R}) = \sum_{p=1}^{\nu} \zeta_p(\underset{\sim}{R}) = \begin{cases} 1 \text{ for } \underset{\sim}{R} \text{ occupied by martensite} \\ 0 \text{ otherwise} \end{cases} \qquad \text{(III-A-4)}$$

In order to establish contact between the superlattice distribution functions $\zeta_p(\underset{\sim}{R})$ and the lattice distributions $C_p(\underset{\sim}{r})$, let $\chi(\underset{\sim}{R})$ be the set of lattice sites which fall within the supercell located at $\underset{\sim}{R}$. Then

the shape of the supercell at $\underset{\sim}{R}$ is described by the function

$$\eta(\underset{\sim}{r}-\underset{\sim}{R}) = \begin{cases} 1 \text{ if } \underset{\sim}{r} - \underset{\sim}{R} \in \chi(\underset{\sim}{r}) \\ 0 \text{ otherwise} \end{cases} \qquad \text{(III-A-5)}$$

With this definition,

$$C_p(\underset{\sim}{r}) = \sum_{\underset{\sim}{R}} \eta(\underset{\sim}{r} - \underset{\sim}{R})\ \zeta_p(\underset{\sim}{R}), \qquad \text{(III-A-6)}$$

which relates the occupation numbers within the two lattices. Taking the Fourier transform of both sides, we have

$$\tilde{C}_p(\underset{\sim}{k}) = \sum_{\underset{\sim}{r}} C_p(\underset{\sim}{r}) e^{-i\underset{\sim}{k} \cdot \underset{\sim}{r}} = N_o \eta(\underset{\sim}{k})\ \tilde{\zeta}_p(\underset{\sim}{k}) \qquad \text{(III-A-7)}$$

where the function $\eta(\underset{\sim}{k})$ is defined by

$$\eta(\underset{\sim}{k}) = \frac{1}{N_o} \sum_{\underset{\sim}{r}} \eta(\underset{\sim}{r} - \underset{\sim}{R}) e^{-i\underset{\sim}{k} \cdot (\underset{\sim}{r} - \underset{\sim}{R})} \qquad \text{(III-A-8)}$$

and

$$\tilde{\zeta}_p(\underset{\sim}{k}) = \sum_{\underset{\sim}{k}} \zeta_p(\underset{\sim}{R}) e^{-i\underset{\sim}{k} \cdot \underset{\sim}{R}} \qquad \text{(III-A-9)}$$

where the $\underset{\sim}{R}$ are the lattice points of the superlattice.

If the total number of cells in the superlattice is M, and if M_p are those occupied by particles of type p, then

$$\overline{\zeta}_p = M_p/M = \overline{C}_p \qquad \text{(III-A-10)}$$

If each supercell contains only one lattice point, then M = N and

$$\eta(\underset{\sim}{k}) = 1 \quad (M = N). \qquad \text{(III-A-11)}$$

If $M \neq N$ there are $N_o = N/M$ lattice points per supercell and $\eta(\underset{\sim}{k})$ has non-zero values over a volume $\sim (2\pi)^3/N_o v$ of k-space about $\underset{\sim}{k} = \underset{\sim}{0}$. When N_o is large the supercell is macroscopic and the long-wavelength approximation is valid.

B. The Elastic Energy

The elastic energy of an arbitrary distribution of elementary martensite particles may be computed by means of the equations developed in section II-B. Ideally, we wish to express the equation in a form identical to that in equation II-B-78 (k-space form) or II-B-69 (real space form) but with the lattice sums renormalized to sums over the superlattice of EMP, so that the free energy of the distribution of EMP can be computed directly, without reference to a microscopic reference lattice.

To accomplish the renormalization we return to equation II-B-62:

$$\Delta\Phi_{el} = \frac{N}{2}\sum_{p}\left(v\lambda_{ijk\ell}\varepsilon^{o}_{ij}(p)\varepsilon^{o}_{k\ell}(p)\right)\overline{C}_p$$
$$- \frac{N}{2}\sum_{pq}\left(v\lambda_{ijk\ell}\varepsilon^{o}_{ij}(p)\varepsilon^{o}_{k\ell}(q)\right)\overline{C}_p\overline{C}_q$$
$$- \frac{1}{2N}\sum_{pq}\sum_{\underset{\sim}{k}}\left(\tilde{F}^{p}_{i}(\underset{\sim}{k})G_{ij}(\underset{\sim}{k})\tilde{F}^{q*}_{j}(\underset{\sim}{k})\right)\Delta\tilde{C}_p(\underset{\sim}{k})\,\Delta\tilde{C}^{*}_{q}(\underset{\sim}{k}). \qquad \text{(III-B-1)}$$

Using equations III-A-7 and III-A-10 this equation may be rewritten

$$\Delta\Phi_{el} = \frac{M}{2}\sum_{p}\left(V\lambda_{ij\ell m}\varepsilon^{o}_{ij}(p)\varepsilon^{o}_{\ell m}(p)\right)\overline{\zeta}_p$$
$$- \frac{M}{2}\sum_{pq}\left(V\lambda_{ij\ell m}\varepsilon^{o}_{ij}(p)\varepsilon^{o}_{\ell m}(q)\right)\overline{\zeta}_p\overline{\zeta}_q$$
$$- \frac{N_o}{2M}\sum_{pq}\sum_{k}\left(\tilde{F}^{p}_{i}(\underset{\sim}{k})G_{ij}(\underset{\sim}{k})\tilde{F}^{q*}_{j}(\underset{\sim}{k})\right)|\eta(k)|^2\,\Delta\tilde{\zeta}_p(\underset{\sim}{k})\,\Delta\zeta^{*}_{q}(\underset{\sim}{k}) \qquad \text{(III-B-2)}$$

where $V = N_o v$ is the volume of an EMP.

To accomplish a renormalization to the superlattice we rewrite the wavenumbers, $\underset{\sim}{k}$, of the elementary lattice as

$$\underset{\sim}{k} = \underset{\sim}{k}_o + \underset{\sim}{k}', \qquad \text{(III-B-3)}$$

where $\underset{\sim}{k}_o$ is a reciprocal lattice vector of the superlattice

$$\underset{\sim}{k}_o \cdot \underset{\sim}{R} = 2\pi n \qquad (n = \text{integer}) \qquad \text{(III-B-4)}$$

Since the volume of the supercell is N_o times the volume of the unit cell of the crystal the volume in reciprocal space of the Brillouin zone of the superlattice is $1/N_o$ times that of the Brillouin zone of the crystal. It follows that there are N_o superlattice reciprocal vectors $\underset{\sim}{k}_o$ within the first Brillouin zone of the crystal and $N/N_o = M$ wave vectors, $\underset{\sim}{k}'$ associated with each. From the definition, III-B-4,

$$\zeta_p(\underset{\sim}{k}_o + \underset{\sim}{k}') = \sum_{\underset{\sim}{k}} \zeta_p(\underset{\sim}{R}) e^{-i(\underset{\sim}{k}_o + \underset{\sim}{k}') \cdot \underset{\sim}{R}} = \zeta_p(\underset{\sim}{k}') \qquad \text{(III-B-5)}$$

By means of the scalar

$$\Gamma_{pq}(\underset{\sim}{k}) = N_o(\tilde{F}_i^p(\underset{\sim}{k}) G_{ij}(\underset{\sim}{k}) \tilde{F}_j^{q*}(\underset{\sim}{k}))\,|\eta(\underset{\sim}{k})|^2 \qquad \text{(III-B-6)}$$

the summation over k on the third term of the right hand side of equation III-B-2 can be written

$$\begin{aligned} &- \frac{1}{2M} \sum_{\underset{\sim}{k}} \Gamma_{pq}(\underset{\sim}{k}) \Delta\zeta_p(\underset{\sim}{k}) \Delta\zeta(\underset{\sim}{k}) \\ &= - \frac{1}{2M} \sum_{\underset{\sim}{k}}{}' \sum_{\underset{\sim}{k}_o} \Gamma_{pq}(\underset{\sim}{k}_o + \underset{\sim}{k}') \; \Delta\zeta_p(\underset{\sim}{k}') \Delta\zeta_q(\underset{\sim}{k}') \qquad \text{(III-B-7)} \\ &= \frac{1}{2M} \sum_{\underset{\sim}{k}}{}' \hat{\Gamma}_{pq}(\underset{\sim}{k}') \Delta\zeta_p(\underset{\sim}{k}') \Delta\zeta_q(\underset{\sim}{k}'), \end{aligned}$$

where

$$\hat{\Gamma}_{pq}(\underset{\sim}{k}') = \sum_{\underset{\sim}{k}_o} \Gamma_{pq}(\underset{\sim}{k}_o + \underset{\sim}{k}'). \qquad \text{(III-B-8)}$$

When the EMP is of reasonable size so that the non-negligible values of $\eta(k)$ are well confined to the first Brillouin zone of the superlattice then

$$\hat{\Gamma}_{pq}(\underset{\sim}{k}') \simeq \Gamma_{pq}(\underset{\sim}{k}'). \qquad \text{(III-B-9)}$$

and only the first Brillouin zone of the superlattice need be considered

in evaluating $\Delta\phi_{el}$.

To complete the task of re-casting equation (III-B-2) into compact form we need to separate out that part of the sum over reciprocal space which is independent of the precise configruation of EMP. Proceeding as in the equations following II-B-62 we re-define the scalar Q_{pq}:

$$Q_{pq} = \langle \Gamma_{pq}(\underset{\sim}{k}') \rangle = \frac{1}{M} \sum_{\underset{\sim}{k}'} \Gamma_{pq}(\underset{\sim}{k}') \qquad \text{(III-B-10)}$$

Using the definitions III-B-8 and III-B-10 and the identity

$$\Delta\zeta_p(\underset{\sim}{k}) = \zeta_p(\underset{\sim}{k}) - \overline{\zeta}_p(\underset{\sim}{k}) = \begin{cases} 0 & \underset{\sim}{k} = 0 \\ \zeta_p(\underset{\sim}{k}) & \underset{\sim}{k} \neq 0 \end{cases} \qquad \text{(III-B-11)}$$

equation III-B-2 may be rewritten

$$\Delta\phi_{el} = M \sum_p \Delta\phi^{el}_{self}\, \overline{\zeta}_p - \frac{M}{2} \sum_{pq} \hat{\Gamma}^{el}_{pq}(0)\, \overline{\zeta}_p \overline{\zeta}_q$$

$$- \frac{1}{2M} \sum_{pq} \sum_{\underset{\sim}{k}'} \hat{\Gamma}^{el}_{pq}(\underset{\sim}{k}') \zeta_p(\underset{\sim}{k}') \zeta_q(\underset{\sim}{k}') \qquad \text{(III-B-12)}$$

where

$$\Delta\phi^{el}_{self} = \frac{1}{2} \left(V \lambda_{ij\ell m} \varepsilon^o_{ij}(p) \varepsilon^o_{\ell m}(p) - Q_{pp} \right) \qquad \text{(III-B-13)}$$

$$\hat{\Gamma}^{el}_{pq}(0) = - \left(V \lambda_{ij\ell m} \varepsilon^o_{ij}(p) \varepsilon^o_{\ell m}(q) - Q_{pq} \right) \qquad \text{(III-B-14)}$$

$$\hat{\Gamma}^{el}_{pq}(\underset{\sim}{k} \neq 0) = \hat{\Gamma}_{pq}(\underset{\sim}{k}') - Q_{pq} \qquad \text{(III-B-15)}$$

and where the summation over k is taken over the first Brillouin zone of the superlattice and the prime on the summation indicates that the $\underset{\sim}{k}' = \underset{\sim}{0}$ term is to be excluded.

Defining the elastic potential

$$\mathcal{L}^{el}_{pq}(\underset{\sim}{k}) = \begin{cases} \hat{\Gamma}^{el}_{pq}(0) & \underset{\sim}{k} = 0 \\ \hat{\Gamma}^{el}_{pq}(\underset{\sim}{k}) & \underset{\sim}{k} \neq 0 \end{cases} \tag{III-B-16}$$

and using the identity

$$\tilde{\zeta}_p(0) = \frac{1}{M}\bar{\zeta}_p \tag{III-B-17}$$

we obtain

$$\Delta\phi_{el} = M \sum_p \Delta\phi^{el}_{self}\bar{\zeta}_p$$

$$- \frac{1}{2M} \sum_{\underset{\sim}{k}} \mathcal{L}^{el}_{pq}(\underset{\sim}{k})\ \tilde{\zeta}_p(\underset{\sim}{k})\ \tilde{\zeta}_q(\underset{\sim}{k}) \tag{III-B-18}$$

where the prime on the summation has been removed. This compact equation is identical in form to the final equation (II-B-78) of the lattice statics model, with the difference that the elementary particles are EMP rather than atomic defects and the sum is taken over the points of the superlattice rather than over those of the fundamental lattice.

The inverse transformation of equation III-B-18 to its real space form yields the final equation

$$\Delta\phi_{el} = \sum_{\underset{\sim}{R}} \sum_P \Delta\phi^{el}_{self}\ \zeta_p(\underset{\sim}{R})$$

$$- \frac{1}{2} \sum_R \sum_{R'} \sum_{pq} \omega^{el}_{pq}(\underset{\sim}{R} - \underset{\sim}{R}')\ \zeta_p(\underset{\sim}{R})\ \zeta_q(\underset{\sim}{R}') \tag{III-B-19}$$

where

$$\omega^{el}_{pq}(\underset{\sim}{R} - \underset{\sim}{R}') = - \frac{1}{M} \sum_{\underset{\sim}{k}} \omega^{el}_{pq}(\underset{\sim}{k}) e^{-i\underset{\sim}{k} \cdot (\underset{\sim}{R} - \underset{\sim}{R}')} \tag{III-B-20}$$

gives the real space interaction between EMP.

C. The Chemical Energy

From equation (II-B-19) the total chemical energy of a crystal containing a distribution of elementary particles of the martensite phase is

$$\Delta\phi_{ch} = \sum_p \sum_{\underset{\sim}{r}} \Delta\mu_p C_p(\underset{\sim}{r}) + \frac{1}{2} \sum_{pq} \sum_{\underset{\sim}{r}\underset{\sim}{r}'} V^{ch}_{pq}(\underset{\sim}{r} - \underset{\sim}{r}')\, C_p(\underset{\sim}{r})\, C_q(\underset{\sim}{r}'). \qquad \text{(II-B-19)}$$

Using the definition

$$C_p(\underset{\sim}{r}) = \sum_{\underset{\sim}{R}} \eta(\underset{\sim}{r} - \underset{\sim}{R})\, \zeta_p(\underset{\sim}{R}) \qquad \text{(III-A-6)}$$

this equation may be renormalized into a sum over the points of the superlattice. Letting $\underset{\sim}{r} = \underset{\sim}{R} + \underset{\sim}{\tau}$,

$$\Delta\phi_{ch} = \sum_{\underset{\sim}{R}} \sum_p (N_o\, \Delta\mu_p)\, \zeta_p(\underset{\sim}{R})$$

$$+ \frac{1}{2} \sum_{RR'} \sum_{pq} \hat{V}^{ch}_{pq}(\underset{\sim}{R} - \underset{\sim}{R}')\, \zeta_p(\underset{\sim}{R})\, \zeta_q(\underset{\sim}{R}') \qquad \text{(III-C-1)}$$

where

$$\hat{V}^{ch}_{pq}(R - R') = \sum_{\underset{\sim}{\tau}\underset{\sim}{\tau}'} V^{ch}_{pq}[(\underset{\sim}{R} - \underset{\sim}{R}') + (\underset{\sim}{\tau} - \underset{\sim}{\tau}')]\, \eta(\underset{\sim}{\tau})\, \eta(\underset{\sim}{\tau}') \qquad \text{(III-C-2)}$$

When the elementary martensite particle has finite size, it is useful to represent the chemical free energy as a conventional sum of bulk free energy and surface energy terms. The bulk-free energy term is the same for all martensite variants ($\Delta\mu^b_o$). If we ignore the temperature dependence of the enthalpy (Δh_o) and entropy (Δs_o) of the transformation, which is reasonable at least for T near T_o, the transformation temperature, then $\Delta\mu^b_o$ may be written in the familiar form

$$\Delta\mu^b_o = \frac{\Delta h_o}{T_o}(T - T_o) = \Delta s_o(T - T_o) \qquad \text{(III-C-3)}$$

where Δh_o is the transformation enthalpy per atom.

The representation of the surface energy is more complex. Two distinct surface energies are relevant to the martensite transformation: the free energy $\Delta\mu_o^s$ of an element of coherent interface with the parent phase and the free energy $\Delta\mu_{pq}^s$ of an element of interface between martensite variants of types p and q. Both interfacial free energies will generally depend on orientation. The total interfacial energy should be computed by integration over the surface of each distinct martensite particle. At least in certain cases, however, this integration may be replaced by a summation over the EMP.

Let the surface energy of a martensite particle be strongly orientation-dependent, as will usually be the case, and assume that the shape which minimizes the surface energy of an isolated particle gives a figure which may be repeated to fill space, i.e., a figure which corresponds to the Wigner-Seitz cell of a periodic lattice. If the EMP is taken to have the shape which minimizes surface energy and if the superlattice of EMP is taken to be the periodic lattice appropriate to this shape, then the surface energy of a martensite particle represented as an agglomeration of EMP is well approximated by summing the surface energies of the exposed facets of the EMP which lie in its periphery. This sum may be evaluated by taking an appropriate sum over all EMP. The relevant equations are simplest when the EMP is a cube, though they may be formulated for any shape which fills the space on periodic repitition.

Assume a cubic EMP, and let its facets have the energy $\Delta\mu_o^s$, if in contact with the matrix, $\Delta\mu_1^s$ if in contact with an EMP of different type, and zero if in contact with an EMP of the same type. Defining

$$V^s_{pq}(\underset{\sim}{R} - \underset{\sim}{R}') = \begin{cases} (\Delta\mu^s_1 - 2\Delta\mu^s_o) - \Delta\mu^s_1\,\delta_{pq} & \text{If } (\underset{\sim}{R} - \underset{\sim}{R}') = \underset{\sim}{R}_o \\ 0 & \text{Otherwise} \end{cases} \qquad \text{(III-C-4)}$$

where R_o is any lattice vector connecting nearest neighbors, it follows that the surface energy may be written

$$\Delta\phi^s = \sum_{\underset{\sim}{R}} \sum_p (Z\Delta\mu^s_o)\ \zeta_p(\underset{\sim}{R})$$

$$+ \frac{1}{2} \sum_{pq} \sum_{\underset{\sim}{R}\underset{\sim}{R}'} V^s_{pq}(\underset{\sim}{R} - \underset{\sim}{R}')\ \zeta_p(\underset{\sim}{R})\ \zeta_q(\underset{\sim}{R}') \qquad \text{(III-C-6)}$$

where Z is the number of nearest neighbors of an EMP (Z = 6 for a cube).

If equation III-C-3 and III-C-6 are substituted into equation III-C-1, and if the direct chemical interaction between EMP is neglected on the grounds that the EMP are finite, the expression for the total chemical energy becomes

$$\Delta\phi_{ch} = \sum_{\underset{\sim}{R}} \left[\frac{N_o \Delta h_o}{T_o}(T - T_o) + \phi^s_o\right] \sum_p \zeta_p(\underset{\sim}{R})$$

$$+ \frac{1}{2} \sum_{\underset{\sim}{R}\underset{\sim}{R}'} \sum_{pq} V^s_{pq}(\underset{\sim}{R} - \underset{\sim}{R}')\ \zeta_p(\underset{\sim}{R})\ \zeta_q(\underset{\sim}{R}') \qquad \text{(III-C-7)}$$

where

$$\phi^s_o = Z\Delta\mu^s_o \qquad \text{(III-C-8)}$$

D. The Total Energy and the Thermoelastic Potential.

Summing equations (III-B-19) and (III-C-6) gives an expression for the total energy of a configuration of elementary martensite particles specified by the set of ν distribution functions $\left\{\zeta_q(\underset{\sim}{R}')\right\}$:

$$\Delta E\left\{\zeta_q(\underset{\sim}{r})\right\} = \sum_{\underset{\sim}{R}} \left(\frac{N_o \Delta h_o}{T_o}(T - T_o) + \phi_o^s + \Delta\phi_{self}^{el}\right) \sum_p \zeta_p(\underset{\sim}{R})$$
$$+ \frac{1}{2} \sum_{\underset{\sim}{R}\underset{\sim}{R}'} \sum_{pq} \left[\omega_{pq}^{el}(\underset{\sim}{R} - \underset{\sim}{R}') + V_{pq}^s(\underset{\sim}{R} - \underset{\sim}{R}')\right] \zeta_p(\underset{\sim}{R})\, \zeta_q(\underset{\sim}{R}') \tag{III-D-1}$$

where we have used the fact that the self energy of all martensite variants is the same. Equation (III-D-1) gives the elastic energy as a sum of bulk free energy, surface energy, and elastic energy contributions, in keeping with the representation for systems of finite particles.

A thermoelastic potential may be defined for the EMP using a procedure identical to that employed in section II-B-3. Given the distribution of EMP specified by the set $\left\{\zeta_q(R')\right\}$ we define

$$\phi_p(\underset{\sim}{R},\left\{\zeta_q(\underset{\sim}{R}')\right\}) = \left[\Delta E\left\{\zeta_q(\underset{\sim}{R}') + \delta_{qp}\delta_{\underset{\sim}{R}\underset{\sim}{R}'}\right\}\right] - \left[\Delta E\left\{\zeta_q(\underset{\sim}{R}')\right\}\right]$$
$$= \frac{N_o \Delta h_o}{T_o}(\Delta T) + \phi_o^s + \phi_{self}^{el} \tag{III-D-2}$$
$$+ \sum_{\underset{\sim}{R}'} \sum_q \left[\omega_{pq}^{el}(\underset{\sim}{R} - \underset{\sim}{R}') + V_{pq}^s(\underset{\sim}{R} - \underset{\sim}{R}')\right] \zeta_q(\underset{\sim}{R}').$$

The thermoelastic potential is the free energy change on introduction of an EMP of type p at position R in the presence of the distribution $\left\{\zeta_q(\underset{\sim}{R}')\right\}$ over sites other than $\underset{\sim}{R}$. If the EMP $(p,\underset{\sim}{R})$ is present in the

initial distribution, then the energy change on removing it is just

$$\Delta F = - \phi_p(\underset{\sim}{R}, \{\zeta_q(\underset{\sim}{R}')\}) \qquad \text{(III-D-3)}$$

where $\{\zeta_q(\underset{\sim}{R}')\}$ again represents the distribution of EMP over sites other than $\underset{\sim}{R}$.

For analysis of the martensite transformation, it is useful to write the thermoelastic potential in a compact form. Let the transformation occur in a body which is finite, though it may be arbitrarily large. If the body is finite the possible distributions of EMP over its lattice sites are denumerable, and may be designated by assigning to each a particular value of a single index, say α. The thermoelastic potential may then be written

$$\phi_\alpha^{pk} = \phi_p(\underset{\sim}{R}_k, \{\zeta_q^\alpha(\underset{\sim}{R}')\}), \qquad \text{(III-D-4)}$$

where the index α assigns specific values to the functions $\{\zeta_q^\alpha(\underset{\sim}{R}')\}$ $(q = 1....\nu)$ and the index k may be used to designate a lattice site $(\underset{\sim}{R}_k)$ since the lattice sites are denumerable.

E. The Path and Kinetics of the Martensite Transformation.

A phase transformation may be described by specifying its path, or the sequence of intermediate microstructures that a body assumes between the time the transformation is initiated and the time it is completed. In the present case the transformation is a martensitic transition which is to be represented by the stepwise addition of elementary martensite particles (EMP) to the lattice. The specific path of the transformation is specified by giving the sequence of distinguishable configurations $\left\{\zeta_q^\alpha(\underset{\sim}{R})\right\}$ which are adopted by the body as the transformation proceeds. If the configurations are numbered in the order of their appearance, and if the transformation is assumed to occur in unit steps which involve the creation or annihilation of single EMP, then each configuration is related to its predecessor by the simple addition

$$\left\{\zeta_q^{\alpha+1}(\underset{\sim}{R})\right\} = \left\{\zeta_q^\alpha(\underset{\sim}{R}) \pm \delta_{RR'}^{qp}\right\}, \qquad \text{(III-E-1)}$$

where

$$\delta_{\underset{\sim}{R}\underset{\sim}{R}'}^{qp} = \delta_{qp}\ \delta_{\underset{\sim}{R}\underset{\sim}{R}'} \qquad \text{(III-E-2)}$$

If the sign in equation III-E-1 is positive, the transformation step is the addition of an EMP of type p at $\underset{\sim}{R}'$ to $\left\{\zeta_q^\alpha(R)\right\}$; a negative sign has the meaning that this EMP is eliminated from $\left\{\zeta_q^\alpha(\underset{\sim}{R})\right\}$ by reverse transformation.

Given a configuration $\left\{\zeta_q^\alpha(\underset{\sim}{R})\right\}$, the set of possible events connecting it to the succeeding configuration $\left\{\zeta_q^{\alpha+1}(\underset{\sim}{R})\right\}$ contains the creation of an EMP of type p (=1, ...ν) in any lattice cell $\underset{\sim}{R}$, which is free of martensite, and the annihilation of any of the existing EMP. The free energy changes associated with each of these events may be simply

expressed in terms of the appropriate thermoelastic potentials:

$$\Delta G_\alpha^{kq} = \begin{cases} \phi_\alpha^{kq} & \text{if } \zeta_q(\underset{\sim}{R}_k) = 0, \quad q = 1,\ldots.\nu \\ -\phi_\alpha^{kq} & \text{if } \zeta_q^\alpha(\underset{\sim}{R}_k) = 1. \end{cases} \tag{III-E-3}$$

All other ΔG_α^{kq} correspond to impossible processes and are undefined.

The thermodynamic stability of the configuration $\left\{\zeta_q^\alpha(\underset{\sim}{R})\right\}$ is determined by the minimum value of the ΔG_α^{kq}. Let

$$\Delta G_\alpha = \min\ (\Delta G_\alpha^{kq}) \tag{III-E-4}$$

If $\Delta G_\alpha < 0$ then there is at least one elementary change of $\left\{\zeta_q^\alpha(\underset{\sim}{R})\right\}$ which will lead to a decrease in the free energy; hence $\left\{\zeta_q^\alpha(\underset{\sim}{R})\right\}$ is thermodynamically unstable. If $\Delta G_\alpha > 0$ then every elementary change in $\left\{\zeta_q^\alpha(\underset{\sim}{R})\right\}$ leads to an increase in the free energy, and $\left\{\zeta_q^\alpha(\underset{\sim}{R})\right\}$ is at least metastable.

The kinetics of the transformation will be governed, at least in part, by the statistics of thermal activation. The formation of an EMP through a thermally activated process will generally be opposed by an activation barrier of height Δg^*. Making the usual assumption that the barrier is maximal at the point of half-completion of the elementary event, it follows that the total activation barrier opposing the event (k,q) is

$$\Delta G_\alpha^{*kq} = \begin{cases} \frac{1}{2}\ \Delta G_\alpha^{kq} + \Delta g^* & \text{if } \Delta g^* > \Delta G_\alpha^{kq} \\ \Delta G_\alpha^{kq} & \text{otherwise} \end{cases} \tag{III-E-5}$$

where ΔG_α^{*kq} is defined only for possible events. Of course, the activation energy, Δg^*, need not be the same for all events; in particular, the activation energy for creation of an EMP may differ from that for

annihilation.

The kinetic stability of the configuration $\left\{\zeta_q^\alpha(\underset{\sim}{R})\right\}$ is determined by the minimum of the activation energy ΔG_α^{*kq}. Let

$$\Delta G_\alpha^* = \min\ (\Delta G_\alpha^{*kq}) \qquad \text{(III-E-6)}$$

When Δg^* is the same for all events

$$\Delta G_\alpha^* = \frac{1}{2}\ (\Delta G_\alpha - 2\ \Delta g^*). \qquad \text{(III-E-7)}$$

If $\Delta G_\alpha^* > 0$ then every elementary change in $\left\{\zeta_q^\alpha(\underset{\sim}{R})\right\}$ is opposed by a finite activation barrier and requires a thermal fluctuation in order to happen. Such a configuration will be termed kinetically stable in the sense that it can be maintained by forbidding positive fluctuations in the energy. On the other hand, if $\Delta G_\alpha^* < 0$ then there is at least one elementary event which represents a thermodynamic instability of $\left\{\zeta_q^\alpha(\underset{\sim}{R})\right\}$ (since $\Delta G_\alpha < 0$ if ΔG_α^* is) and which is unopposed by an activation barrier. This event will occur spontaneously even in the absence of thermal fluctuation. The configuration $\left\{\zeta_q^\alpha(\underset{\sim}{R})\right\}$ is hence kinetically unstable.

The analysis of the kinetics of transformation through kinetically unstable configurations poses problems which are beyond the scope of the present investigation and which have their source in the finite speed of sound in real crystals. The theory leading to the definition and evaluation of the free energy change ΔG_α is based on equations which assume static elastic equilibrium. But, if an elementary transformation occurs at a point $(\underset{\sim}{R})$ within a crystal, the associated elastic disturbance propagates only at the speed of sound (c). It will not be sensed at a point R' until after a time interval $\Delta t \sim \frac{|\Delta \underset{\sim}{R}|}{c}$, and the modified static equilibrium state cannot be assumed until several of these time intervals

have passed. The kinetics of transformations which evolve at speeds near that of sound are strictly bound beyond the scope of a static equilibrium model.

However, an error in the precise kinetics of unstable events is of no great concern so long as the sequence of these events is reasonably well represented. In the time frame which is usally of interest in the kinetics of phase transformations, the distinction between a process which happens at sound speed and one which happens instantaneously is immaterial. The sensible kinetics of the phase transformation are controlled by those configurations along the transformation path which are kinetically stable, and which, consequently, require either finite time or additional undercooling before they transform. The nature of the kinetically stable configurations which are reached along the transformation path may depend on the sequence in which unstable configurations are sampled, but does not depend on the kinetics of their evolution.

Given this analysis, we shall represent the martensite transformation by model which ignores the finite speed of sound and assumes that elastic equilibrium is instantaneously reestablished after each elementary event. The resulting kinetic equations will give a good estimate for the transformation rate provided that the model is reasonably successful in selecting the intermediate configurations along the transformation path.

(1) Statistics of Thermal Activation

The kinetics of a martensite transformation which occurs through the thermally activated formation or annihilation of elementary martensite particles may now be developed. The treatment follows that in reference (64) for a formally similar, though physically distinct problem.

Let the transforming crystal have the configuration $\left\{\zeta_q^\alpha(\underset{\sim}{R})\right\}$ which may be changed by adding the EMP $(p,\underset{\sim}{R})$ at any untransformed site $\underset{\sim}{R}$ or by eliminating any EMP $(q,\underset{\sim}{R})$ which is present in $\left\{\zeta_q^\alpha\underset{\sim}{R})\right\}$. Let the attempts at each of these events be uncorrelated and random in time with mean frequency ν_o.

An attempt to achieve event $(q, \underset{\sim}{R}_k)$ has two possible outcomes: a success, which would require overcoming the activation barrier ΔG_α^{*kq} defined in equation (III-E-5) or a failure, for which the activation barrier is zero. If the temperature is T (written in energy units, kT, for simplicity) the normalized probability for the event $(q,\underset{\sim}{R}_k)$ in one attempt is

$$p_\alpha^{kq} = \exp\ (-\beta\Delta G_\alpha^{*kq})/[1 + \exp(-\beta\Delta G_\alpha^{*kq})]$$
$$= [1 + \exp\ (\beta\Delta G^{*kq})]^{-1} \qquad \text{(III-E-8)}$$

where

$$\beta = 1/T \qquad \text{(III-E-9)}$$

The probability $[R_\alpha^{kq}(j)]$ that $(q,\underset{\sim}{R}_k)$ has not happened after j trials is

$$R_\alpha^{kq}(j) = (1 - p_\alpha^{kq})^j \qquad \text{(III-E-10)}$$

If the activation trials occur randomly in time with expectation one per unit of dimensionless time

$$t^* = \nu_o t \qquad \text{(III-E-11)}$$

then the probability of exactly j trials in time t^*, $p(j,t^*)$ is

$$p(j,t^*) = \frac{(t^*)^J}{j!} \exp\ (-t^*) \qquad \text{(III-E-12)}$$

and the probability that no success has been achieved in time t^* is

$$R_\alpha^{kq}(t^*) = \sum_{j=o}^{\infty} (j!)^{-1} (t^*)^j \exp(-t^*) (1 - p_\alpha^{kq})^j \qquad \text{(III-E-13)}$$

$$= \exp(-p_\alpha^{kq} t^*).$$

The configuration of EMP will be changed if any one of the possible elementary events occurs. Hence, the probability $P_\alpha(t^*)$ that the configuration $\left\{\zeta_q^\alpha(\underset{\sim}{R})\right\}$ is retained for a time greater than t^* is equal to the probability that no elementary event happens in time t^*:

$$P_\alpha(t^*) = \prod_{kq} R_\alpha^{kq}(t^*) = \exp(-P_\alpha t^*) \qquad \text{(III-E-14)}$$

where the product is taken over all possible events and

$$P_\alpha = \sum_{kq} P_\alpha^{kq}, \qquad \text{(III-E-15)}$$

the sum of the probabilities of all possible events. It follows that the probability $P_\alpha(t^*)dt^*$ that the configuration transforms in the time interval $(t^*, t^* + dt^*)$ is

$$P_\alpha(t^*)dt^* = -\frac{\partial}{\partial t^*}\left[\exp(-p_\alpha t^*)\right] dt^*. \qquad \text{(III-E-16)}$$

The expected lifetime of configuration α is hence

$$\langle t^* \rangle = \int_o^\infty t^* p_\alpha(t^*)\, dt^*$$

$$= (P_\alpha)^{-1}, \qquad \text{(III-E-17)}$$

and its variance is

$$\sigma_\alpha^2 = \langle t_\alpha^{*2} \rangle - \langle t_\alpha^* \rangle^2 = P_\alpha^{-2}$$

$$= \langle t^* \rangle^2 \qquad \text{(III-E-18)}$$

Equations (III-E-16) and (III-E-17) give the mean and variance of the time required for the first elementary transformation to happen from the configuration $\left\{\zeta_q^\alpha(\underset{\sim}{R})\right\}$, irrespective of its identity. The probability $p(q,k)$ that the specific event $(q,\underset{\sim}{R}_k)$ is the first to occur may be easily shown to be

$$p(q,k) = p_\alpha^{kq}/P_\alpha \qquad \text{(III-E-19)}$$

as would be expected intuitively.

Equations III-E-17 to III-E-19 give the activation time, variance, and site for evolution of the configuration, $\left\{\zeta_q^\alpha(\underset{\sim}{R})\right\}$. They are expressed in terms of the set of probabilities p_α^{kq}, defined in equation III-E-8, which can be computed from a knowledge of the thermoelastic potentials and activation energies for each of the possible elementary transitions from $\left\{\zeta_q^\alpha(\underset{\sim}{R})\right\}$ via equations III-E-3 and III-E-5. It is important to recognize that under the assumptions we have made, particularly the assumption of instantaneous equilibrium, the probabilities p_α^{kq} are fixed by the current configuration and are not influenced by the prior transformation path.

(2) The Statistical Transformation Path and Transformation Time

The statistics of the martensite transformation are complicated by the fact that, except under very restrictive assumptions, the sequence of configurations assumed during the transformation (the transformation path) is not unique. Given finite temperature and activation energy any one of the elementary processes permitted by the instantaneous configuration of the transforming body is possible. The sequence of subsequent configurations will generally depend on the specific event which occurs. The problem is, however, somewhat simplified by the fact that the

configurations assumed during the transformation form an irreducible Markov chain.[64]

The Markovian character of the transformation path follows immediately from the fact, emphasized at the end of the previous subsection, that the probabilities of all possible elementary transformation steps are uniquely determined by the current configuration of the EMP. If the αth configuration is $\left\{\zeta_q^{\alpha}(\underset{\sim}{R})\right\}$ then the $(\alpha+1)^{th}$ configuration is determined by the particular event $(p,\underset{\sim}{R}_k)$ which continues the transformation from step α. Since the probability that $(p,\underset{\sim}{R}_k)$ will occur at step α is uniquely fixed by $\left\{\zeta_q^{\alpha}(\underset{\sim}{R})\right\}$ then the probability that a particular configuration will be the $(\alpha+1)^{th}$ member of the chain is fixed once $\left\{\zeta_q^{\alpha}(\underset{\sim}{R})\right\}$ is known, independent of previous events. Hence, the transformation path is Markovian.

The irreducible character of the Markov chain follows so long as the transformation can be assumed to go to completion in a number of steps which is less than some finite upper bound, where completion is defined as the first realization of a configuration having EMP at all lattice sites. There are, then, a finite number of possible transformation paths, which may be labelled by the index, χ, and a finite number of distinguishable configurations, which may be labelled by the index, α'. The elements of the set of all distinguishable configurations $\left\{\alpha'\right\}$ form an irreducible chain since any given configuration of EMP may be created by adding EMP to an empty lattice, and, hence, may lie along the transformation path.

It follows from the property of irreducible Markov chains that the probability, μ_χ, that the transformation takes path χ is defined and that $\sum_\chi \mu_\chi = 1$ (III-E-20)

The probability $\mu_{\alpha'}$ that the transformation passes through the particular configuration α' is just the sum of μ_χ over all paths which contain α',

$$\mu_{\alpha'} = \sum_{\alpha' \in \chi} \mu_\chi, \tag{III-E-21}$$

and

$$n = \sum_{\alpha'} \mu_{\alpha'} \tag{III-E-22}$$

is the expected number of configurations assumed. Both $\mu_{\alpha'}$ and μ_χ will, of course, be rather complex functions of temperature.

Let the transformation follow a particular path, χ, which has n configurations whose activation parameters are $P_\alpha (\alpha=1,\ldots,n)$. Using the properties of Markov chains it may be shown[63] that the expected value of the time required for the transformation is

$$\langle t^*_\chi \rangle = \sum_{\alpha=1}^{n} \langle t^*_\alpha \rangle = \sum_{\alpha=1}^{n} (P_\alpha)^{-1} \tag{III-E-23}$$

and that variance, σ^2_χ, of t^*_χ is

$$\sigma^2_\chi = \sum_{\alpha=1}^{n} \sigma^2_\alpha = \sum_{\alpha=1}^{n} (P_\alpha)^{-2}. \tag{III-E-24}$$

More specifically, if n is large the distribution of the transformation times, t^*_χ, approaches a normal distribution with the density function

$$\rho(t^*) = (12\pi\sigma^2_\chi)^{-\frac{1}{2}} \exp \frac{\left[- (t^*_\chi - \langle t^*_\chi \rangle)^2 \right]}{\alpha\sigma^2_\chi} \tag{III-E-25}$$

giving the probability that the time required to complete the transformation lies in the range $(t^*, t + dt^*)$.

F. The Minimum-Energy Path

The analysis of the preceding section reduces the problem of determining the kinetics of the phase transformation to the problem of determining the sequence of configurations assumed as the transformation proceeds. Even with the help of computer simulation, however, this problem remains formidable in the analysis of a transformation which occurs at finite temperature. The transformation path will be determined by what amounts to a random walk over the set of possible configurations. Particulary if there are metastable intermediate states during the transformation, the transformation may not go at all monotonically toward completion, but rather oscillate for long periods of time before making a net positive step.

To construct a tractable treatment of the phase transformation, it is useful to have a representation of the transformation path which is both reasonably accurate and relatively simple to analyze. The obvious choice is the minimum-energy path, which is the path found if at each step of the transformation the transformation progresses in a way which minimizes the total activation energy.

An examination of the equations in the preceding section will show that at each step of the transformation that event which involves the least value of the activation energy is most likely to happen, and is also least likely to be reversed by back-transformation in the following step. Hence, while the transformation may take many paths, there will be a tendency for it to follow the path which progresses toward completion through those steps which involve the minimum activation energy. This tendency will become increasingly strong as the temperature goes down.

A simple way to locate the minimum-energy path in computer simulation, which will be used in the following, is to assume that the transformation cannot reverse itself, that is, that it goes monotonically to completion, and to choose each transformation step so that the incremental energy is as low as possible. If we rule out the possibility of reverse transformations, then the computation of transformation kinetics along the minimum-energy path is straightforward and simple. In the more realistic case in which reverse transformation is allowed the kinetics may be approximated by using equations analogous to diffusion through random-walk processes, in which the kinetic consequences of the reverse transformation are gathered into a "correlation factor".

Specification to the minimum-energy path defines the particular sequence of configurations $\alpha = 1, \ldots, n$ assumed as the reaction goes to completion. This particular sequence of configurations may be readily found through computer simulation of the transformation, as is done, for example, in the following sections.

The predicted kinetics of transformation along the minimum-energy path depend on the assumed reversibility of the transformation. If the transformation is assumed to be irreversible, but is confined to the minimum-energy path then the time required for the αth step is

$$\langle t_\alpha \rangle = 1 + \exp\,(\beta \Delta G^*_\alpha), \qquad \text{(III-E-26)}$$

where ΔG^*_α is defined in the previous section. If the transformation is assumed to be reversible, but biased in the forward direction by the chemical driving force, $\Delta\mu$, then a first approximation to the net rate of forward progress may be phrased as follows:

If the body has the αth configuration along the transformation path

then the probability that the body will move to the $(\alpha+1)^{st}$ configuration in a single attempt is

$$P_\alpha = (1 + \exp(\beta\Delta G^*_\alpha))^{-1} \qquad \text{(III-E-27)}$$

To obtain the net probability for forward progres the probability P_α must be weighted by the probability $P_{\alpha'}$ that the transformation will not subsequently reverse itself to regenerate the configuration α. Since the body may perform a rather complicated random walk along the transformation path before regenerating the configuration α, $P_{\alpha'}$ will be difficult to compute exactly. If the thermodynamic driving force $N_o\Delta\mu$ is large and negative, however, it is unlikely that the body will return to from configurations $\alpha + \alpha'$ where α' is large.

As a first approximation, we account for returns to α from $\alpha+1$, but ignore returns from $\alpha+\alpha'$ when $\alpha' > 1$. The probability $P_{\alpha'}$ is then approximated by the probability that the configuration $\alpha+1$ will evolve to $\alpha+2$ before reverting to α, or:

$$P_{\alpha'} \simeq \exp(-\beta\Delta G^*_{\alpha+1}) / \left[\exp(-\beta\Delta G^*_{\alpha+1}) + \exp(\beta\Delta G^*_\alpha)\right]$$
$$= \left[1 + \exp\beta(\Delta G^*_\alpha + \Delta G^*_{\alpha+1})\right]^{-1} \qquad \text{(III-E-28)}$$

It follows that the net probability for forward progress, P^+_α, is

$$P^+_\alpha \simeq \left[1 + \exp(\beta\Delta G^*_\alpha)\right]^{-1} \left[1 + \exp\beta(\Delta G^*_\alpha + \Delta G^*_{\alpha+1})\right]^{-1} \qquad \text{(III-E-29)}$$

giving the net activation time

$$\langle t^+_\alpha \rangle = (P^+_\alpha)^{-1}$$
$$\approx \exp \beta\left[2\Delta G^*_\alpha + \Delta G^*_{\alpha+1}\right] \qquad \text{(III-E-30)}$$

when $\Delta G^*_\alpha >> \beta$ and $(\Delta G^*_\alpha + \Delta G^*_{\alpha+1}) > 0$.

As $T \to 0$ ($\beta \to \infty$) the probability of transition approaches one for $\Delta G_\alpha^* < 0$ and zero for $\Delta G_\alpha^* > 0$.

IV. COMPUTER SIMULATION OF MARTENSITIC TRANSFORMATION

Before presenting the results of computer simulation of the martensite transformation, we briefly recapitulate the more important features of the model employed.

The computer simulation of the martensite transformation in 3-dimensions requires the employment of three kinds of EMP whose tetragonal axes (or Bain axes) lie along the [100], [010] and [001] directions of the cubic parent phase respectively. For a reasonably large crystal, the calculations will take considerable computer time. The resulting structure inside the 3-dimensional volume of the parent phase cannot be displayed with the same clarity and simplicity as the structure in the 2-dimensional case. The latter can be presented simply on a sheet of paper.

On the other hand, the main pecularities of the martensitic transformation appear in a 2-dimensional model as well as in a 3-dimensional one. We have, therefore, chosen a 2-dimensional model for the initial computer simulation studies.

In the specific model used below the crystal is assumed to be a pseudo 2-dimensional body, in that each point in its plane represents a line extending to infinity in either direction. The 2-dimensional crystal is represented by a square grid of points, forty on a side, in a square array. Each point represents an EMP of the type discussed in the previous section. The array is assumed to be periodic across each of its boundaries.

The array initially consists of elementary volumes of the parent phase together with one or more defects which may serve as heterogeneous nucleation sites for the martensite transformation. For simplicity,

and since we are interested in the growth of martensite rather than in the details of its nucleation, these initial defects are modeled as elementary volumes of the martensite phase.

The martensite transformation is assumed to involve a Bain strain in two dimensions: a contraction along one of the axes together with an expansion along the other axis of the grid (See Figure 5). In most of the cases reported below, the Bain strain is assumed to involve no dilatation; the transformation strain is therefore a pure shear. The two variants of the stress-free distortion are then described by the two tensors

$$\varepsilon^{o}_{ij}\ (1) = \varepsilon^{o} \begin{pmatrix} 1 & 0 \\ 0 & \bar{1} \end{pmatrix} \qquad \varepsilon^{o}_{ij}\ (2) = \varepsilon^{o} \begin{pmatrix} \bar{1} & 0 \\ 0 & 1 \end{pmatrix} \qquad \text{(IV-1)}$$

where ε^{o} is the magnitude of the shear.

Elementary volumes of the martensite phase (EMP) interact with one another through elastic interactions as discussed in the previous section. The calculation of the invariant plane in three dimensions was described in Section II-A. The orientation of the invariant plane, which corresponds to the plane with minimum lattice mismatch, can also be calculated for the two dimensional case. When the transformation strain is a pure shear, the invariant planes are found to be (11) and $(1\bar{1})$.

The martensitic transformation is assumed to occur through the discrete formation of elementary volumes of the martensitic phase (EMP). The net energy change on introduction of an EMP is the sum of three terms: a chemical energy, which is described in the previous section and is assumed to depend linearly on the undercooling, ΔT; an elastic self energy, which is equal to the elastic energy required to accomplish

the Bain strain; and an elastic relaxation term which was derived in the previous section and includes the elastic two-body interaction with all other particles which are present.

The thermoelastic potential $\phi_p(\underset{\sim}{R})$ is calculated by the computer in accordance with the equation (III-D-2) applied for the 2-dimensional case, for all sites $\underset{\sim}{R}$ of the grid and for p = 1 or 2, corresponding to the two possible variants of the EMP. The code employs the stress-free strains (IV-1) and carries out the integration over $\underset{\sim}{k}$ in equation (III-B-18). Figure 6 shows a 3-dimensional plot of potential $\phi_p(\underset{\sim}{R})$ at every site, $\underset{\sim}{R}$, for a configuration, α, which contains a single type p EMP on the center of the net, in the case of elastic isotropy. The potential field varies dramatically with direction near the EMP. The absolute value of $\phi_p(\underset{\sim}{R})$ decreases quickly, approximately as $1/R^2$.

Since the surface energy, which includes the martensite-austenite interphase energy and the interplane energy for the martensite transformation, is much less than the elastic strain energy, we neglect the surface energy term in equation (III-D-2).

For each configuration formed by EMPs, the computer calculates all local potentials $\phi_p(\underset{\sim}{R})$ for every point $\underset{\sim}{R}$ on the net and for both values of p, finds the $\phi_p^o(\underset{\sim}{R}) = \min \phi_p(\underset{\sim}{R})$ and, if $\phi_p^o(\underset{\sim}{R})$ is negative, creates a new EMP of the kind of P_o at the point $\underset{\sim}{R}_o$. Therefore $\phi_p^o(\underset{\sim}{R})$ is the 'quantum' of the free energy, i.e., the elementary martensite formation energy (EMFE) of one EMP at $\underset{\sim}{R}_o$. In all cases discussed below, the energies are in the unit of $\mu\varepsilon_o^2 V$, where μ is the shear modulus, ε_o is the amount of transformation strain, and V is the volume of one EMP. The local potential $\phi_p(\underset{\sim}{R})$ is the sum of the terms $\Delta\phi_{ch}$, the chemical energy term and $\Delta\phi_{el}(\underset{\sim}{R})$, the elastic energy term. As in eq. (III-C-7), the

chemical energy $\Delta\phi_{ch}$ is proportional to the amount of supercooling $\Delta T = T - T_o$, which is expressed in units of $V\mu\varepsilon_o^2 T_o / N_o \Delta h$. $\Delta\phi_{ch}$ is constant over all lattice sites while $\Delta\phi_{el}(R)$ varies. For convenience, we define the Elementary Martensite Elastic Energy (EMEE) for each cycle during the transformation process where

$$\text{EMEE} = \text{EMFE} - \phi_{ch} \qquad \text{(IV-2)}$$

The energy EMEE is also given in units of $\mu\varepsilon_o^2 V$ in the following.

To establish the kinetics and path of the transformation in these initial experiments, the transformation is assumed to follow the deterministic minimum emergy path in the limit of low temperature. This transformation path is defined by the dual requirements that transformation can only occur if the energy associated with the formation of an additional particle is negative, and that, if several such particles are possible, that having the lowest energy will be the one formed. The transformation hence occurs so as to maximize the energy decrease per elementary step and only occurs if the incremental energy change is negative.

As should be clear from the preceding section, most of the more restricitive assumptions cited above can be relaxed within the context of the model. Some exploratory experiments in these directions have already been carried out. However, the work associated with this thesis has focused on the attempt to gain a fuller understanding of the simplest possible case, which appears to be that cited above.

V. COMPUTER SIMULATION RESULTS

A. The Single Nucleus Case

The simplest case of the transformation os that in which the two-dimensional body is elastically isotropic, initially contains only a single nucleating defect, and transforms via a Bain strain which is a simple shear. The starting point for this case is shown in Fig. 7-1. The subsequent development of the microstructure is illustrated in the other figures presented in Fig. 7. The companion Fig. 8 shows the incremental change in the elastic relaxation energy for the first 800 steps of the martensitic transformation. The companion Fig. 9 plots the average of the elastic energy per martensite particle for the first 400 transformation steps.

Referring to the microstructural sequence shown in Fig. 7, it will be seen that the martensite transformation begins from its single nucleus as a three-layer twinned plate along the (11) habit, which may be easily seen to be the preferred habit plane for the growth of the martensite plate in the case in which the Bain strain is a simple shear. The reason for the three-layer initial thickness may be readily seen from Fig. 7-4. The first three elementary martensite particles which develop from the initial nucleus position themselves so as to form a closed box, the sum of whose tetragonal distortions is zero. This configuration minimizes but does not eliminate the elastic energy. As discussed in previous sections, the elastic energy is always minimal for the morphology of a thin plate. The box shown in Fig. 7-4 hence tends to extend itself into a thin plate along the (11) plane. Since the box occupies three parallel (11) planes in its initial configuration, the initial plate is three planes in thickness. An intermediate configura-

tion in the development of the three-layer plate is shown in Fig. 7-5, 7-6.

The plate extends throughout the periodic array until it finally closes on itself, as shown in Fig. 7-6.

The incremental elastic energy associated with the growth of the three-layer plate is shown in the first segment of Fig. 8. The regular oscillation of the incremental elastic energy during growth of the three-layer plate is evident. When the plate eventually closes on itself, at the 120th cycle, a situation of invariant plane strain is created. There is essentially no elastic driving force for further growth of the plate, and the additional transformation would involve a rather high elastic energy as shown in Fig. 8.

The gradual decrease of the elastic energy during growth of the three-layer initial plate is perhaps even more evident in Fig. 9, which shows the average elastic energy per martensite particle. As is apparent from the figure the elastic energy is initially high and decreases dramatically towards zero as the three-layer plate develops. On the closure of this plate, at the 120th cycle, the elastic energy becomes essentially equal to zero.

Once the initial three-plane plate has completed itself, the residual interaction terms almost vanish and there is, therefore, very little elastic driving force to continue the martensitic transformation. It is apparent from the graphs shown in Figs. 8 and 9 that the transformation of particles to continue the transformation requires a very high elastic energy, and would consequently require a rather large chemical driving force as might be achieved through severe undercooling. The details of the two-body elastic interaction do, however, create a

slight bias for additional transformation to occur at a particular point in the microstructure. As shown in Fig. 7-7 and 8, this slight bias causes the martensite plate to thicken on further transformation by the addition of a two-layer twin plate that spreads along the surface of the pre-existing martensite plate. The plate hence thickens by what in usual metallurgical terminology is known as a ledge growth mechanism. The two-layer twin nucleates and spreads to completion along the surface of the pre-existing plate, giving finally a five-layer internally twinned plate. At this point the transformed region again consists of an infinite plate along the habit plane, and the average value of the elastic energy per martensite particle is again almost identically zero as shown in Fig. 8 at the 200 cycle point.

Following completion of the five-layer plate it is again necessary to nucleate a new plate under a situation requiring a rather high activation energy. Again the details of the two-body interaction create a small but finite bias for further transformation to initiate at a particular point within the lattice. The resulting nucleation is shown in Fig. 7-9 and differs from the previous nucleation event in that this time the preferred site for the nucleus is spatially separate from the pre-existing plate. As shown in the subsequent figures this nucleated plate develops into a three-layer martensite plate that grows in parallel to the pre-existing plate leaving a layer of retained austenite in the interim. Interestingly, as can be seen in Fig. 7-10, the growing plate is, in aggregate, twin related to the initial martensite plate.

The reason for the spatial separation between the parent and the autocatalytically nucleated plates appears to derive from the particular shape of the two-body elastic interaction, as diagrammed in Fig. 6

The two-body elastic interaction has a weakly oscillating tail, which, if it is constructively reinforced by the overlapping interactions from properly configured plates, can introduce a bias for the formation of martensite particles at some distance from the pre-existing particles. The weak oscillation of the long range interaction is in this particular case a consequence of the periodic boundary condition and hence may be a spurious feature of the model. It is, however, interesting that the transformation through formation of crystallographically-related martensite variants at some distance from the initial martensite plate is a not uncommon experimental feature of the martensitic transformation[68].

As shown in Fig. 8 the incremental energy pattern following autocatalytic nucleation of the second three-layer plate is essentially identical to that for the development of the original three-layer plate. As shown in Fig. 9 the average value of the elastic energy increases slightly during the growth of this plate and returns to zero when the plate development is completed at the 320th cycle.

The remainder of this martensitic transformation essentially repeats the features we have already seen. Following the growth to completion of each twinned plate the elastic energy returns to a value very close to zero and a new nucleation event is required in order to continue the transformation. Depending on the precise configuration of the martensite particles the preferred site for this nucleation event may be on the surface of an existing plate, in which case the plate thickens by a ledge growth mechanism with the ledge being a two-layer twin plate, or the preferred nucleation site may be spatially separated from any of the pre-existing plates, in which case the growth of a new three-layer plate is autocatalytically triggered. Some elements of this process are

apparent in the energy curves presented in Figures 8 and 9.

The thermal characteristics of the martensite transformation from a single nucleus are relatively uninteresting. A finite supercooling, of approximately 0.3 in energy units is required to start the transformation on its way. Following the growth to completion of the initial plate, an additional supercooling of approximately 0.3 energy units is required to continue the transformation. The sum of these undercoolings, 0.6, is nearly equal to the chemical driving force required to balance the elastic self energy of the martensite particle in the absence of any favorable interaction terms. Once this undercooling has been established a transformation will continue to completion along the energy path shown. Hence, as a function of temperature the transformation contains only two steps: a first step which causes the initial nucleus to develop into a full plate along the habit plane, and a second step at a much more substantial undercooling, which completes the transformation of the body.

B. Multi-Nuclei Transformations

To simulate a wider range of interesting features of the martensite transformation, it is necessary to assume that multiple nuclei are present within the periodic forty by forty cell of initial volumes. The presence of the distribution of nucleating defects serves two functions: it helps to eliminate the effect of the periodic boundary conditions, and it strongly influences the character of the martensite transformation.

The specific example that we shall discuss begins from ten initial martensite embryos which are randomly distributed over the forty by forty grid. Again, the strain is assumed to be a pure shear (no dilatation), the

the matrix elastic constants are assumed isotropic, and the transformation path is taken to be the deterministic (low temperature limit) one by one transformation path, in which the transformation proceeds if and only if it is possible to form a particle which decreases the energy of the system, and the transforming particle is chosen from among the admissable events so as to provide the maximum energy decrease.

The particular example discussed here has been used to create a computer movie of the martensite transformation, which is in fact rather more informative than the following discussion, based on a limited number of figures, is likely to be.

The transformation is represented in the composite Figures 10, 11 and 12. Figure 10 shows the variation of the martensite fraction with undercooling, with the temperature measured in energy units. The composite Figure 11 shows the transformation through the successive stages of its development in the microstructure. The two variants of martensite are again represented by horizontal and vertical lines and the parent austenite is represented by open squares. The example microstructures are chosen to emphasize the stages of the transformation at which the undercooling would have to be increased in order to maintain the process. The composite Figure 12 plots the energy change associated with each successive elementary transformation. The horizontal lines in these figures show the chemical driving force, and hence the undercooling which is necessary to maintain the transformation at the stage in question. The oscillating line shows the total elastic energy involved in each elementary transformation event. The driving force, or undercooling required is simply that necessary to insure that the total energy is negative for every preceding transformation event.

As discussed earlier the elastic self energy for the formation of a martensite particle in the periodic array is large and positive, 0.6447 in dimensionless energy units. If there were no relaxation due to interaction with other inhomogeneous defects the self energy would have to be provided by the chemical driving force of the transformation, requiring an undercooling equivalent to 0.6447. However in the presence of the distribution of initial defects shown in Figure 11-1 the required driving force is much smaller. The total elastic energy change involved on the addition one elementary martensite particle in the most favorable site (Figure 11-2) is 0.09, and only this supercooling, approximately 1/7th of that required for the homogeneous nucleation of martensite, need be established to initiate the transformation.

As shown in Figure 10 the martensitic transformation is initiated at an undercooling of 0.09, which defines the M_s temperature for this particular example, and the initiated transformation proceeds by some finite amount before coming to a halt. The nucleation site shows that it lies in the vicinity of two preexisting defects, which are so configured that they are naturally incorporated in a two layer twinned martensite plate extending from one to the other. At an undercooling of 0.09 this two layer twin plate nucleates and begins to propagate rapidly through the array. Its growth is illustrated in Figures 11-1 through 11-7. As can be seen from Figure 12-1, the elastic energy change per elementary event during the growth of this twinned plate is small and oscillates about zero. This situation maintains until the twinned plate almost closes on itself (Figure 11-7) at which point the transformation ceases abruptly. Reference to Figure 12 shows that the continuation of the transformation beyond the point shown in Figure 11-7 would involve

an elastic energy exceeding the chemical driving force; the transformation can, therefore, proceed only if the temperature is lowered further. Examination of Figure 11-7 indicates the source of the transformation arrest: the twin plate is trying to grow through a region of the crystal that contains pre-existing defects whose strain fields interfere with and oppose the continued growth of the plate.

The development of this initial martensite plate as pictured in Figures 11-1 through 11-7 illustrates the dual role played by pre-existing defects. In favorable configuration these defects act as preferential nucleation sites to initiate and promote the martensite transformation. The defect distribution is also, however, responsible for the energetic barrier that forces the transformation to stop, and necessitates a continual increase in the undercooling if the transformation is to be maintained.

On a slight lowering of the temperature the transformation is restarted and proceeds ultimately through the nucleation and growth of a short plate that is in a branching orientation to the original twinned martensite plate (Figs. 11-10 through 11-12). The development of this plate is again stopped by its impingement on the strain field of pre-existing embryos, Fig. 11-12. A further decrease of the temperature, to an undercooling of 0.1375, Fig. 12-1, is required to trigger a significant additional transformation, that is shown in Figs. 11-14 to 11-17. It will be noted from Fig. 12-1 (Cycles 100 to 144) that during the growth of this new plate, the incremental elastic energy continues to oscillate about 0. The increased undercooling is only necessary to overcome specific barriers which bring the transformation to a halt.

Several further drops of temperature are necessary after cycle 146

to maintain the transformation; they correspond to the formation of new plates and the thickening of the initial plate (Figure 11-18) until cycle 229 (Figure 11-21). The increase in the energy required to sustain the transformation during the impingement process is clear from Figure 12.

At this stage of the transformation, the temperature must be lowered still further to an undercooling of 0.27 to continue the process. The next nucleation event is the activation of a pre-existing defect which is spatially separated from the part of the microstructure which is already transformed. Once this nucleus is activated the propagation of an associated plate is energetically quite easy and fast (Figure 11-26, 27). At the completion of the growth of this plate, other events are triggered at the same driving force. The transformation proceeds at this value of the undercooling for 663 steps. The transformation involves the thickening of the martensite plates and the transformation of the space between plates, as illustrated in Figures 11-28 through 11-33. The relatively high amplitude oscillation of the energy change from cycles 980 to 1170, shown in Figure 12-3, corresponds to the formation of the thick twinned plate which fills up the space between two widely separated transformed plates Figs. 11-(33-36). At the completion of the transformation permitted at this value of the undercooling, the martensitic transformation is much more than 50% complete, and the microstructure, illustrated in Figure 11-38 has come to bear a very strong resemblance to that observed in a number of real systems at the approximately 50% transformation point. Discrete internally twin plates are present, they branch along the two variants of the (11) habit plane, and they are separated by regions of retained austenite.

At this point in the transformation, all of the pre-existing defects have been consumed by transformation. The undercooling required to accomplish this transformation is less than one-half of that which would be required to initiate the martensite transformation by a homogeneous nucleation process.

The martensite transformation is brought essentially to completion by an additional lowering of the temperature to an undercooling of 0.355. At this value of the undercooling, further transformation is triggered by the annihilation of a layer of retained phase lying between two martensite plates (Figures 11-39,40). Transformation continues until almost all the crystal lattice sites are transformed. Only fifty-three austenite elementary volumes remain at the completion of this step.

The undercooling $\Delta T = 0.355$, resulting in the microstructure shown in Figure 11-40, may be reasonably regarded as the martensite finish temperature. Very few austenite volumes remain, and, as shown in Figure 12-4, the elimination of these requires a substantial and increasing undercooling. Further transformation is, in fact, only accomplished by a rather substantial undercooling which results in the elimination of the residual austenite particles in almost a step by step process. This retention of an austenite phase which is very difficult to eliminate is a common experimental observation, and is also a natural consequence of the model transformation exhibited here. The complete elimination of the residual austenite requires an undercooling $\Delta T = 0.62$, which is still less than but almost equal to the undercooling required for homogeneous nucleation of the martensite transformation.

Three additional figures have been included, Figures 13 to 15, to

provide other useful illustrations of the energy change during the martensite transformation. Figure 13 shows the average elastic energy per martensite particle during the transformation. At the beginning of the transformation, the elastic energy per particle is high. As the transformation proceeds, the high elastic energy is relaxed and the average elastic energy decreases. The elastic energy ultimately decreases to an average value very close to zero, though it does not quite reach zero because of the irregular arrangement of the elementary martensite particles.

Figure 14 shows the average values of the self energy per particle, including the elastic and chemical energy but excluding the elastic interaction term, and the average total energy per particle during the transformation. The upper curve represents the self energy. Each step in the curve is associated with a decrease in the chemical energy resulting from the decrease in temperature. The self energy is positive definite through the entire transformation, reflecting the very large value of the elastic self energy. Inclusion of the interaction energy, however, has the consequence that the average total energy becomes increasingly negative causing the transformation to proceed in an increasingly favorable manner.

Figure 15 plots the total energy change during the martensite transformation. Again the total value of the self energy is positive and increases with the extent of transformation, while the relaxation term has the consequence that the total energy is negative and decreases as the transformation proceeds. It should be clear from this figure why earlier models of the martensite transformation, which effectively considered only the self energy term, had some difficulty in interpreting

why it is that the martensite transformation occurs spontaneously. The elastic interaction term along the most favorable transformation path, is, in fact, large and negative, and effectively cancels out a substantial part of the high elastic self energy involved in the transformation of the martensite particle.

In summary it should be noted that the model transformation described above reproduces most of the characteristic features of observed martensitic transformations in a simple and intriguing correspondence. The transformation proceeds through the growth of discrete martensite plates which are twinned. In the earlier stages of transformation, these plates are heterogeneously nucleated at pre-existing defects in the lattice. The driving force for the transformation is provided by undercooling, which must be continuously increased to maintain the transformation; the transformation occurs over a range of temperatures between a martensite start and a martensite finish point. Some austenite phase is retained in the microstructure until the undercooling becomes extremely large. As observed experimentally, this austenite phase tends to be retained in thin lamella separating adjacent martensite plates. Finally, the martensite transformation occurs spontaneously on cooling in situations in which the self energy of the martensite particles is large and positive.

C. Variations on the Multi-Nucleus Case

The martensite transformation beginning from ten randomly distributed nuclei which was discussed in detail in the previous subsection is typical of the results obtained when the two-dimensional martensite transformation occurs in an array containing a distribution of initial nuclei. Of course, given the small size of the array and the random

distribution of nuclei, there are statistical variations in the martensite start temperature and in the specifics of the transformation path which depend on the particular number and distribution of initial nuclei. Some additional results are shown in Figures 16-1 to 3, which present the fraction of martensite as a function of undercooling for three cases containing ten, twenty and forty initial nuclei in random distribution. The resulting transformation curves are somewhat different from, though qualitatively similar to that obtained in the ten-nucleus case discussed in detail.

There is an expected statistical tendency for the martensite start temperature, M_s, to increase as the number of randomly distributed nuclei is made greater. Recognizing that the martensite transformation will begin from the most favorable local configuration of pre-existing nuclei, this tendency simply reflects the increased likelihood of a particularly favorable configuration when the number of nucleating defects is increased. A particularly favorable configuration may even cause the martensitic transformation to occur to a slight extent above the equilibrium temperature ($\Delta T = 0$). An example is shown in Figure 16-3, for a martensite transformation in a case containing forty initial defects. In this case a slight transformation occurs at a temperature for which the undercooling ΔT is negative. The source of the transformation is the large negative energy which may be obtained by introducing a martensite particle in the environment of a particularly suitable configuration of initial defects. It is, however, not possible for the martensite transformation to progress significantly at negative values of the undercooling.

The tendency for the martensite transformation to occur at increas-

ing temperatures with the introduction of additional defects is analogous to the phenomenon of deformation-induced martensite, in which the martensite transformation temperature is raised by deforming a crystal.

It will also be noted that as the number of initial defects is increased the transformation becomes more smooth, that is, it occurs more uniformly as the temperature is decreased. This behavior also has a relatively straightforward interpretation. As we discussed in the two previous sections, the halting of the martensite transformation at a given temperature has one of two causes: either previous transformation has led to the completion of a twin plate along the habit plane, which dramatically reduces the elastic driving force for further transformation, or the plate has progressed to a point in which it encounters opposing strain fields from other plates which have previously formed, or from previous defects that have not yet been activated. The latter case is much more common when many initial defects are present. As a consequence, the extent of transformation per thermal step tends to be much less in the many defect case. On the other hand, the presence of many initial defects provides a smoother energy spectrum of heterogeneous nucleation sites. As a consequence, the degree of supercooling required to reinitiate a transformation that has halted tends to be smaller when many nuclei are present.

The tendency toward a higher martensite start temperature and a smoother transformation curve of percent martensite vs. temperature in the presence of the larger number of initial nuclei are, of course, statistical trends rather than determined phenomena. Significant statistical variations in both these features of the transformation do occur when a particular transformation case is repeated with a differ-

ent distribution of additional nuclei. An example may be seen by comparing the transformation curve given in Figure 16-1, for a ten-nucleus case, with that presented earlier in Figure 10 for the ten-nucleus case which was discussed in detail. Because of the difference in the initial defect configuration, the example shown in Figure 16-1 exhibits a substantially lower martensite start temperature and a much narrower range of temperatures over which the transformation is brought to completion. One would, of course, expect these statistical variations to disappear if the array size were made arbitrarily large. The martensite start and finish temperatures would then become dependent only on the type and concentration of initial defects.

The martensite finish temperature, M_f, at which the last of the austenite particles disappears, tends to decrease as the density of the initial defects increases. This effect also has a relatively straightforward interpretation in the model. As the number of initial defects increases, the transformation becomes more irregular and the martensite plates become less well-developed. The residual austenite is stabilized by the elastic interference of the adjacent martensite plates which leads to high values of the elastic energy required to complete transformation in certain unfavorable sites. As the transformation becomes more irregular, the number and unfavorability of such sites has a statistical tendency to increase, requiring greater undercooling to fully complete the martensitic transformation.

D. Variation of Array Size and Dimensionality

Experience with the computer simulation model seems to show that the characteristics of the two-dimensional transformation are not very sensitive to the array size employed so long as the array size is forty by

forty or greater and so long as the density of the initial defects is reasonable, for example, ten or more in a forty by forty array. A forty by forty array is sufficient in size to largely eliminate fluctuations in the two-body elastic interaction due to the periodic boundary condition, so that the nature of the elastic relaxation term does not change significantly as the array size is made larger. There is a slight tendency for the martensite start temperature to increase as the array size is made bigger, again as a consequence of the fact that the martensite transformation is nucleated by the most favorable configuration of defects initially present, but the effect does not seem to be pronounced in the cases studied to date.

Much more pronounced effects are expected if the dimensionality of the array is increased from two to three. In three dimensions there are three rather than two simple variants of the elementary martensite particle, corresponding to the three different orientations of the tetragonal axis of the Bain strain. Moreover, in three dimensions there is a considerably enhanced freedom for the martensite particle to take non-simple habit planes, for example, the (259) plane often observed in real systems. The problem of elastic constraint also changes somewhat in three dimensions since one must recognize the three-rather two-dimensional confinement of an isolated martensite particle. It is clear that a three-dimensional simulation which incorporates these qualititative changes must be carried out if we hope to obtain quantitative simulation of the martensitic transformation in a real crystal.

In anticipation of the need for three-dimensional simulation studies, a computer code was written which permits the modeling of the martensitic transformation in three dimensions. To date this code has only

been used for some preliminary experiments for debugging purposes. The three-dimensional transformation is not only much more difficult and expensive to simulate in the computer, but is also much more difficult to analyze insofar as the progress of the transformation is concerned, since the three dimensional development of martensite particles is not easy to represent in a way which permits simple visualiztion. We therefore adopted a research strategy that contemplates a thorough investigation and understanding of the two-dimensional transformation case before proceeding to three-dimensional studies.

A preliminary example of a martensitic transformation in three dimensions is shown in Figure 17. In this case the transformation was allowed to occur in a fifteen by fifteen by fifteen array, the initiating defect was a single martensite variant in the center of the array, and the three martensite variants are modeled by lines along the x, y or z axes. A section through the transforming cube is shown in Figure 17. The transformation tends to proceed through the growth of (110) twinned plates in three dimensions. Only two of the three possible variants appear in a single plate, as expected from either the crystallographic or elastic energy model of the martensite plate. The results of this simulation seem to show that the computer code is working properly, but since detailed studies of the three-dimensional transformation have not been carried out, no more specific discussion of these results can be given.

E. The Introduction of Elastic Anisotropy and Dilatation

The martensite transformation studied in detail in this work concerned the simplest possible case, in which the elastic constants were assumed to be isotropic and the Bain strain was taken to be a simple

shear. The modification of the model to treat cases in which the elasticity is anisotropic and the Bain strain involves a dilatation as well as a shear is straightforward and some preliminary investigations have been carried out. While these investigations have not been taken to the point at which a thorough discussion of the consequences of anisotropy or dilatation can be given, preliminary results are available.

Figure 18 shows a series of micrographs illustrating the development of the martensitic transformation in a two-dimensional forty by forty array in which the elastic constants were chosen to be the anisotropic elastic constants of iron-nickel austenite, and the transformation was assumed to involve a large dilatation, roughly corresponding to the dilatation involved in the Bain strain of iron-nickel austenite when only the tetragonal and perpendicular axes are included. This dilatation is unrealistically large, and it exaggerates the relevant effects.

The habit plane of the martensitic transformation in this case can be computed using relations developed in Section III. Since the dilatation is non-zero, the preferred habit plane is rotated somewhat away from (1 1) and lies close to the plane (5 4). An examination of the effect of the dilatation on the pair-wise interaction of martensite particles brings out a second effect. The dilatation modifies the short range two-particle interaction so that the preference for unlike neighbor particles is slightly reduced. Unlike or twinned neighbors are still preferred, but less so than when the transformation strain is a pure shear.

The transformation illustrated in Fig. 18 occurs in an array which contains a distribution of twenty initial nuclei. The nucleating defect is a like pair of initial defects, located near the center of the

array on the right hand side, which are fortuitously in nearest neighbor relation to one another. As shown in Fig. 18-2 and 18-3 the transformation begins to develop in the form of a twinned plate roughly along the (1 1) direction. In contrast to the pure shear case, however, the central rib of this plane is two layers in thickness.

As shown in Figures 18-4 and 18-5, shortly after it begins to grow the plate branches in a somewhat irregular pattern. It becomes a thick wavy plate which contains (1 1) and (1 0) segments. An examination of the microstructure reveals two sources for the waviness of the plate. First, since the habit plane of the particle is not strictly (1 1), the growing plate can deviate from its initial orientation without a substantial loss of energy. Second, the array through which the plate is growing contains initial defects, some of which are attractive to the growing plate and promote deviations in the direction of its growth.

After some growth the plate crosses the array in roughly a (1 0) direction. However, the plate is displaced slightly as it is wrapped around the periodic array, so that the two ends of the plate are slightly offset and bypass one another rather than meeting, leaving a region of retained austenite in the intervening region. The plates do ultimately join together, as shown in Figure 18-6, and the intermediate austenite is gradually transformaed as shown in Figures 18-7 to 18-12 to yield an essentially complete plate traversing the array in a (1 0) direction. The process of transforming the austenite between the bypassing plates is accomplished primarily through the thickening of the upper plate in the figure; however, secondary nucleation is also involved. The transition from the state of Figure 18-8 to that of Figure 18-9 is accomplished by a clear case of autocatalytic nucleation. The new

particle forms within an island of austenite in a position which is spatially separate from any of the previously formed martensite.

The transformation subsequent to that shown in Figure 18-12 is relatively simple. The thick (1 0) plate shown in the figure gradually thickens, and by this thickening, eventually accomplishes the complete transformation of the array. Some residual austenite is left behind in this thickening process, as, for example, is seen in the microstructure 18-12. This austenite is eventually eliminated at large undercooling. Its tendency to lie in thin platelets along the (1 0) orientation will be noted.

The internal structure of the transformed region shown in Figure 18-12 is typical of the structure observed in the late stages of the transformation. The internal structure of the plate is largely made up of twineed sub-plates which are often two layers rather than one layer in thickness. These two-layer platelets lie approximately along the (1 1) direction, but have occasional steps within them, which presumably reflect the preference of the system for a habit that is slightly rotated with respect to (1 1).

The pattern of the transformation in this case of anisotropic elastic constants and transformation strains involving non-zero dilatation is decidedly more complex than that observed in the transformation of an isotropic array through a pure shear transformation strain. The details of this case are under continuing investigation. We are particularly seeking to separate the effect of the elastic anisotropy from that of the dilatational component of the transformation strain in their relative effects on the morphology of the transformation products.

VI. DISCUSSION

The purpose of this thesis was to construct and study a theoretical model of the martensitic transformation, which would be simple enough to permit detailed study in computer simulation while being sufficiently profound to shed new light on the manner in which the martensitic transformation proceeds. Since the martensite transformation is believed to be dominated by the problem of elastic accomodation between the two phases, the model that was constructed emphasizes the elastic interaction, and in its simplest form, deemphasizes other possible factors. The assumptions are strong in keeping with the desire to create the simplest reasonable initial model. We have hence made a linear elastic approximation, assumed homogeneous elastic constants, and modeled the reaction over a finite lattice of elementary volumes which is formally treated as a discrete lattice of points.

A. Comparison with Experiment

Despite the relative simplicity of this model of the transformation, the results are encouragingly real. Many of the most important qualitative features of the martensite transformation are already reproduced in this simplest case. Apparent qualitative points of contact with experimental results occur in the heterogeneity of the martensite phenomenon, the thermal characteristics of the transformation, and the retention of austenite at very large undercoolings.

As is believed to be the case experimentally, the martensite transformation is nucleated from heterogeneous sites[63], which are in this case elastic defects in the lattice modeled as martensite embryos. When many initial defects are present, the nucleation occurs preferentially at the most favorable configuration of defects, an observation

in contact with the suggestion that arrays of defects form the preferential nucleation sites[23]. The nature of the favorable configurations might be discussed in detail by considering the interacting strain fields defects in the configuration. However, in the cases analyzed to date the most favorable configurations have a simple characteristic form. They consist of an association of defects, such as those illustrated in Figure 11-1, which are so oriented with respect to one another that a simple twinned plate will naturally incorporate them during its growth.

The growing martensite plate is an internally twinned plate two or three layers in thickness. From the point of view of the two-body interaction, the source of the preference for the twinned plate is clear; as illustrated in Figure 7-2 for the case of a transformation strain of the pure shear type, the most favorable interaction between particles promotes the appearance of a particle in twin orientation along a (1 0) direction from the initial particle. Neighboring twin particles along the (1 1) habit plane. The qualitative preference for the formation of the twinned plate has an obvious interpretation in terms of the tendency of the martensite particle to try and minimize its net tetragonal strain. This feature of the transformation is most clearly evident in the growth of the plate from a single nucleation center, as illustrated in Figure 7-3. The first four martensite particles appear so as to form a square configuration in which the tetragonal strains are mutually compensating. This box is the embryo of a three-layer twin plate. Fig. 19 shows one example of twinned martensite.

The driving force for the growth of a martensite plate is the decrease in the elastic energy associated with the spreading out of a plate along its habit plane to form a completed plate along an invariant

plane. This process is clearly revealed in the case of the growth of a martensite plate from a single strain center, as illustrated in Figure 7-6, in which the twin particle grows to form a twinned plate along the (1 1) habit plane. After this growth has been completed the total elastic energy of the system decreases to an extremely small value.

In the case of transformation in a lattice containing a number of initial defects, the martensite particle attempts to grow to complete the formation of a plate along the habit plane, but it is prevented from doing so by the interference of the strain fields of other defects already present in the lattice. In typical experimental cases the preventing defects are grain boundaries or martensite particles that have previously developed. These serve as internal defects which prevent platelet growth from reaching completion.

A continuation of the martensite transformation through the autocatalytic nucleation of additional plates is a consequence of the arrested growth of the initial plate due to the mutual interference of the strain fields of the defects in the lattice. These have the consequence that the strain field of the lattice after partial completion of the transformation is irregular, and there are hence sites within the lattice at which the transformation can favorably proceed on slight further undercooling. Two types of autocatalytic nucleation are observed: first, and most predominately, is the activation of pre-existing defects, or continued growth of previously created plates, through the addition of particles in favorable positions in the internal strain field. However, the homogeneous nucleation of new plates is also occasionally observed. While the homogeneous nucleation of martensite is normally a very difficult process, a circumstance in which the strain fields of

adjacent particles strongly interfere can create the large elastic driving force necessary to bring about homogeneous nucleation as a means of continuing the transformation.

The thermal characteristics of the transformation also strongly resemble those of low-temperature martensitic transformations in real systems. The transformation proceeds by an amount which is a function of the final temperature, but not of time. To continue the transformation the temperature must be continually decreased. The transformation proceeds through a series of bursts as the undercooling is increased, each of which involves the formation and growth of one or more martensite plates or the discontinuous extensions of plates which already exist. Figure 20 shows the variation of the martensite fraction with temperature in a typical experimental case[67], which will be seen to be similar to the results of the computer model as illustrated in Figures 10, 16-1∿3.

During the course of the transformation the energy released per elementary event is a noisy function, due to the strong variation in the relaxation energy associated with each elementary transformation. Experimentally, this irregular energy release should be observable in a noisy contribution to both the thermal and acoustic emission during the transformation. A typical result of the acoustic emission measurements during the course of a martensite transformation is shown in Figure 21[67]. The function is quite irregular as anticipated from the theoretical model.

The retention of austenite in the later stages of the model martensite transformation also bears a strong resemblance to austenite retention in many experimental cases. Initially the retained austenite tends to form continuous bands in the interstices between adjacent martensite

plates. For experimental comparison Figure 22 shows the form of austenite as observed by transmission electron microscopy in a low alloy steel, following Thomas and coworkers[67,68]. The retention of bands of austenite is evident. In the later stages of transformation these bands of austenite are eliminated, and the retained austenite occurs in the form of small isolated particles within the lattice. This final morphology bears a strong resemblance to that of the final residual austenite in, for example, ferritic cryogenic steels, in which the austenite takes the form of small particles that are the residues of bands of austenite that have transformed thermally. In the computer simulation model the austenite is stabilized by the elastic strain, which is such that both martensite variants are unfavorable at the site at which the austenite is retained. This austenite can be quite stable. The example discussed in the previous section is typical, in which very large undercoolings are necessary to eliminate the final fraction of austenite and bring the transformation to completion. It is, however, interesting that the elastic stabilization of the austenite is typically less than that which would be achieved by simply eliminating all martensite particles and nucleation sites from the lattice. While the last few particles of retained austenite are very stable agains transformation, they are, interestingly, less resistant to transformation than they would be if they existed as isolated particles free of the partly transformed lattice. This result is also in qualitative agreement with recent experimental evidence.

The correspondence between the martensite transformation as simulated in this simple model and qualitative features of the transformation

observed in real systems has an important implication that should be noted. One of the objectives of the theoretical study of metallurgical processes is to separate those features of the process that are relatively obvious, in the sense that they are straightforward consequences of the nature of the process itself, from those which are subtle and require a substantial theoretical interpretation for their understanding. In the metallurgical literature the martensitic transformation is often treated as if it were mysterious in many of its most important features. The reproduction of many of these features in what appears to be the simplest realistic model of the transformation suggests that the dominant features of the martensite transformation are not mysterious at all, but they are relatively straightforward results of the large role that elastic strain plays in the transformation process.

B. Extensions of the Model.

The model developed here is capable of a number of extensions which might be useful in increasing understanding of martensitic transformations, and in obtaining a semi-quantitative match with experimental results. In considering such modifications one should, however, keep in mind that the feature of the model which permits us to construct a straightforward computer simulation is the linearization which leads to a two-body elastic interaction and permits the computation of the strain field as a simple superposition of the strain fields of individual particles. Modifications of the model that preserves linearization may be readily incorporated; those which destroy it will be very difficult to include. Features of the model which would bear examination or modification in future work include the following:

1. The two-particle interaction. The precise form of the two-body elastic interaction would appear to be a critical feature of this model.

Examination of the interaction field (Figure 6) shows that the interaction is maximal for the near neighbor terms. It is, of course, precisely these near neighbor terms which are least accurately treated in an elastic model which relies on the long wavelength approximation. As we have used it, the long wavelength approximation introduces two sources of error. First, the finite volume of the elementary martensite cell is not taken into account; the cell is treated as an equivalent point. Second, the deviation of the harmonic dispersion relation at higher values of the wave number, $\underset{\sim}{k}$, is ignored, introducing an approximation that becomes increasingly bad for near neighbor terms. Some preliminary investigation of the influence of the shape of the dispersion relation has, however, been done, with the surprising result that the elastic interaction does not appear to be markedly sensitive to the precise shape of the dispersion relation as long as that relation has a reasonable form. However, a more detailed investigation does appear to be warranted. As discussed in previous sections, the introduction of surface or twin boundary energy may also be formally incorporated as a change in the nearest neighbor interaction in the two-body interaction function. A preliminary investigation suggests that the principal effect of including surface or twin boundary energies will be to change the undercooling in which the transformation occurs, and simultaneously to modify the form of the plate so that somewhat thicker martensite plates are favored. The influence of these parameters also warrants further investigation.

The effects of finite elementary volume size, non-linear dispersion relations, and surface and twin boundary energies can, at least, be

simply incorporated into the model. Interesting features that are more difficult to include are the influence of inhomogeneous elastic constants and anharmonic effects. The elastic constants of the austenite and martensite phases are, of course, different. In some important cases the martensitic transformation introduces a change in overall symmetry, which will cause certain elastic constants that identically vanish in the parent phase to take non-zero values in the product. Methods for incorporating non-uniform elastic constants are now under investigation, but the problem is not a trivial one since at least part of the effect of inhomogeneous elastic constants is to introduce coupling terms that cannot easily be accounted for in a two-body interaction mode. Inhomogeneity of the elastic constants may also destroy the simple linear superposition which permits the computer code to be written in an efficient way. It is, however, possible that at least the greater part of the elastic modulus effect may be taken into account within the context of the present model and we are currently investigating ways in which this might be done. Other interesting anharmonic effects, such as those introduced by the severity of the deformation in the course of the phase transformation, are three-body effects which are probably beyond the domain of models of the present type.

2. The Transformation Strain. Changes in the stress-free strain associated with the transformation are known to change the preferred habit plane of the martensite particle, but may also influence the transformation path in ways that are not yet clearly specified. Incorporation of different tetragonal strains into the computer code is straightforward, and it should be possible to investigate the influence of changes in the transformation strain in some detail in future work.

The simplest modification, which we have investigated in a preliminary way, involves including some dilatation into the Bain strain of the two-dimensional transformation. Some preliminary results of a simulation of this type were included in the preceding section. More general changes would include changes in the symmetry of the transformation, to simulate, for example, the martensitic transformation to the hexagonal epsilon phase in steel.

3. Martensite Nucleation. Since our principal interest in the present research has been on the development of the martensitic transformation rather than on its nucleation, a particularly simple nucleation site, the martensite embryo, was assumed. Even with this simple assumption, the research has shown that the true nucleation site in a crystal containing a distribution of defects tends to be a particular configuration of embryos. In most of the cases analyzed to date the preferred nucleation site can be simply analyzed in terms of the compatibility of the local configuration of embryos with a hypothetical martensite particle. The configurations which are most compatible with a resulting particle seem to be the most potent as far as nucleation is concerned. This subject does, however, deserve a more detailed analysis.

There is, moreover, no inherent reason why the nucleation site in the model must be a martensite embryo. Any strain center might serve as a nucleating defect, and should behave in a qualitatively similar way. In real crystals the nucleating defects are believed to be dislocations, dislocation pileups, or grain boundaries of particular types. Our simulation code offers an efficient means for studying the nucleation behavior and catalytic potency of hypothetical arrangements of defects of these types. Such an investigation should be carried out.

4. The Development of the Transformation. The modifications of the model which are perhaps of greatest potential interest are those which involve more realistic treatments of the development of the transformation. The needed modifications included particularly incorporation of thermal activation and the shift to three-dimensional arrays.

At least some of the effects of introducing thermal activation are obvious from the work which has already been done. If we consider a case in which the thermal activation is weak, that is where only those events which involve a very small activation energy have any possibility of occurring sponataneously, then the principal effect of thermal activation is almost certainly going to be to increase the burst-like character of the transformation. In the thermal case which was studied in this research and discussed in the previous section, each of the major bursts of transformation tended to be separated by a few mini-bursts in which only one or two activation events would occur before the temperature had to be lowered. The energy barriers separating these mini-bursts was, in general, very small. As a consequence we can expect that the first effect of thermal activation will be to eliminate these intervening steps between the major bursts of the martensite transformation.

If thermal activation is made easier still, we should begin to observe a tendency for a significant amount of isothermal transformation of austenite. That is, if a system is held at a fixed value of the temperature for reasonable periods of time, thermal activation may intervene to cause an increasing transformation with time. A character of this isothermal transformation should strongly resemble that observed experimentally: a martensite plate nucleates and grows rapidly to completion, after which one observes a finite time period before the

second thermal activation even occurs, after which the new plate grows rapidly until it reaches completion. Since, as discussed in the previous section, only those events which trigger the growth of the plate require significant elastic energy, this burst-stop-nucleate-burst pattern is quite clearly anticipated when thermal activation is allowed to occur.

At the same time that the ease of thermal activation will permit isothermal formation of martensite, it will also modify the transformation path and make the features of the transformation much less certain than in the cases studied to date. In a situation in which thermal activation is facilitated any one of several activation events may occur. The subsequent development of the transformation will depend on which of these events happens.

A final consequence of thermal activation will be to cause the martensite start temperature, and the progress of the transformation, to become sensitive to the rate at which the system is cooled. It is a common experimental observation that martensite transformations which occur at relatively high temperature exhibit martensite start temperatures which depend on quenching rate. As the rate of cooling is decreased, the martensite start temperature increases. This phenomenon would appear to be the straightforward result of a thermally-activated process. In a thermally-activated process the probability that an event will occur increases with the time and temperature. If there is a range of temperatures over which the event is not unlikely, and if the system is continuously cooled, then the temperature at which the event is observed to happen will increase as the cooling rate goes down. Since the character of the simulated martensite transformation is such

that the transformation may develop easily once it has been nucleated, one would expect to see a pronounced start to the transformation at an increasingly high temperature as the cooling rate is made lower.

It is planned to demonstrate these and other features of the thermally-activated transformation in the near future.

The generalization of the simulation to the 3-dimensional case poses a somewhat different problem. While the simulation in three dimensions is straightforward, and while a working computer code has been developed, and initial results presented in the preceding section, the extension is difficult to carry out because of the time required to conduct a 3-dimensional transformation, and because of the small size of a 3-dimensional cube compatible with the memory of the computer. The extension to three dimensions is, however, important since only the 3-dimensional case can promise a quantitative reproduction of martensite transformations observed experimentally, and because such qualitative features of the transformation as the irrational habit plane of typical iron martensites can only be found in the 3-dimensional case. We hope to conduct these studies in the near future.

A final aspect of the growth process that is important to consider, though the simulation procedure is not obvious, is the possibility of accomodating the transformation strain through a dislocation rather than a twinning mechanism. In many of the most important examples of the martensite transformation in structural alloys the transformation product is dislocated rather than twinned. It is not at the moment clear how transformation-induced dislocations may be incorporated into simulation models of the sort that have been used in this research. However, the need to simulate dislocated martensite is real, and the

problem of identifying suitable representations should be given consideration.

5. Mechanical and Magnetic Effects. An important problem in the engineering control of martensitic transformation in structural alloys is the influence of the interacting environment on the initiation and progress of the transformation. The imposition of a mechanical load will not only influence the onset of the transformation, but it will also modify the microstructure in that it influences the types of martensite particles which form. If the mechanical load results in a plastic strain, the results are not only striking but also puzzling; the transformation is sometimes promoted and sometimes suppressed. Incorporation of a mechanical stress into the computer simulation model is straightforward. The stress will provide a simple additive contribution to the relaxation energy. The contribution will, of course, be such that it is favorable for those martensite particles which relax the external load and unfavorable for those which oppose it, and as a consequence certain characteristic variants will tend to be promoted in the presence of a given external stress. This simulation is well within the capabilities of the present model and will be performed in the near future.

The influence of plastic deformation is somewhat more difficult to simulate, but still appears to be within the capabilities of the model. The simulation approach will in this case have to begin from some previous work on the nature and configuration of defects introduced by the plastic deformation. These may then be allowed to develop in the array before and during the transformation, and their influence on the transformation may then be assessed. Some of the effect of the introduction

of defects through mechanical deformation can be foreseen from the results we have already obtained. The simulation results obtained in this research show that the defects play two roles: they introduce sites which may serve as heterogeneous nucleation sites for either the initiation or continuation of the martensite transformation, and they also introduce internal strains which may inhibit the transformation and cause it to arrest. Since the net transformation observed will depend on the balance of these two effects, it is not surprising that one would empirically find cases in which deformation promoted the transformation, while finding other cases in which the deformation tended to bring the transformation to a halt. Suitable specific simulation should shed further light on this phenomenon.

A rather different type of environmental interaction that has recently taken on special interest is the promotion of the martensitic transformation by magnetic fields. Since in iron the martensite phase is ferromagnetic while the austenite phase is not, the introduction of a magnetic field promotes the appearance of martensite. When the field is high the effect may be significant and has become of some technological importance because of potential problems in the use of austenitic structural steels for the containment walls of high-field superconducting magnets. These operate at very low temperatures at which almost all austenitic steels are at least metastable with respect to the martensite transformation. The incorporation of magnetic fields into the simulation model utilized here is again straightforward. The external field will introduce a direct contribution into the particle self-energy. We plan to perform simulations of this interesting case in the near future.

In summary, the simulation of the martensite transformation as a

simple transformation of elastic elements appears to be a very fruitful approach to enhance our understanding of the transformation. Even the simplest model reporduces many of the qualitative features that are associated with the martensite transformation including some of those previously regarded as rather mysterious. The model is capable of generalization in a number of different directions and may realistically be expected to lead to a much richer understanding of martensitic transformation phenomena in the future.

VII. CONCLUSIONS

The principal results of the work reported here may be summarized as follows:

1. The equations governing the energy of an arbitrary distribution of substitutional point defects in an elastic lattice have been formullated under the dual assumptions that the Born-von Karman constants of the lattice are uniform and that anharmonic effects may be neglected. It has been shown that under these assumptions the elastic energy may be written as a sum of terms which are independent of the configuration of defects and a term which involves a simple sum of binary interactions between the defects.

2. The equations governing the elastic energy of a distribution of elementary point defects on an elastic lattice have been generalized to treat a distribution of elementary defects of finite size. Therefore, the energy associated with arbitrarily distributed inclusions with arbitrary shape (which can be considered as an aggregation of the elementary defects of finite size) can be readily calculated. The resulting equations again have the form of a sum of terms which are independent of the configuration of the defects plus a sum of simple binary interactions between them.

3. A general model of a transformation was developed and described in which the transformation occurs through the sequential appearance or disappearance of elementary defects. Statistical equations were formulated which govern the choice of the transformation path, or sequence of elementary transformation events, and which also give the kinetics of transformation along any particular transformation path. In general the transformation path is statistically chosen and complex. A simple,

useful representative path, the "minimum energy" path, was hence defined and described.

4. The general transformation model was used to simulate a martensitic transformation in the particular case of a simple, pseudo two-dimensional lattice. The path of the transformation and the resulting microstrucute were studied as a function of the number and distribution of the initial nucleating defects within the model lattice, the characteristics and transformation strain, and the nature of the elastic constants. It has been shown that many of the most important qualitative features associated with martensitic transformations in real solids are well reproduced in this simple model.

Table 1

fcc → bcc	Fe, Fe-Ni, Fe-Ni (Co, Ti, Nb, V, Si), Fe-Cr, Fe-Co-W-Cr.
fcc → bct	Fe-C, Fe-C-(N, H, Mn, Cu, Si, Ni, Cr, Mo, V, W, Al, Co).
fcc → hcp	Co, Co-Ni, Co-Fe, La, Ce.
fcc → hcp bcc	Fe-Mn, Fe-Mn(C, Ni, Ni-Cr, Cr), Fe-Cr-Ni, Fe-(Ru, Os, Pt, Ir).
fcc → fct	Mu-Cu, In-Tl, In-Tl-Li, In-Pb.
bcc → hcp	Na, Zr, Zr (Nd, Y, Hg, Ho, Er), Tl, Hf, Ti, Ti(H_2, Al, Cu, Cr, Fe, Mn, Mo, Zr, V, Al-V, Al-V-Mn, Al-C, Cr-Mo, Ta, Nb, W) Zr-U, Cu-Al-N.
bcc → Monoclinic orthorhombic	Cu-Al, Ag-Cd
bcc → orthorhombic tetragonal	Au-Cd-Cu, Au-Cd.
bcc → hcc fcc	Li, Li-Mg, Cu-Zn
hcp → fcc	A-N_2
tetragonal	U. U-Cr
rhombohedral → bct	Hg.
A15 (cubic-tetragonal).	

REFERENCES

1. Reed, R. P. and Breedes, J. F.: Low Temperature Phase Transformations in "Behavior of Metals at Cryogenic Temperatures", ASTM-STP-38. Am. Soc. Testing Mats., 1966, p. 60.
2. Bain, E. C.: Trans, AIME 70, 25 (1924).
3. Kurdjumov, G. and Sachs, G.: Z. Physi K, 64, 325 (1930).
4. Nishiyama, Z: Sci. Rept. Tohoku Univ., Sendai, 23, 637 (1934).
5. Lysak, L. I. and Nikolin, B. I.: Fiz, Met Metalloved, 20, 547 (1965), 20, 540 (1965), 24, 299 (1967).
6. Vanables, J. A.: Phil. Mag., 7, 35 (1962).
7. Fujita, F. E.: Nippon Kinzolu Grakkai, 13, 713 (1974), Nippon Kinzoku Gakkaishi, 39, 1082 (1975).
8. Khachaturyan, A. G. and Kurdjumov, G. V.: "New Aspects of Martensitic Transformation" Proceedings of the First JIM International Symposium held at Kobe, May, 1976, Supplement to Trans. JIM, Vol. 17 (1976).
9. Greninger, A. B. and Troiano, A. R.: Trans. AIME 185, 590 (1949).
10. Lieberman,D. S., Wechsler, M. S., and Read, T. A.: J. Apply Phys., 26, 473 (1955).
11. Bowles, J.S. and Mackenzie, J. K.: Acta Met., 2, 129 (1954) 2, 138 (1954) 2, 224 (1954), 5, 137 (1957), 10, 625 (1962).
12. Wayman, C. M.: "Introduction to the Crystallography of Martensitic Transformation", Macmillan Series in Materials Science (1964).
13. Khachaturyan, A. G. and Rumynina, A. F.: Phys. Stat. Sol. (a) 45, 393 (1978).
14. Khachaturyan, A. G.: Sov. Phys. Solid Stat. 8, 2163 (1967).

15. Khachaturyan, A. G. and Shatalov, G. A.: Sov. Phys. - JETP, 29, 557 (1969).

16. Shibata, M. and Ono, K.: Acta Met. 23, 587 (1975).

17. Eshelby, J. D.: Progress in Solid Mechanics, 2, 89 (1961).

18. Eshelby, J. D.: Proc. Roy Soc., A241, 376 (1957).

19. Kaufman, L and Cohen M.: Progr. Metal Phys. 7, 169 (1958).

20. Christian, J. W.: "The Mechanism of Phase Transformations in Crystaline Solids", Proceedings of an International Symposium organized by the Institute of Metals and held in the University of Manchester, July 1968. Monograph and Report Series No. 33.

21. Easterling, K. E. and Thölén, A. R.: Acta. Met. 24, 333 (1976).

22. Frank, F. C.: Acta. Met. 15, 1 (1952).

23. Olson, G. B. and Cohen, M.: Met. Trans. A, 17A, 1897 (1976).

24. Labbe', P. J. and Friedel, J.: Le Jo. De Physique, 27, 303 (1966), 27, 708 (1966).

25. Pytte, E.: Phys. Rev. B., Vol. 3 #10, 15, 3503 (1971).

26. Pytte, E.: "Mechanism of Structural Phase Transformation", Structure Phase Transitions and Soft Modes, E. J. Samuelson, E. Anderson and J. Feder. Proceedings of the NATO Advanced Study Institute at Geilo, Norway, April 1971, p. 133.

27. Gorkov, L. P.: JETP Lett. 17, 379 (1973).

28. Gorkov, L. P.: Sov. Phys.-JETP. 38, 830 (1974).

29. Gorkov, L. P. and Dorokhov, O. N.: J. Low Temp. Phys. 22, 1 (1976).

30. Gorkov, L. P. and Dorokhov, O. N.: JETP Lett. 21, 310 (1975).

31. Mattheiss, L. F.: Phys. Rev. 138 A 112 (1965), Phys. Rev. 12 B 2161 (1975).

32. Clapp, P. C.: Phys. Stat. Sol. (b) 57, 561 (1973).

33. Suzuki, T. and Wuttig, M.: Acta Met. 23, 1069 (1975).

34. Khachaturyan, A. G.: Soviet Phys.- Solid Stat. Vol. 9 #9, 2040 (1968), Vol. 4 #10, 2081 (1963), Vol. 9 #10, 2249 (1968), Vol. 13 #8, 2024 (1972).

35. Khachaturyan, A. G. and Shatalov, G. A.: Acta Met. 23, 1089 (1975).

36. Khachaturyan, A. G.: Soviet Physics-Crystallograph, Vol. 10 #3, 248 (1965).

37. Khachaturyan, A. G. and Hairapetyan, V. N.: Phys Stat. Sol. (b), 57, 801 (1973).

38. Khachaturyan, A. G.: Progress in Materials Science 22, 1 (1978).

39. Tanner, L. E.: Phil. Mag. 14 (127) 111 (1966).

40. Lee, J. K., Barnett, D. M. and Aaronson, H. I.: Met. Trans. Vol. 8A, 963 (1977).

41. Johnson, W. C. and Lee, J. K.: To be published.

42. Matusbara, T. J.: J. Phys. Soc., Japan 7, 270 (1952).

43. Born, M. and Huang, K.: "Dynamical Theory of Crystal Lattice", Oxford University Press (1954).

44. Kanzaki, H.: J. Phys. Chem. Solids, 2, 24 (1957).

45. Hardy, J. R.: J. Phys. Chem Solids, 15, 39 (1960).

46. Hardy, J. R. and Bullough, R.: Phil. Mag. 15, 237 (1967), Phil. Mag. 17, 833 (1968).

47. Tewordt, L.: Phys. Rev., 109, 61 (1958).

48. Ho, P. S. and Benedek, R.: J. of Nuclear Materials, 69-70, 730-733 (1978).

49. Ho, P. S.: Phys. Rev. B, Vol. 7 #8, 3550 (1973).

50. Siems, R.: Phys. Stat. Sol. 42, 105 (1970).

51. Maradudin, A. A.: J. Phys. Chem. Solids, 9, 1 (1958).

52. Celli, V.: J. Phys. Chem. Solids, 19, 100 (1961).

53. Gallotto, C. P. and Omini, M.: Phys. Stat. Solids, 8, 239 (1965) 10, 601 (1965).

54. Brialsford, A. D.; Phys. Rev. 142, #2, 383, 388 (1966).

55. Brailsford, A. D.: J. Appl. Phys. 37 (7), 2842 (1966).

56. Boyer, L. L. and Hardy, J. R.: Phil. Mag. 24, 647 (1971).

57. Esterling, D. M.: J. Appl. Phys. 47 (2), 486 (1976); 49 (7), 3954 (1978); 49 (7), 3960 (1978).

58. Hsei, C. and Thomson, R.: J. Appl. Phys. 44, 2051 (1973).

59. Friedel, J.: Adv. Phys. 3, 446 (1954).

60. Eshelby, J. D.: Sol. State Phys. 3, 79 (1966).

61. Cahn, J. W.: Acta Met. 9, 795 (1961); 10, 907 (1962).

62. Cook, H. E. and De Fontaine, D.: Acta Met. 17, 945 (1969); 18, 189 (1970), 19, 607 (1971).

63. Nishiyama, Z: "Martensitic Transformation", M. E. Fine, M. Meshii and C. M. Wayman ed. Academic Press, New York, San Francisco, London, 1978.

64. Morris, Jr., J. W. and Klahn, D.: J. Appl. Phys. 44, 4882 (1973).

65. Feller, W.: "An Introduction to Probability Theory and its Applications". 3rd ed. (Wiley, New York, 1968).

66. Speich, G. R. and Fisher, R. M.: "Acoustic Emission", ASTM Special technical publication 505, a symposium of ASTM. Bal Harbour, Florida, 1971, p. 140.

67. Rao, B. and Thomas, G.: Proceeding of ICOMAT-77, March 16-20, 1977, Kiev, USSR, In Russian (1978) LBL-8013, UC-25 July (1978).

68. Rao, B.: Ph.D. Thesis, U. C. Berkeley (1978).

FIGURE CAPTIONS

Figure 1. The hypothetical procedures to create a multi-component substitutional solid solutions

Figure 2. The Bain distortion.

Figure 3. The martensite twin plate.

Figure 4. The superlattice of cells, each of which is of the size of an EMP (elementary martensite particle).

Figure 5. Bain strain in two dimensions.

Figure 6. Three dimensional plot of the thermoelastic potential $\phi_p(\underset{\sim}{R})$ at every site $\underset{\sim}{R}$, due to a type p EMP on the center of the net, in the case of elastic isotropy.

Figure 7. The development of the microstructure in the two-dimensional isotropic body, initially contains only a single nucleating defect, and transforms via a Bain strain which is a simple shear.

Figure 8. The companion figure to Figure 7. It shows the incremental change in the elastic relaxation energy for the first 800 steps of the transformation.

Figure 9. The companion figure of Figures 7 and 8. It shows the average elastic energy per martensite particle.

Figure 10. The prototype simulation of the martensite transformation of multi-nucleus. The variation of the martensite fraction with undercooling, with the temperature measured in energy units ($\mu\varepsilon_o^2 VT_o/N_o\Delta h_o$).

Figure 11. The successive stages of the development in the microstructure associated with the same transformation described in Figure 10.

Figure 12. The energy change associated with each successive elementary transformation associate with Figures 10 and 11. The horizontal lines in these figures show the chemical driving forces, and hence the undercooling, which is necessary to maintain the transformation in progress.

Figure 13. The average elastic energy change per EMP during the transformation associate to Figure 10~12.

Figure 14. The average values of the self energy per EMP including the elastic and chemical energy but excluding the elastic interaction term, and the average total energy per particle during the transformation.

Figure 15. The total energy change during the martensite transformation. The companion figure of Figure 10~14.

Figure 16. The fraction of martensite as a function of undercooling (1) Ten initial nuclei (2) Twenty initial nuclei (3) Forty initial nuclei.

Figure 17. A preliminary example of a martensitic transformation in three dimensions. The section of (001) plane.

Figure 18. The development of the microstructure in a two-dimensional anisotropic crystal and the transformation was assumed to involve a dilatation.

Figure 19. An example of twinned martensite.

Figure 20. The variation of the martensite fraction with temperature in Acoustic Emission test and the electrical resistance test[67].

Figure 21. The Acoustic Emission measurements during the course of a martensitic transformation[67].

Figure 22. The transmission Electron Micrograph of the martensite phase in Fe-Cr-C steel. The retained austenite is shown in the dark field which is obtained from the diffraction spot of the austenitic phase[68,69].

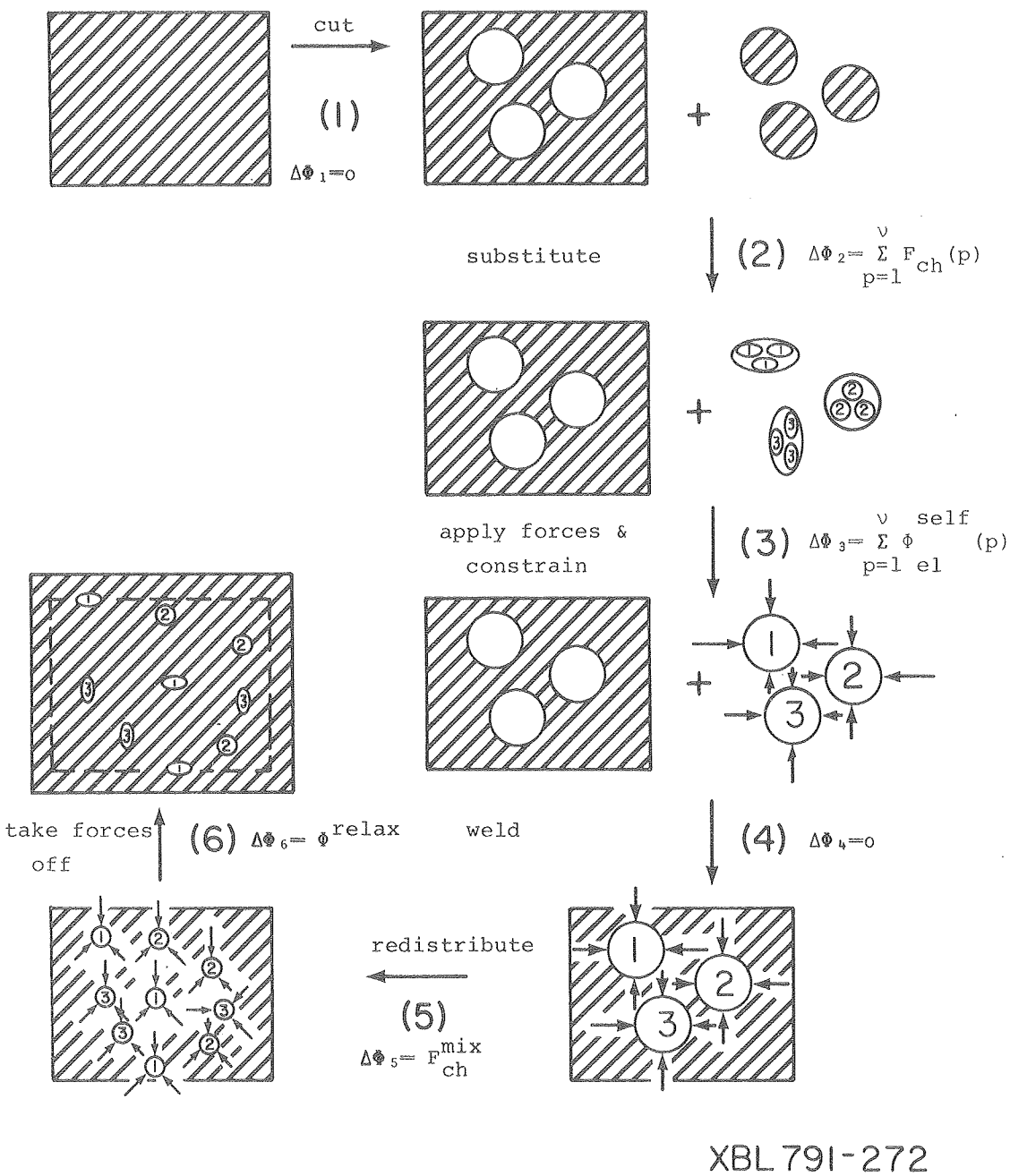
cut
(1)
$\Delta\Phi_1 = 0$
substitute
(2) $\Delta\Phi_2 = \sum_{p=1}^{\nu} F_{ch}(p)$
apply forces & constrain
(3) $\Delta\Phi_3 = \sum_{p=1}^{\nu} \Phi_{el}^{self}(p)$
weld
(4) $\Delta\Phi_4 = 0$
redistribute
(5) $\Delta\Phi_5 = F_{ch}^{mix}$
take forces off
(6) $\Delta\Phi_6 = \Phi^{relax}$
XBL 791-272

Fig. 1

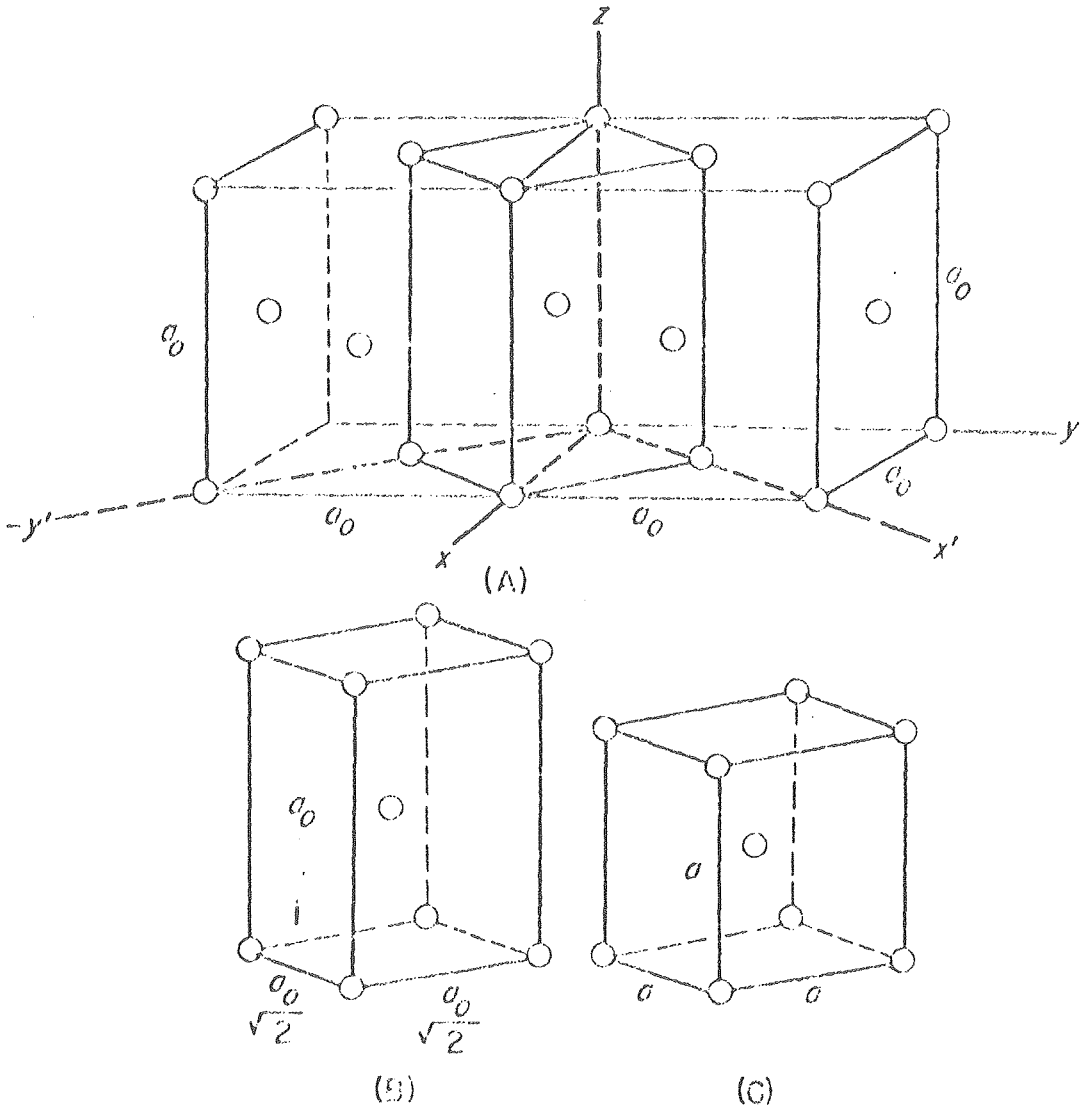

XBL 791-8134

Fig. 2

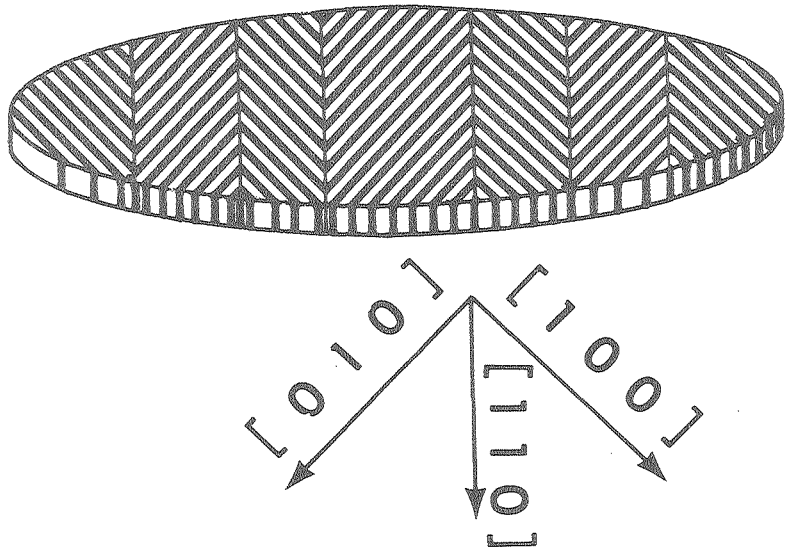

XBL 791-276

Fig. 3

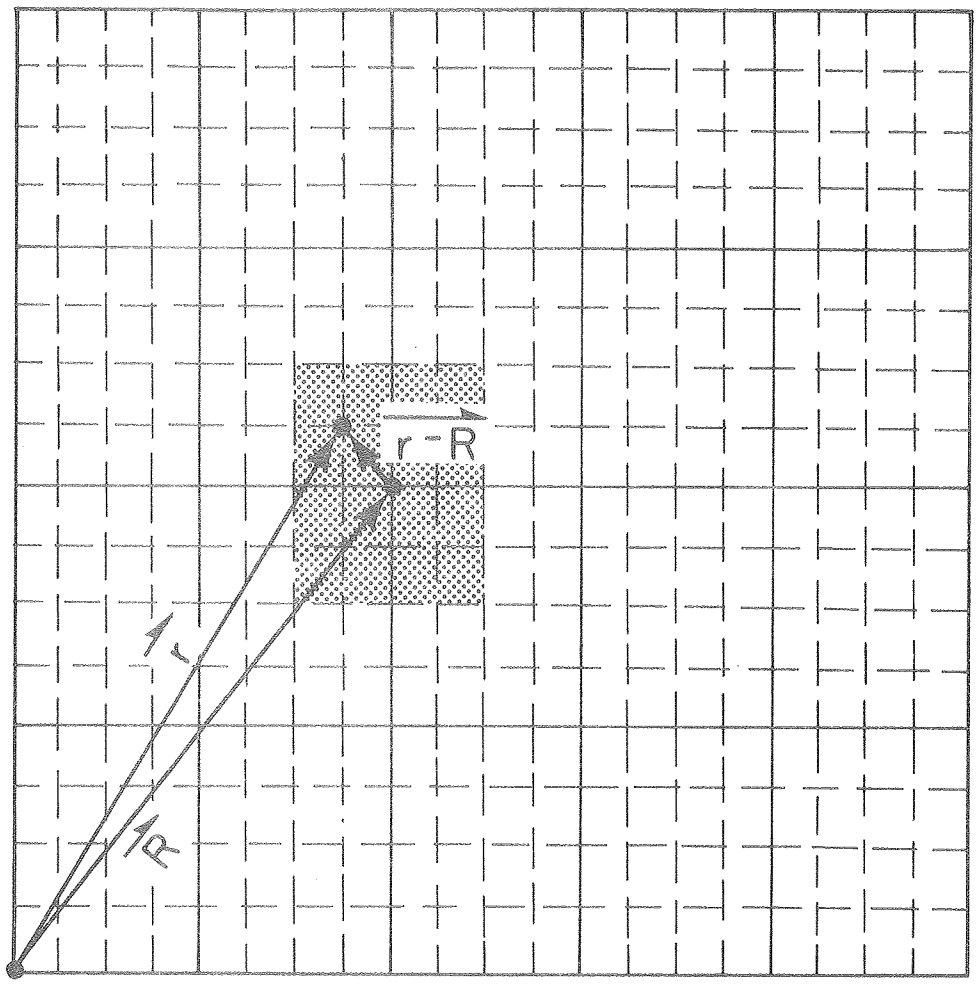

XBL 791 - 275

Fig. 4

Two Dimensional Case

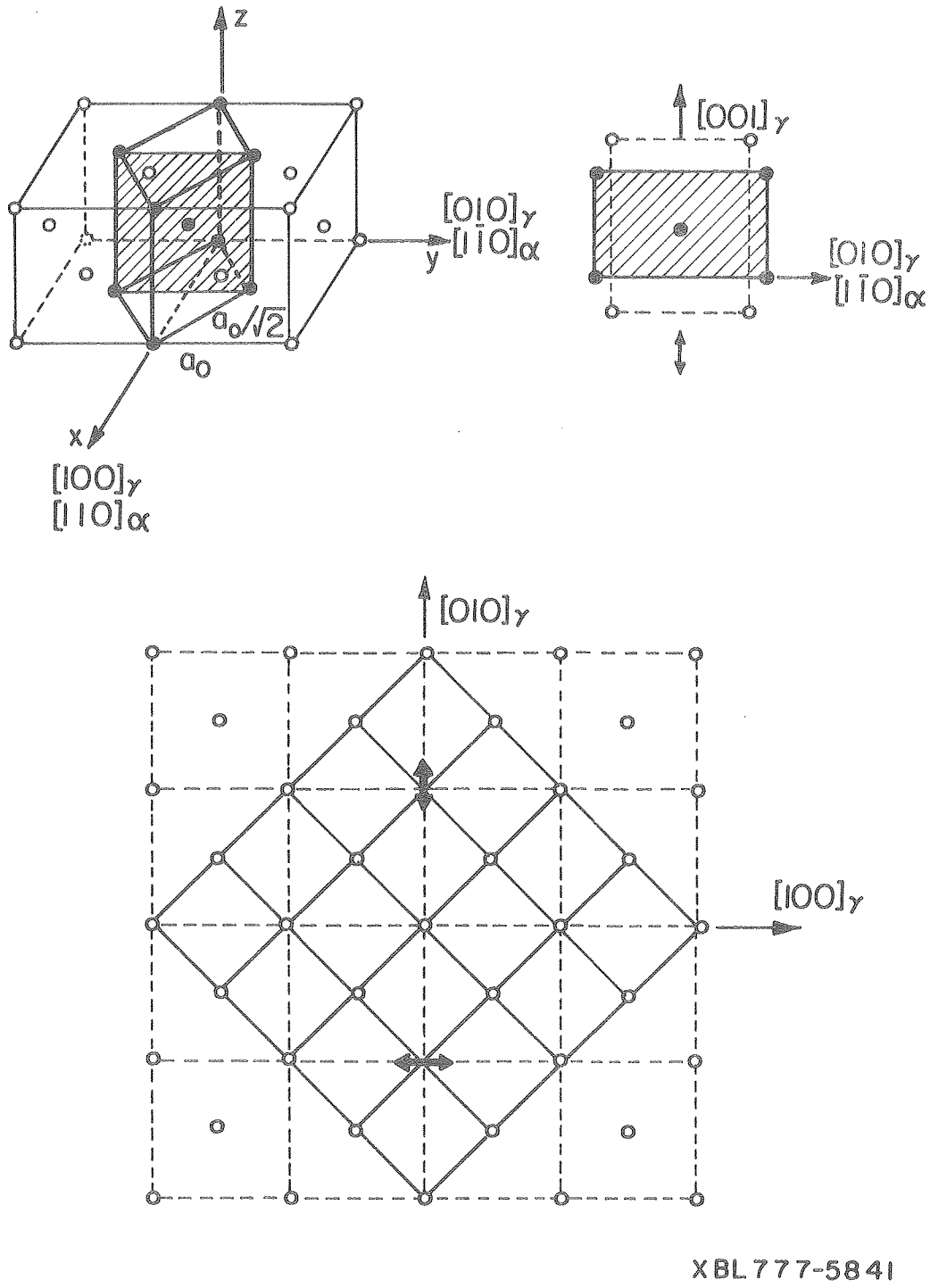

XBL777-5841

Fig. 5

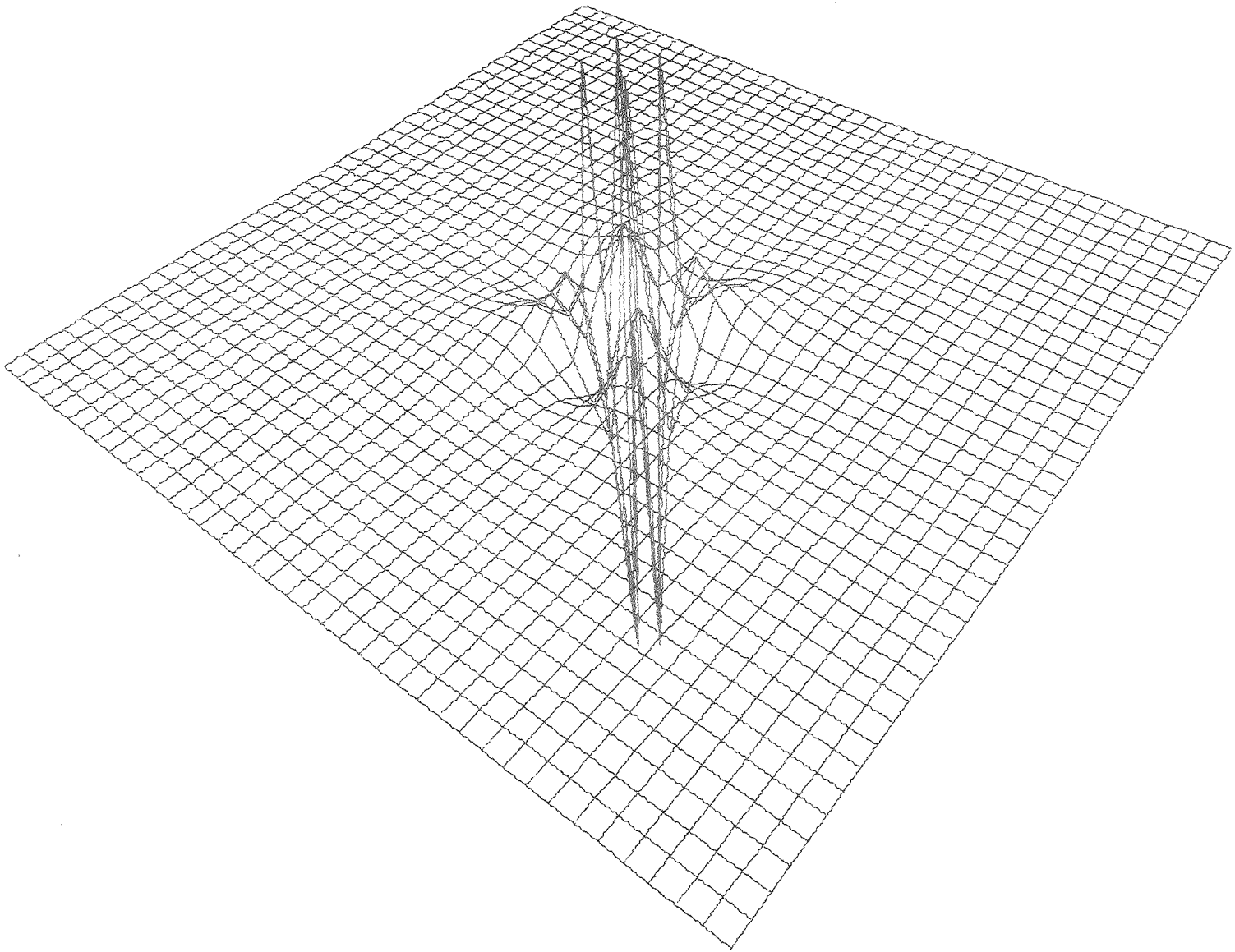

Fig. 6

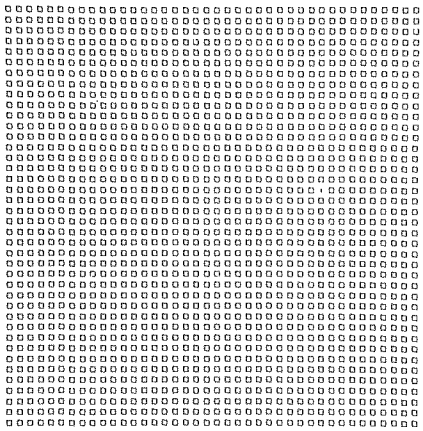

(1)

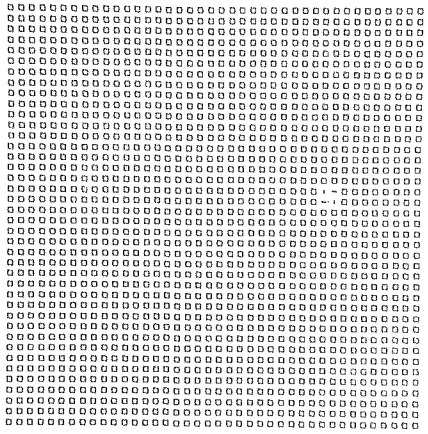

(4)

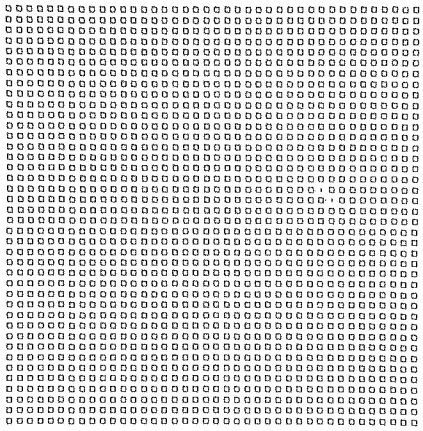

(2)

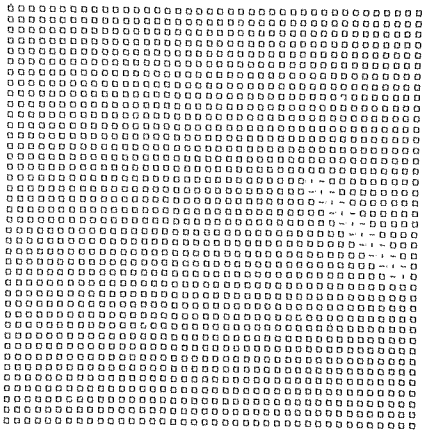

(5)

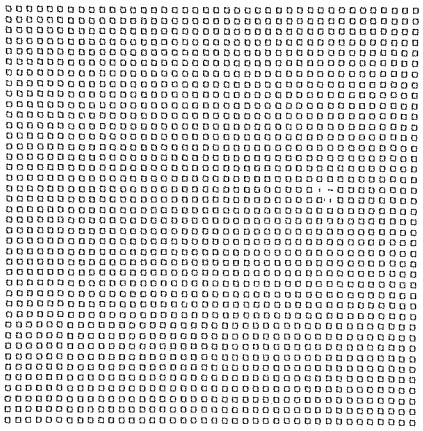

(3)

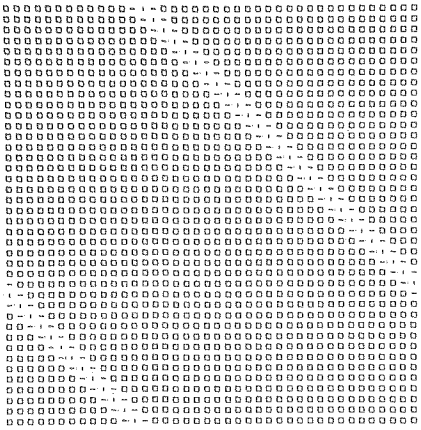

(6)

Fig. 7

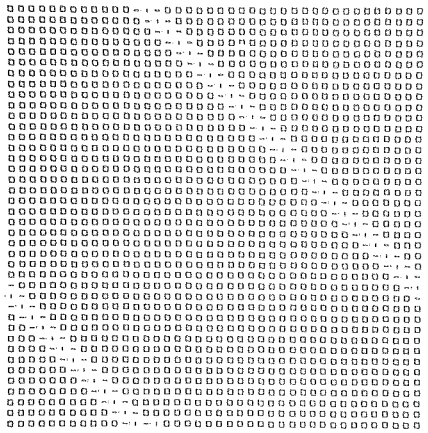

(7)

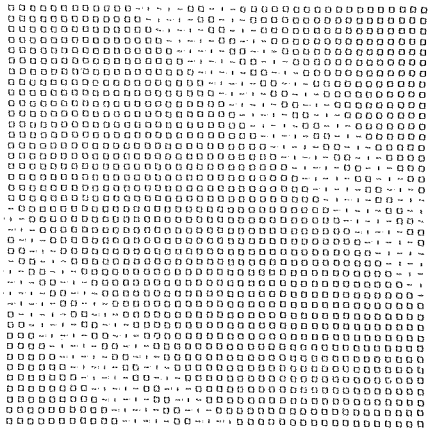

(10)

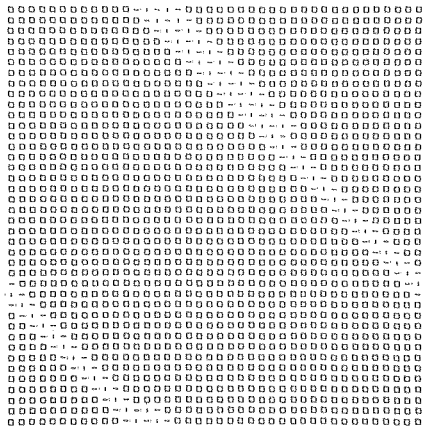

(8)

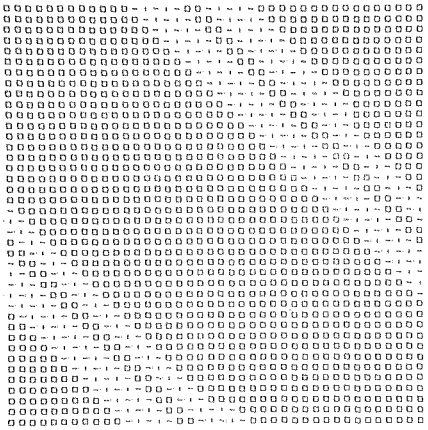

(11)

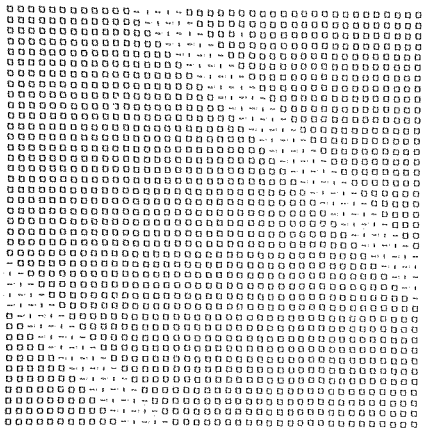

(9)

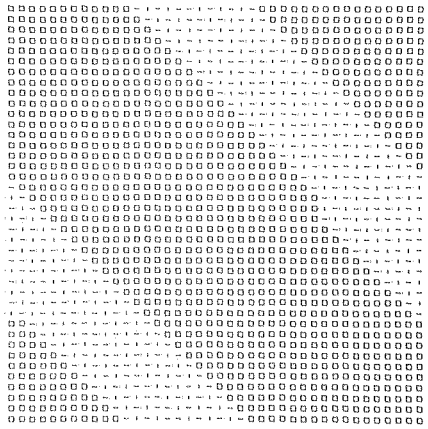

(12)

Fig. 7

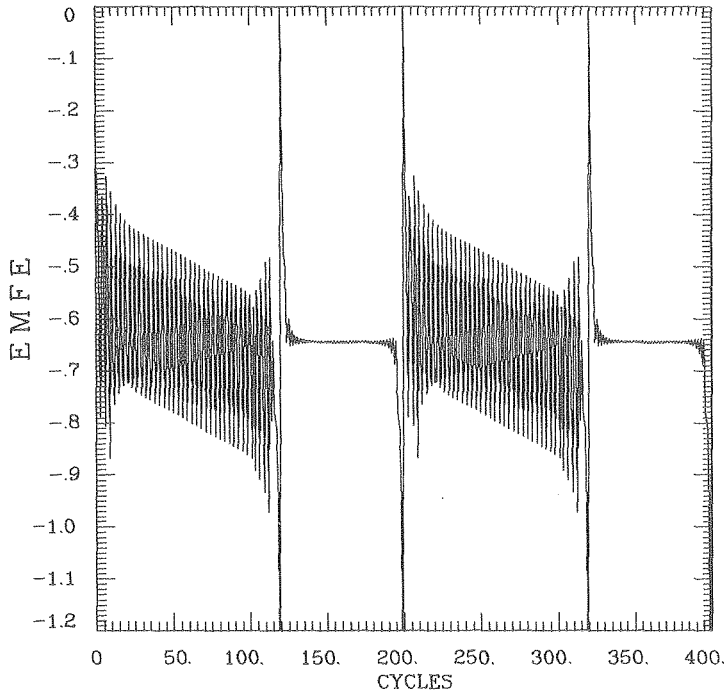
0
-.1
-.2
-.3
-.4
-.5
-.6
-.7
-.8
-.9
-1.0
-1.1
-1.2
EMFE
0
50.
100.
150.
200.
250.
300.
350.
400.
CYCLES

(1)

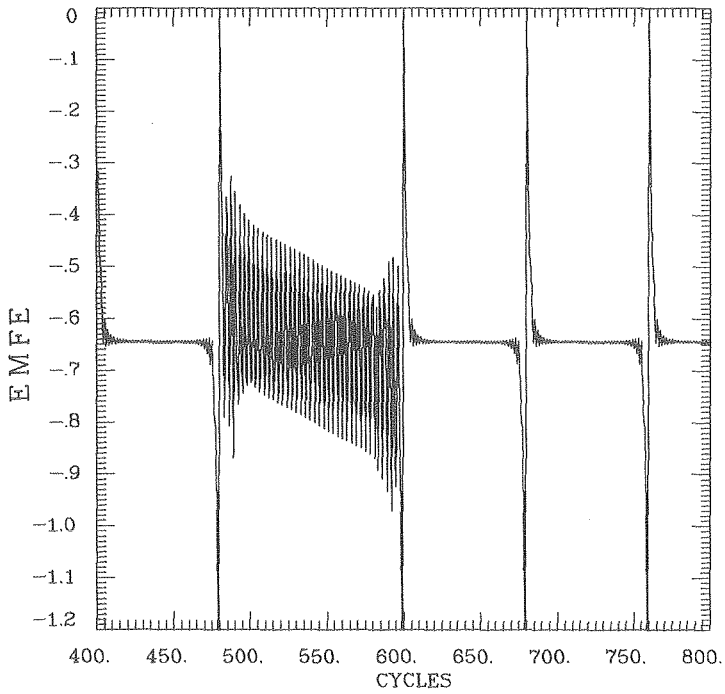
0
-.1
-.2
-.3
-.4
-.5
-.6
-.7
-.8
-.9
-1.0
-1.1
-1.2
EMFE
400.
450.
500.
550.
600.
650.
700.
750.
800.
CYCLES
XBL 792-8217

(2)

Fig. 8

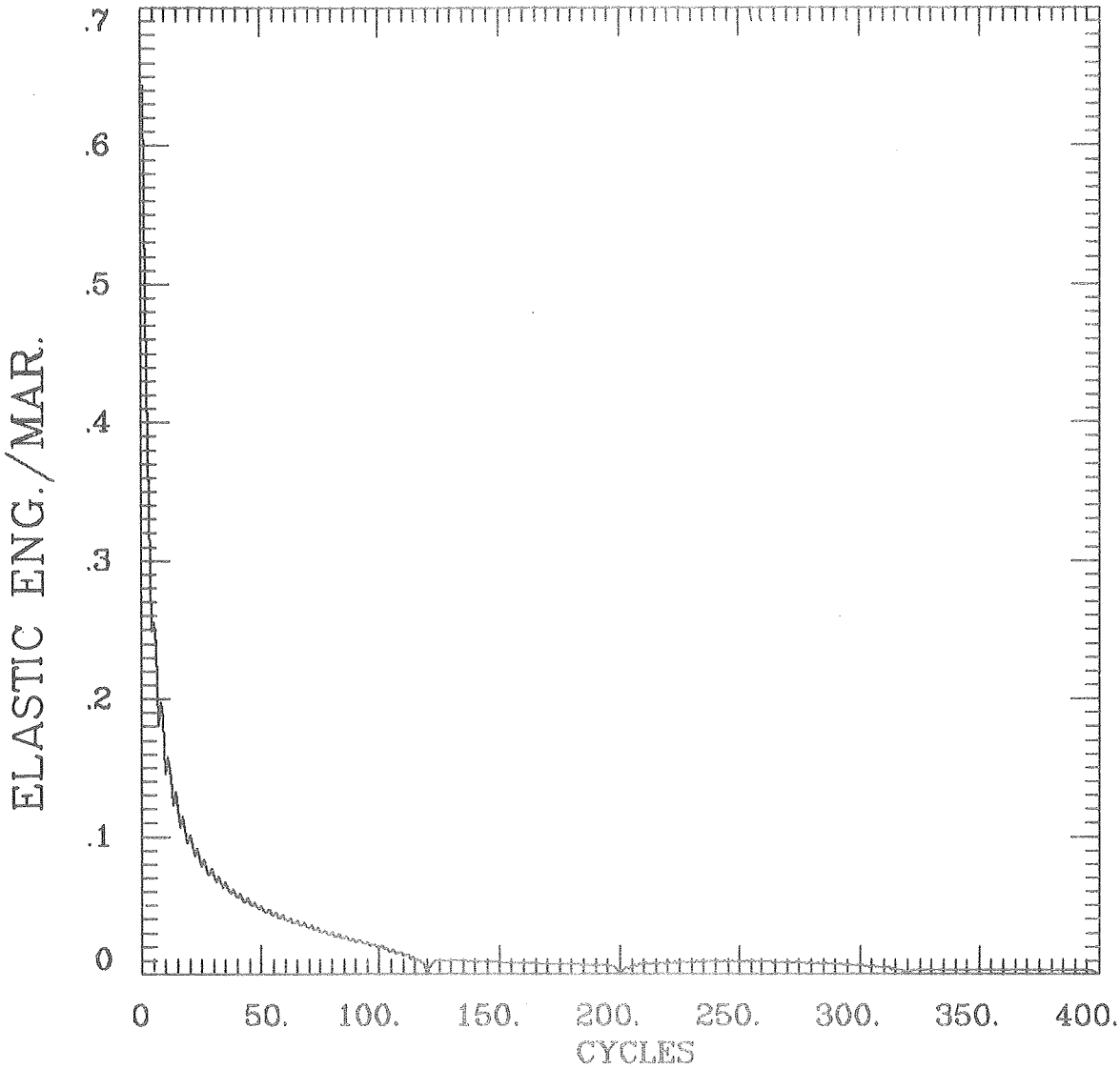

XBL 792-8193

Fig. 9

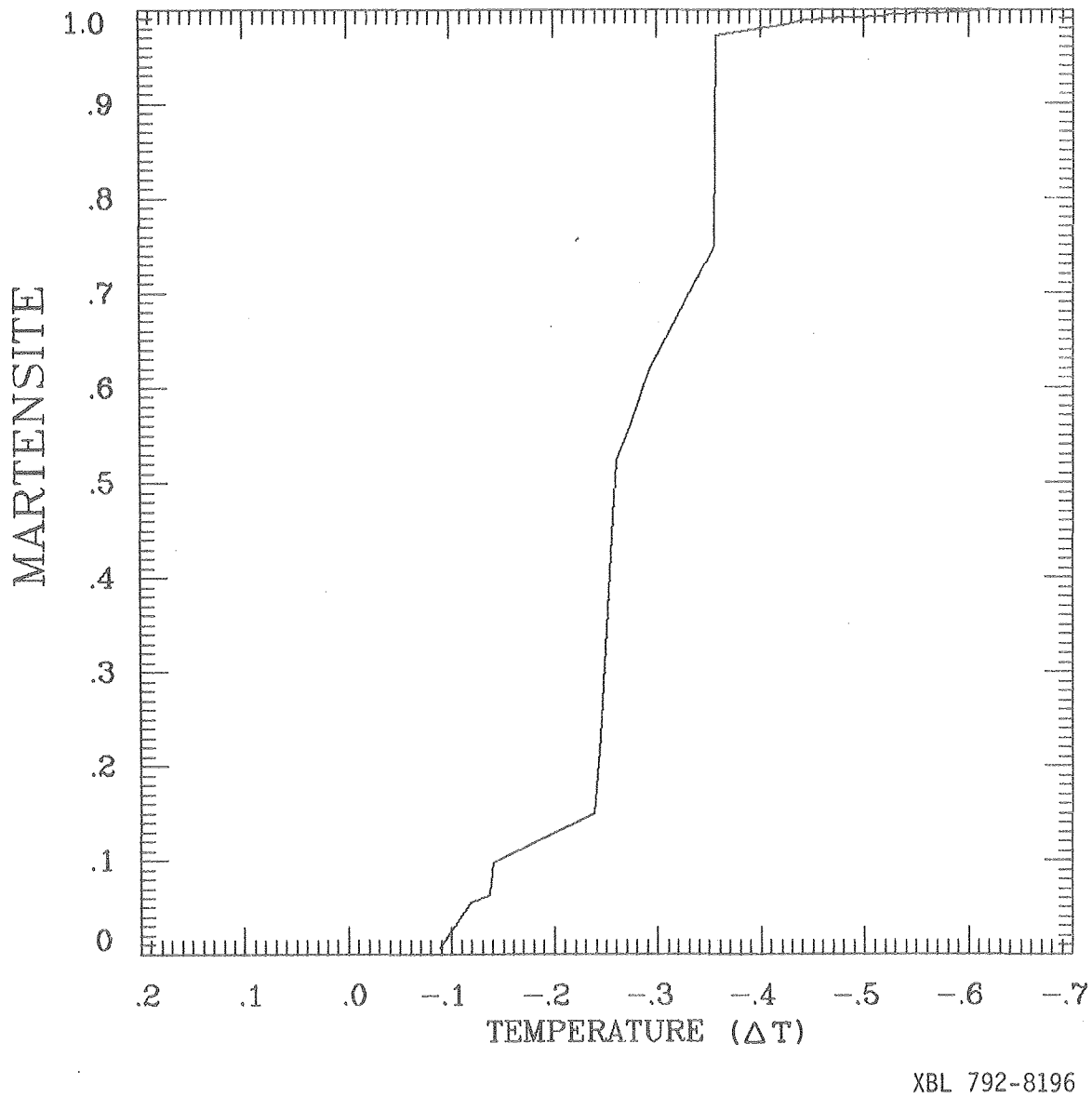

XBL 792-8196

Fig. 10

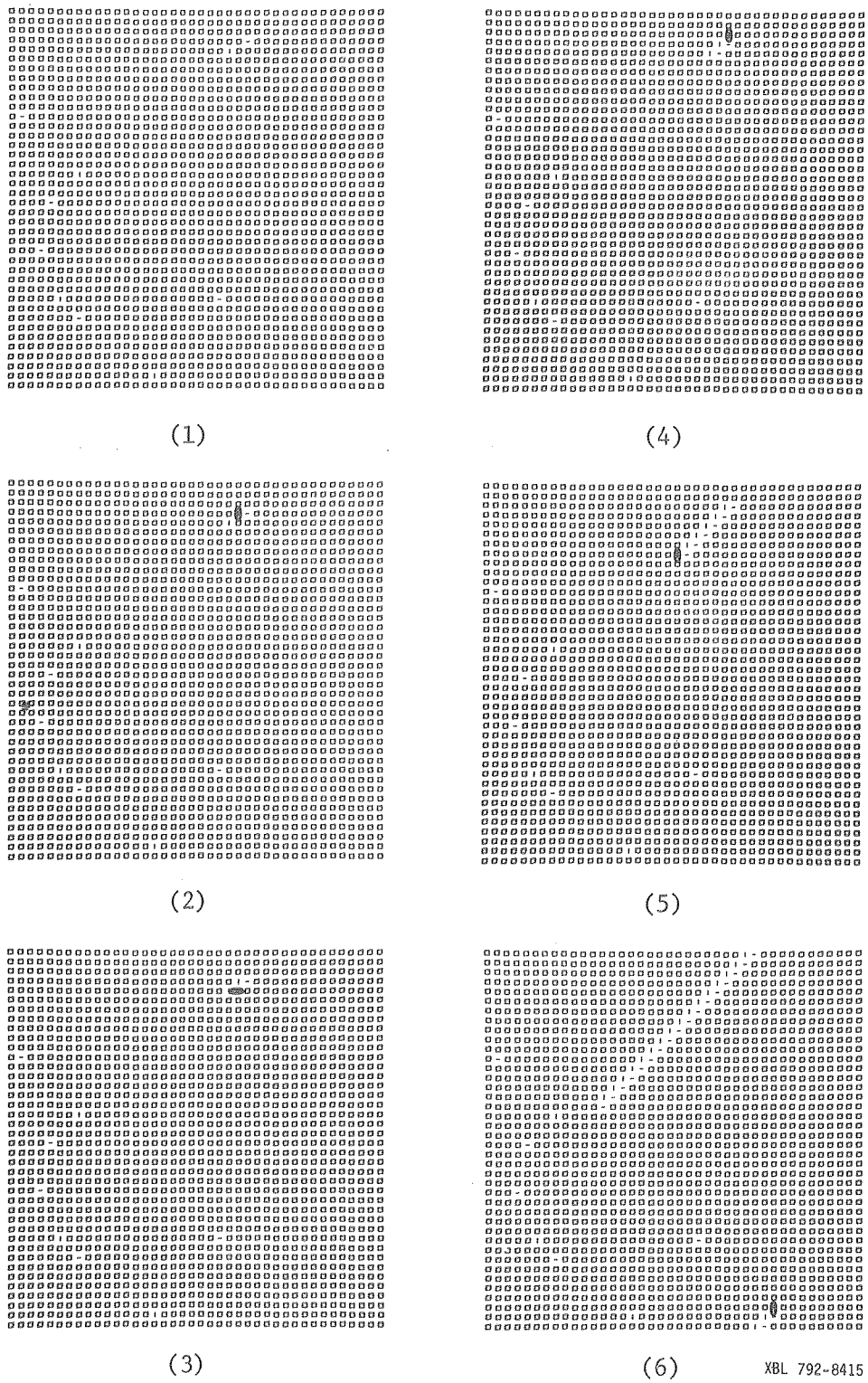

Fig. 11

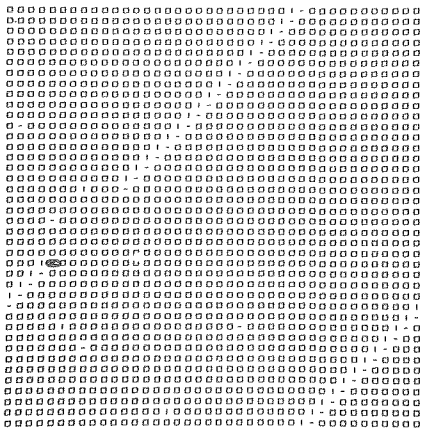

(7)

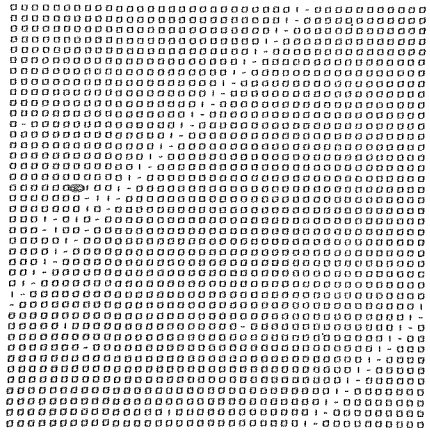

(10)

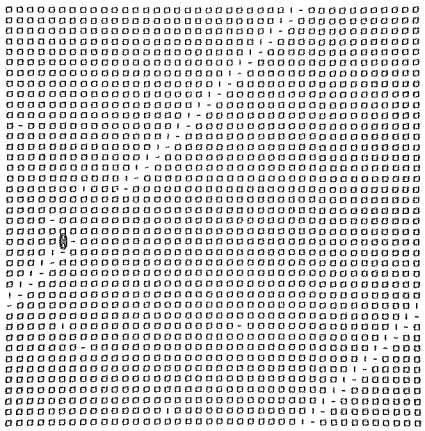

(8)

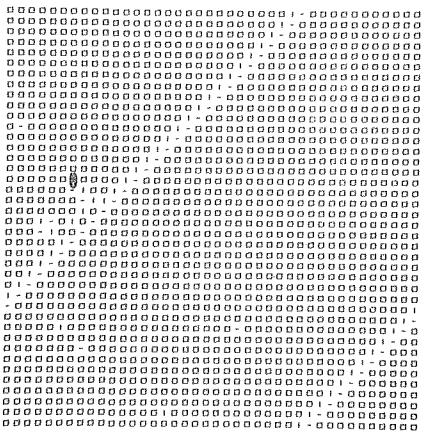

(11)

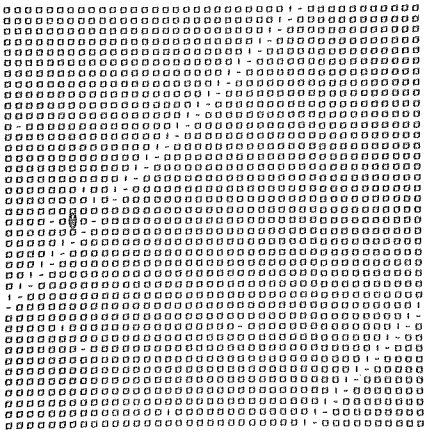

(9)

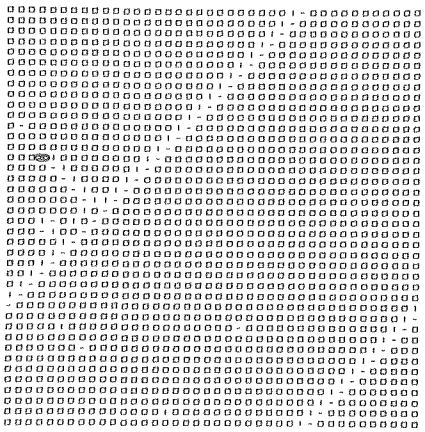

(12)

XBL 792-8420

Fig. 11

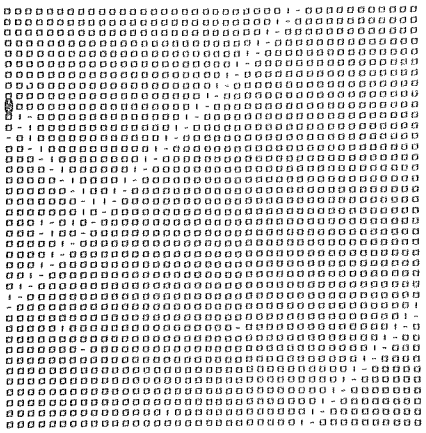

(13)

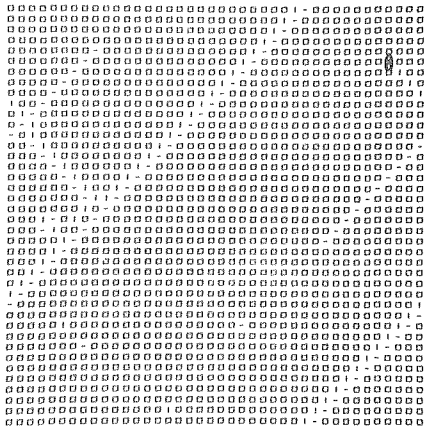

(16)

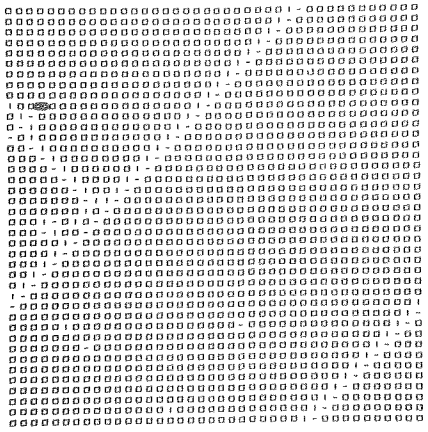

(14)

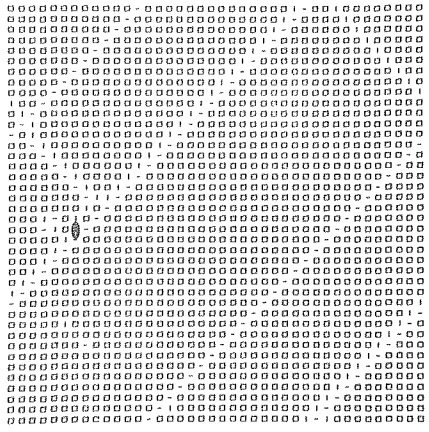

(17)

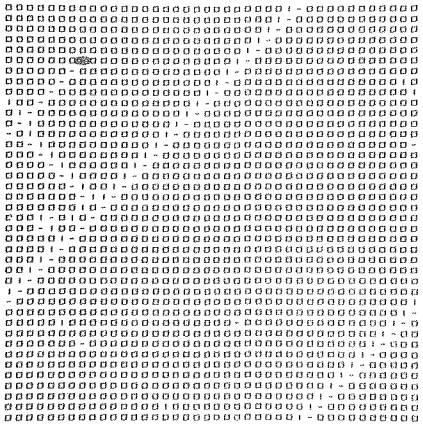

(15)

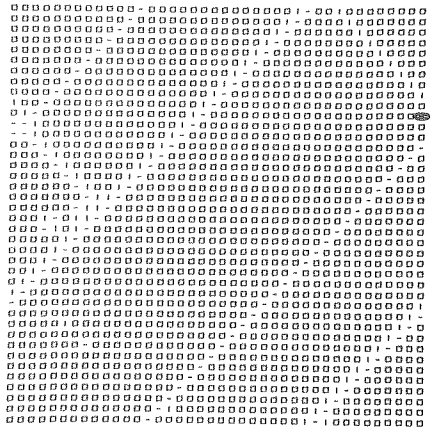

(18)

XBL 792-8412

Fig. 11

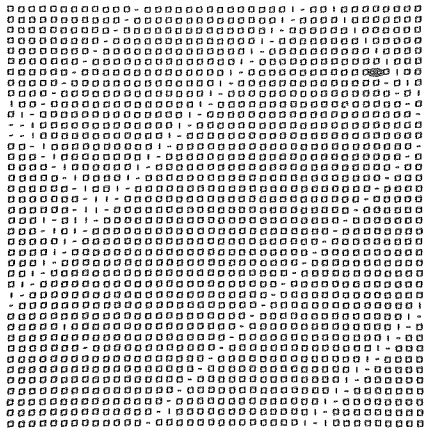

(19)

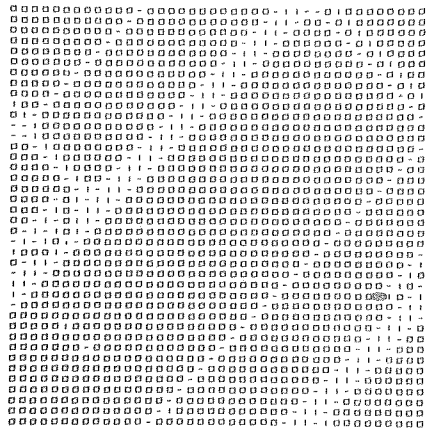

(22)

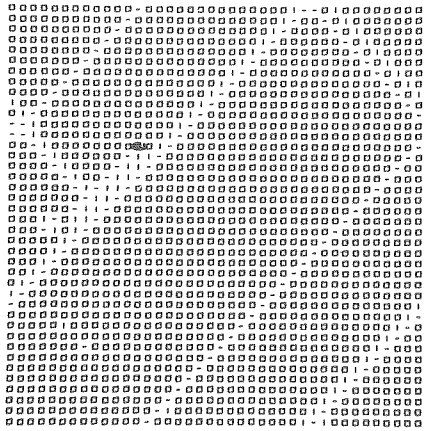

(20)

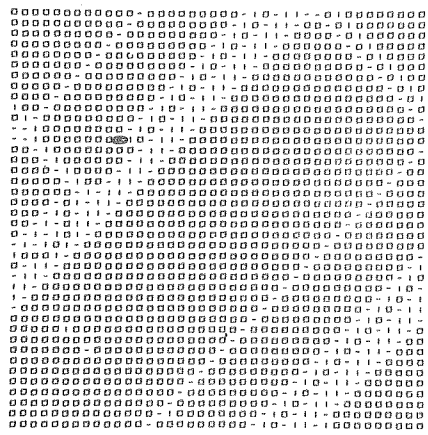

(23)

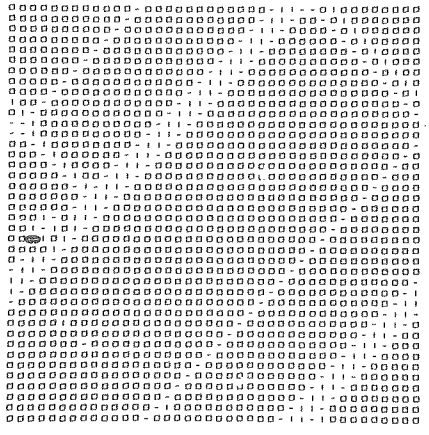

(21)

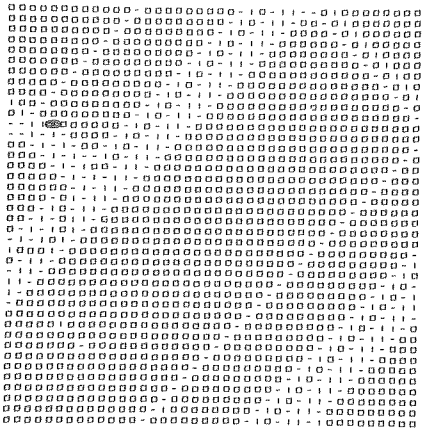

(24)

XBL 792-8413

Fig. 11

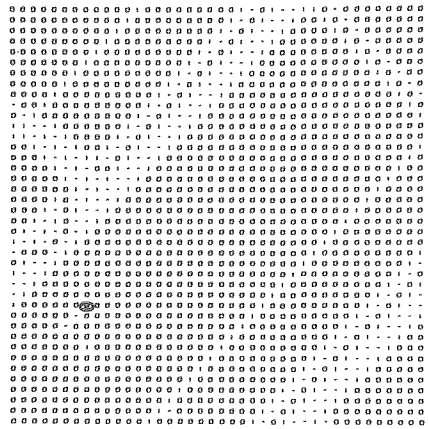

(25)

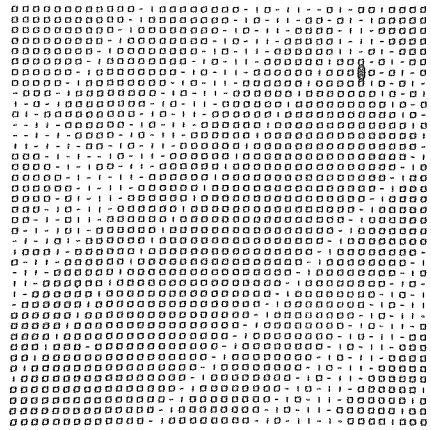

(28)

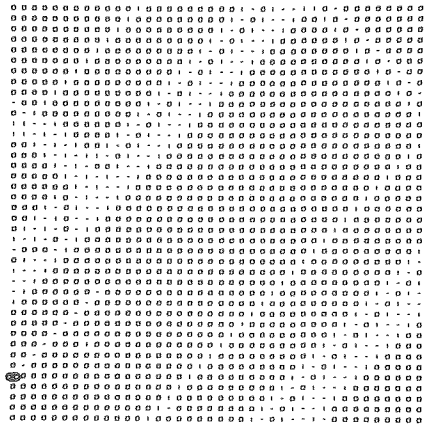

(26)

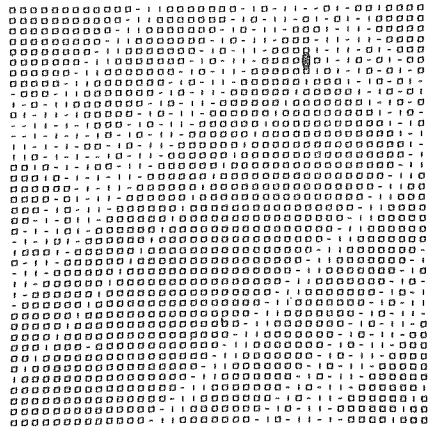

(29)

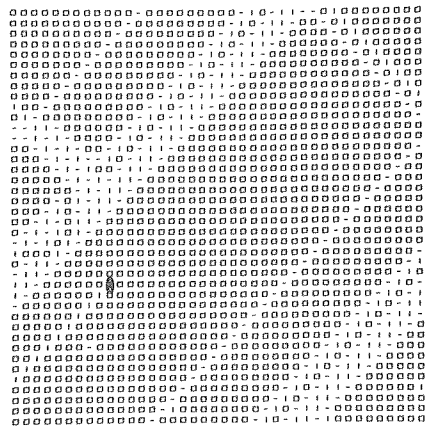

(27)

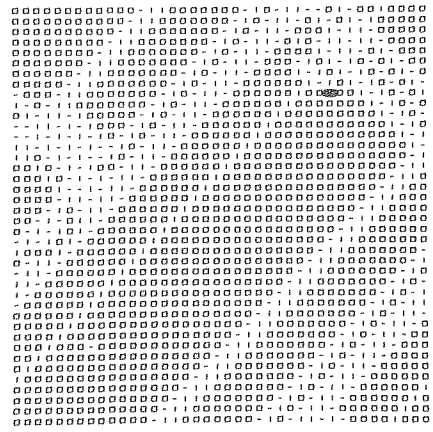

(30)

XBL 792-8416

Fig. 11

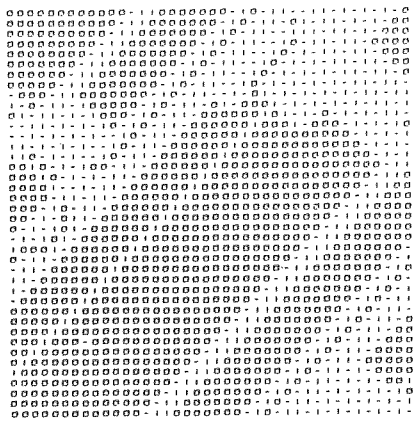

(31)

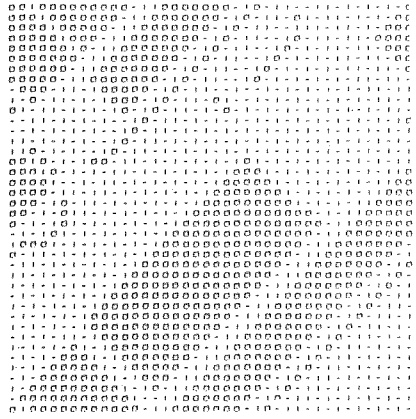

(34)

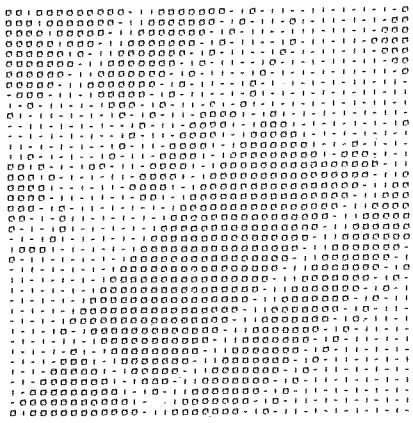

(32)

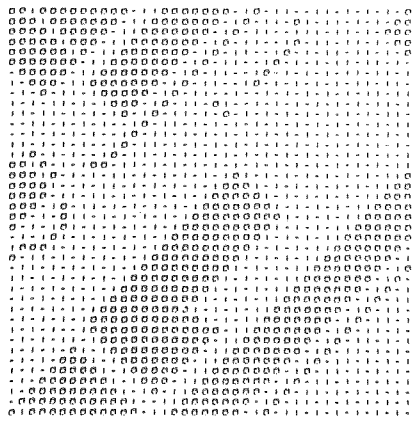

(35)

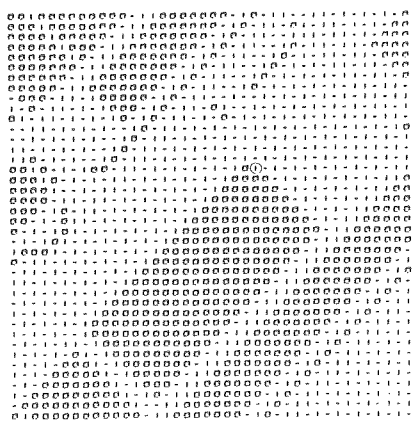

(33)

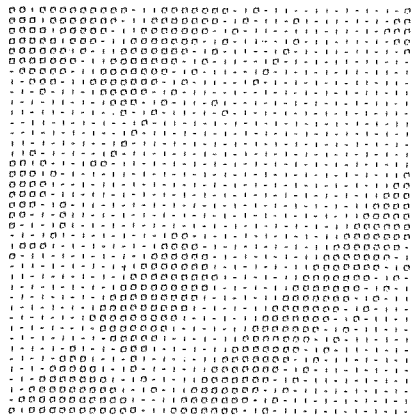

(36)

XBL 792-8417

Fig. 11

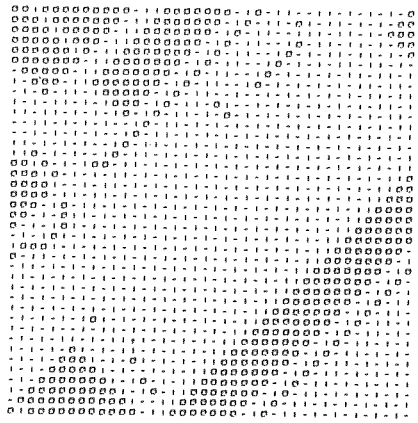

(37)

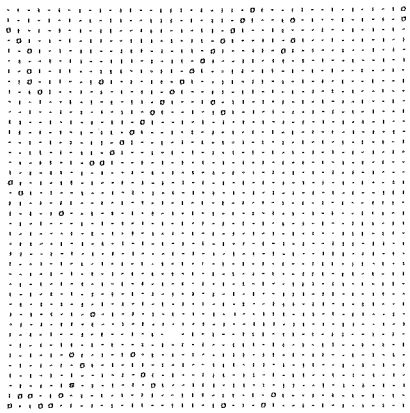

(40)

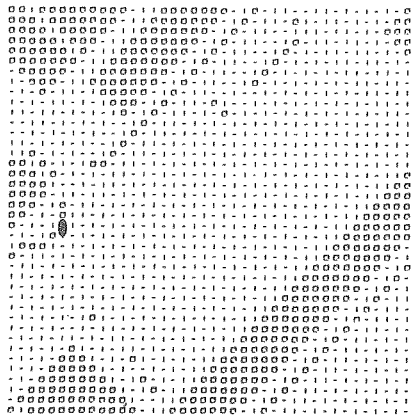

(38)

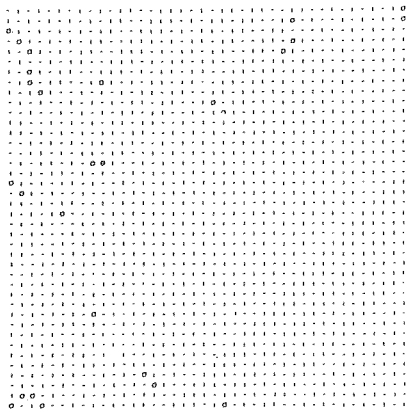

(41)

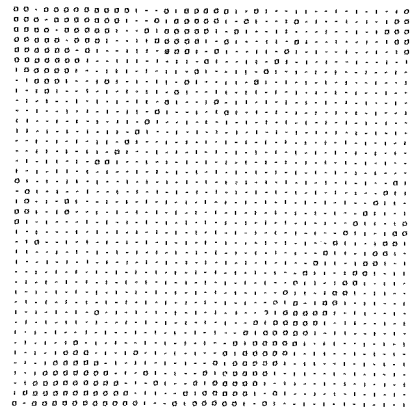

(39)

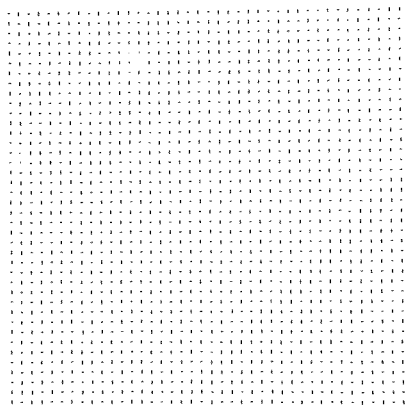

(42) XBL 796-10030

Fig. 11

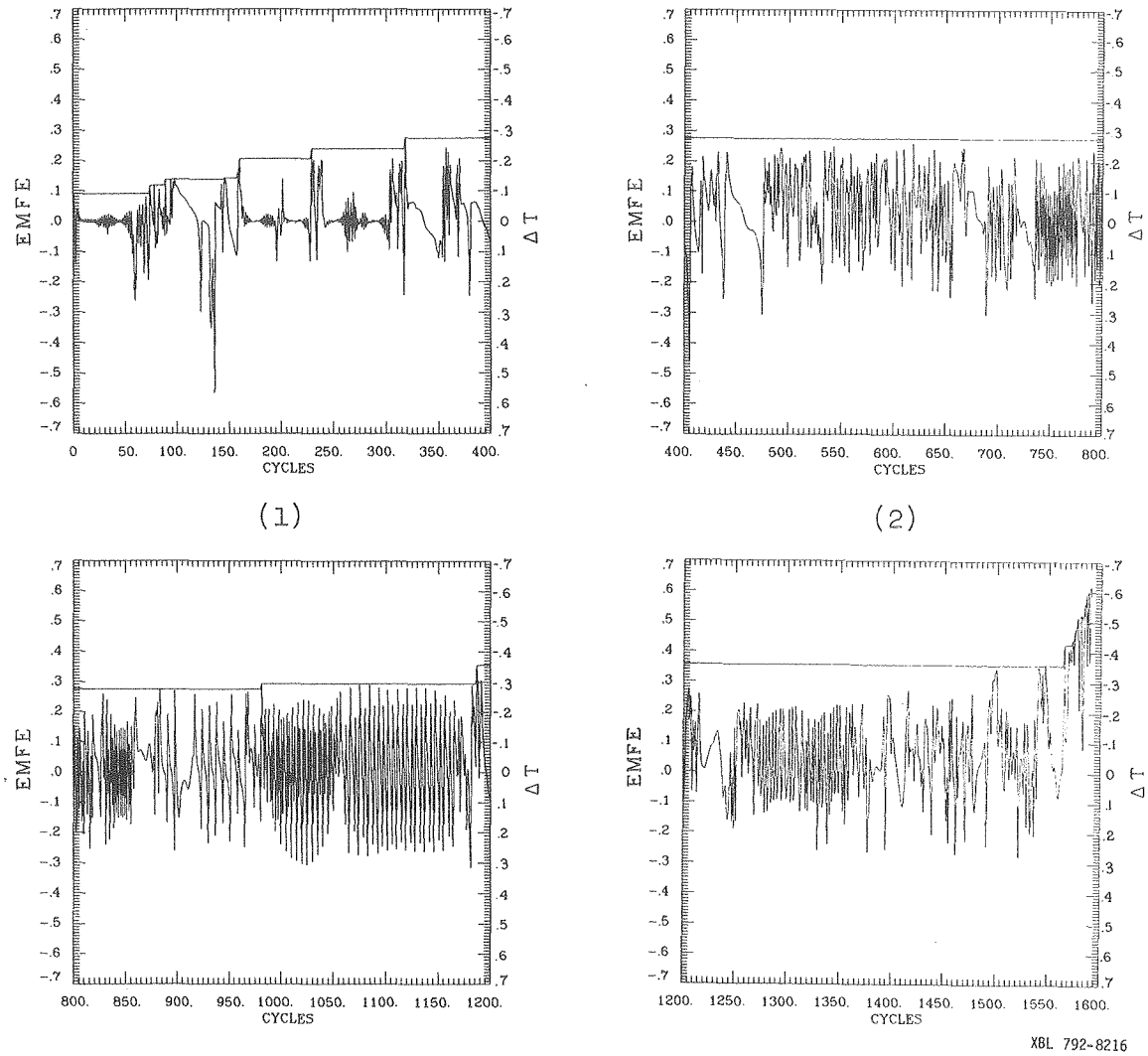

Fig. 12

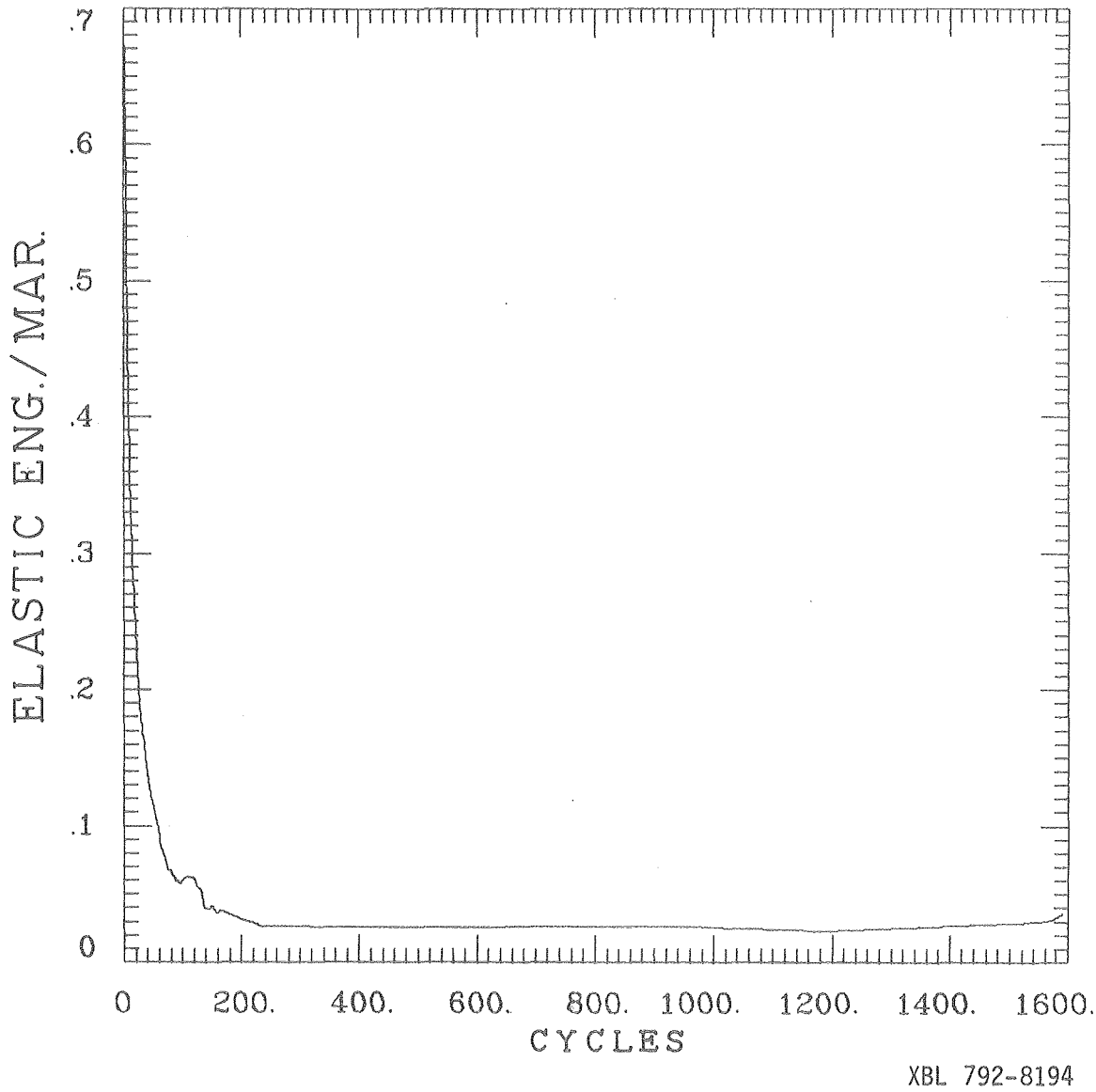
ELASTIC ENG./MAR.
.7
.6
.5
.4
.3
.2
.1
0
0
200.
400.
600.
800.
1000.
1200.
1400.
1600.
CYCLES
XBL 792-8194

Fig. 13

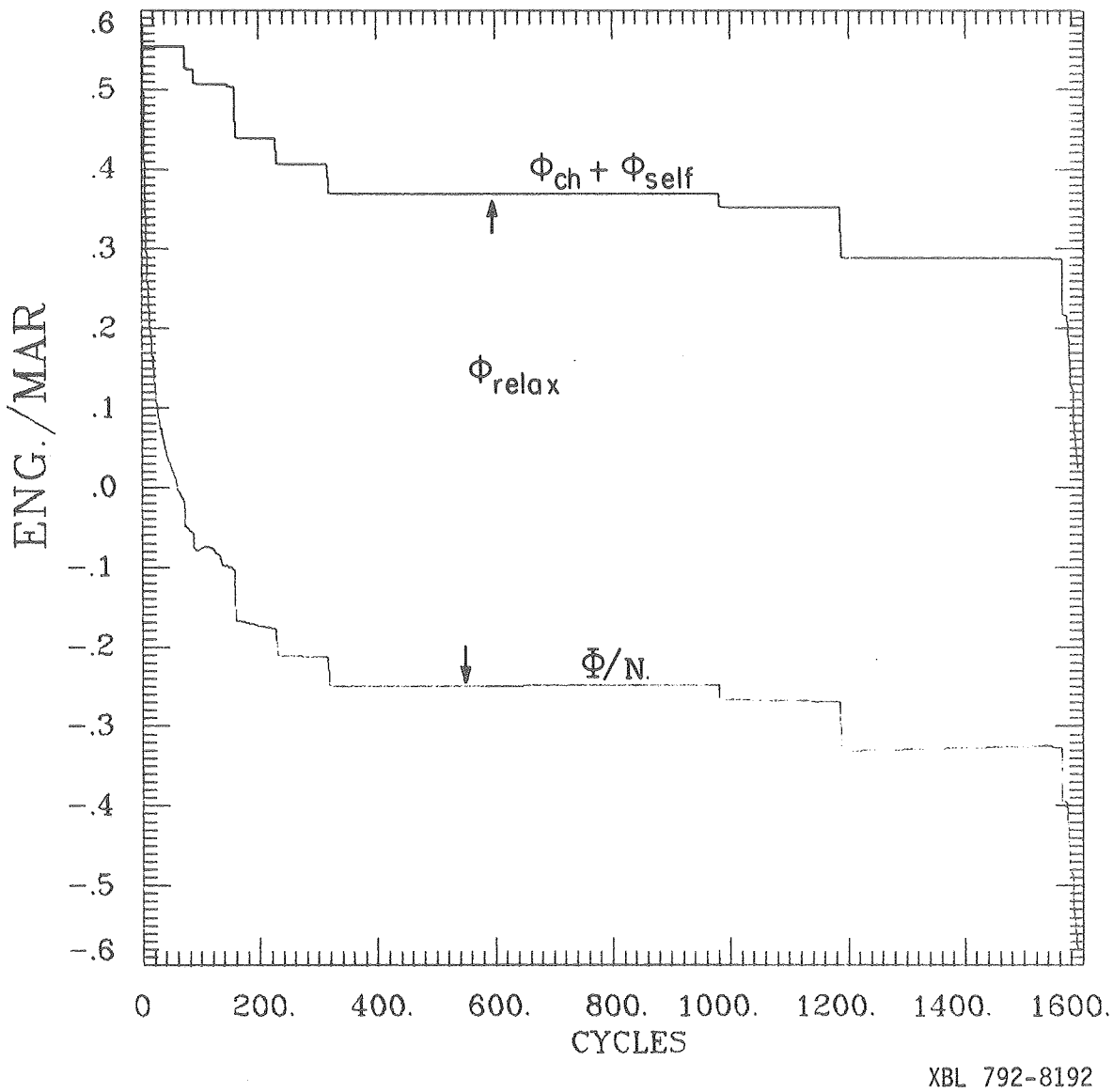
.6
.5
.4
.3
.2
.1
.0
-.1
-.2
-.3
-.4
-.5
-.6
ENG./MAR
$\Phi_{ch} + \Phi_{self}$
Φ_{relax}
Φ/N
0
200.
400.
600.
800.
1000.
1200.
1400.
1600.
CYCLES
XBL 792-8192

Fig. 14

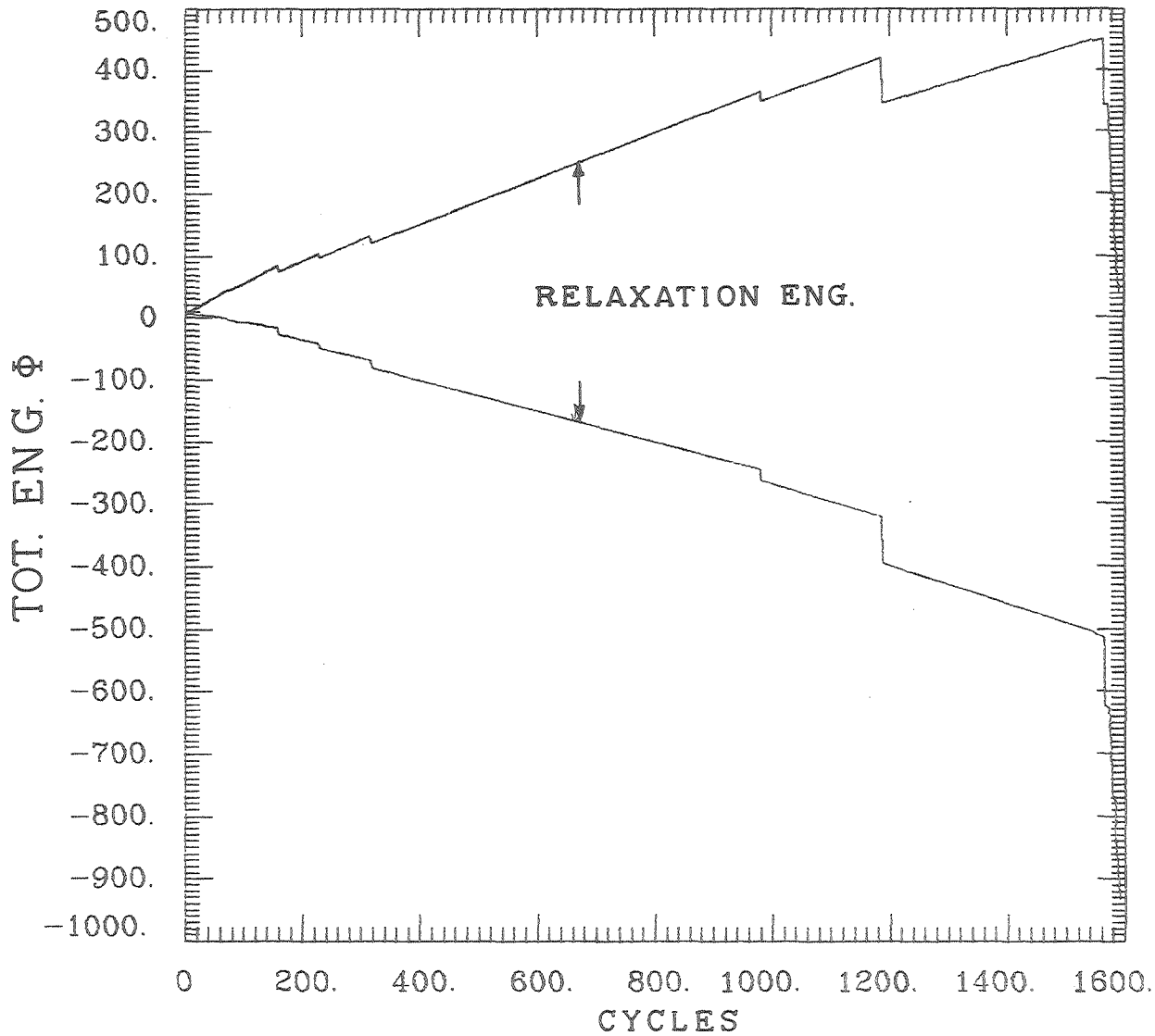

XBL 792-8195

Fig. 15

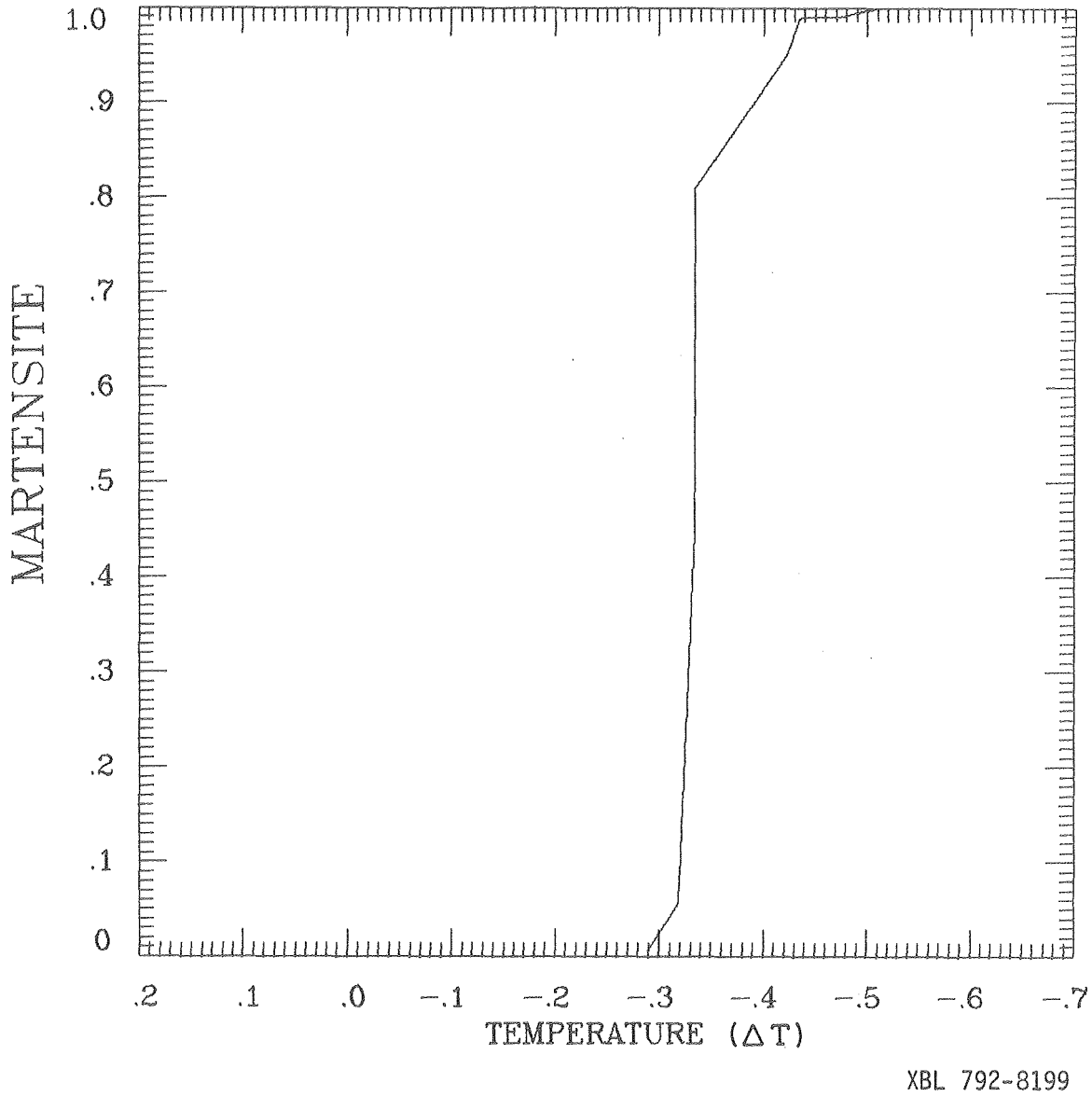
1.0
.9
.8
.7
.6
.5
.4
.3
.2
.1
0
MARTENSITE
.2
.1
.0
−.1
−.2
−.3
−.4
−.5
−.6
−.7
TEMPERATURE (ΔT)
XBL 792-8199

Fig. 16-1

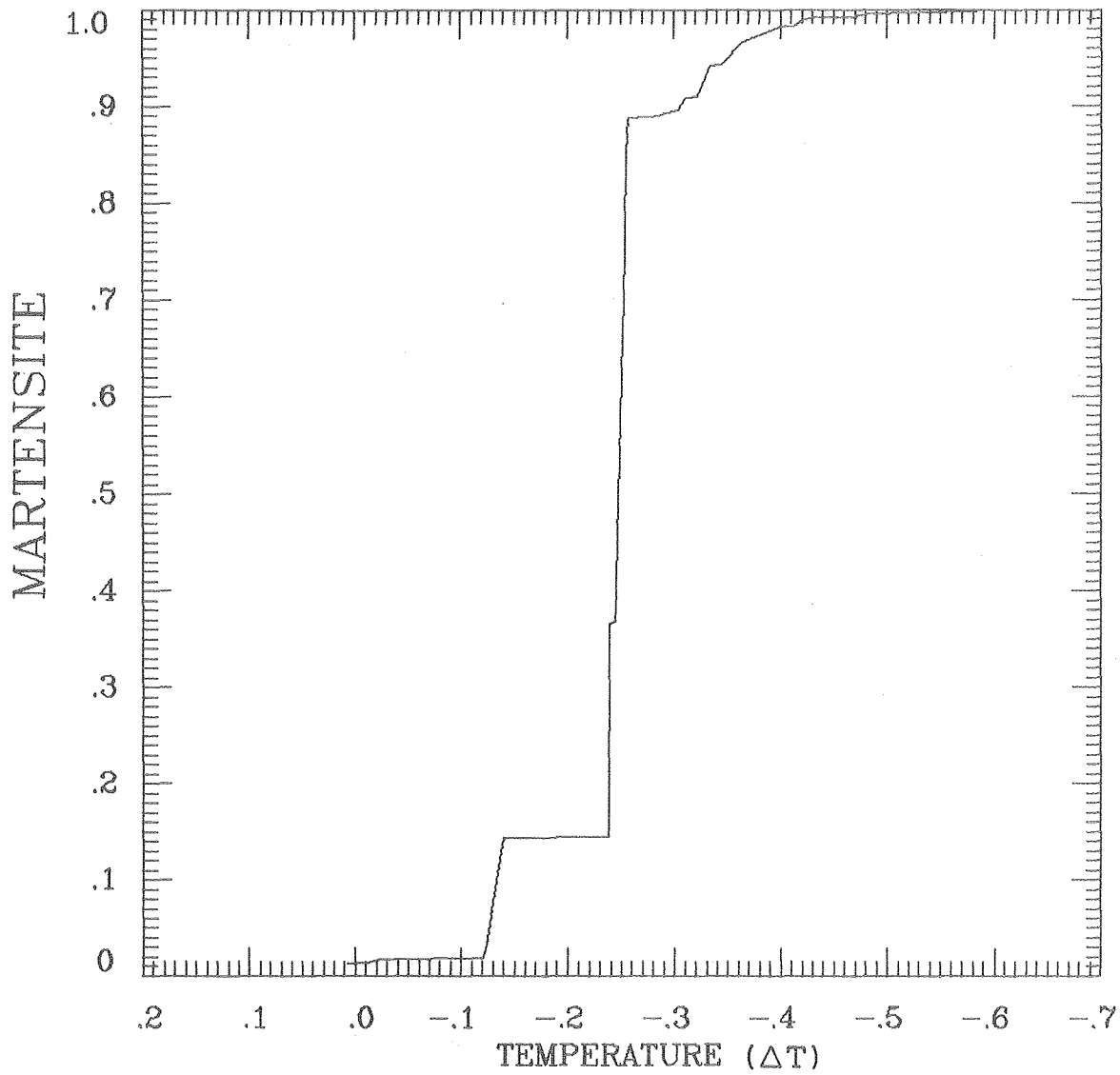

XBL 792-8198

Fig. 16-2

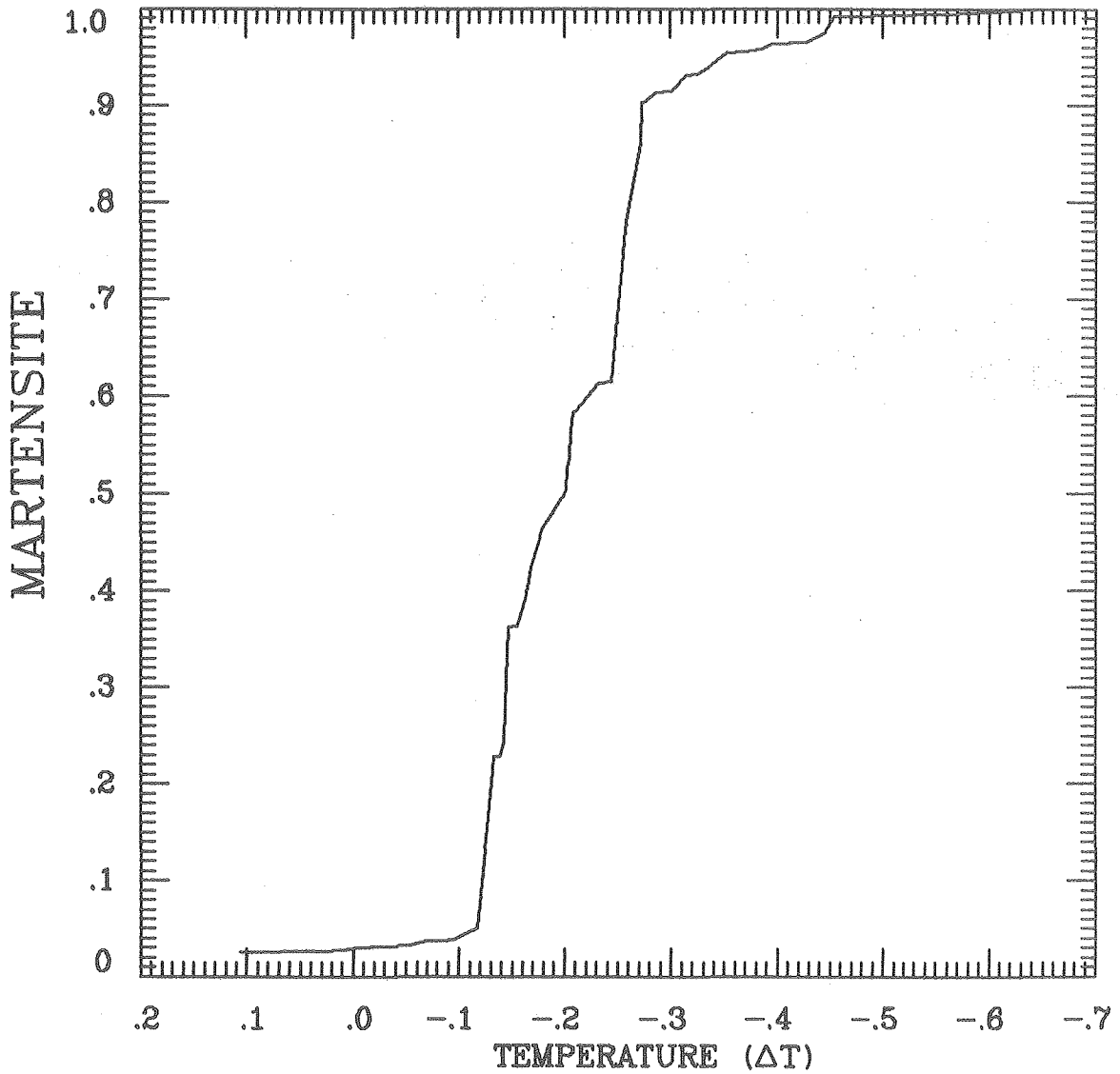

XBL 792-8197

Fig. 16-3

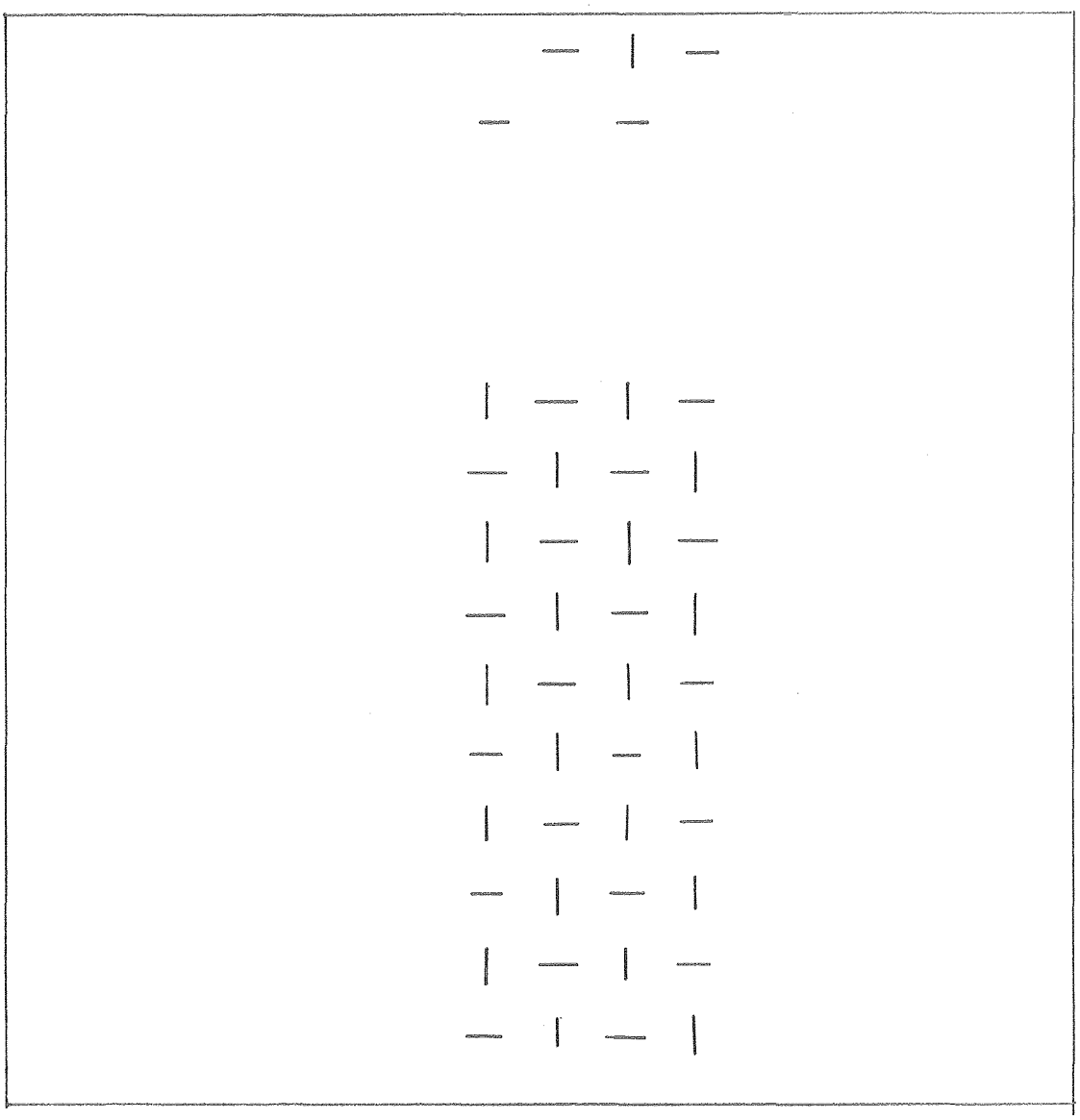

Fig. 17

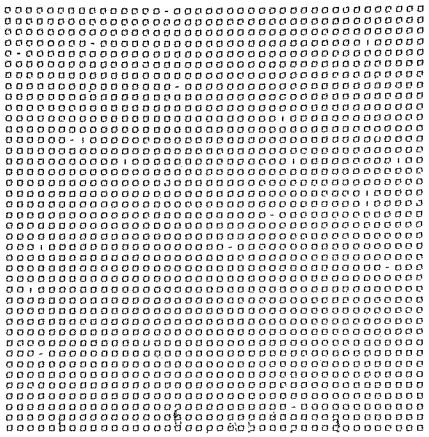

(1)

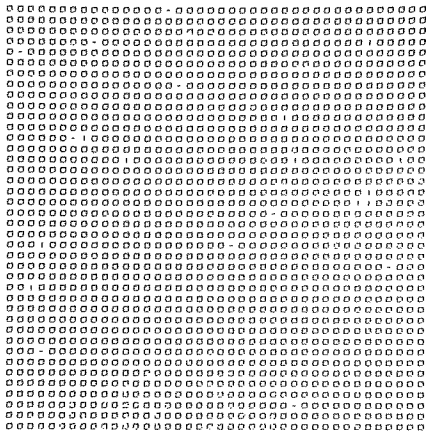

(2)

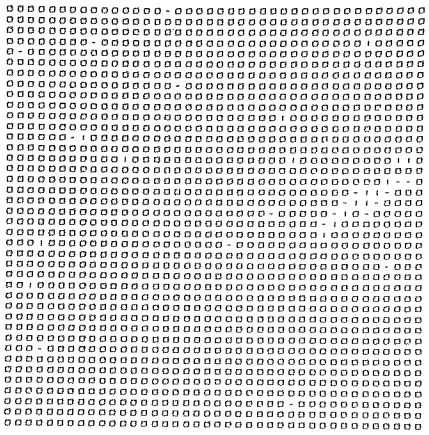

(3)

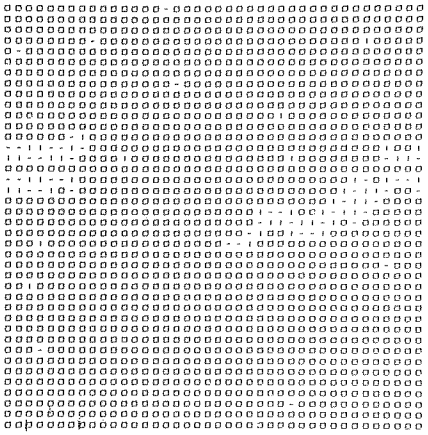

(4)

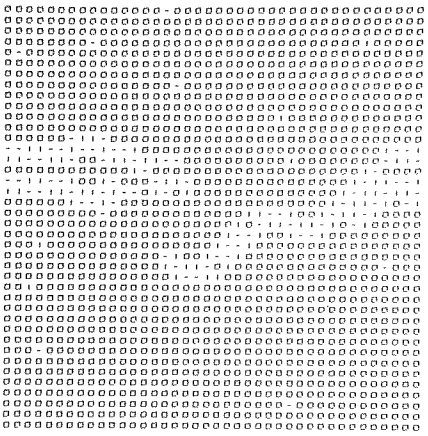

(5)

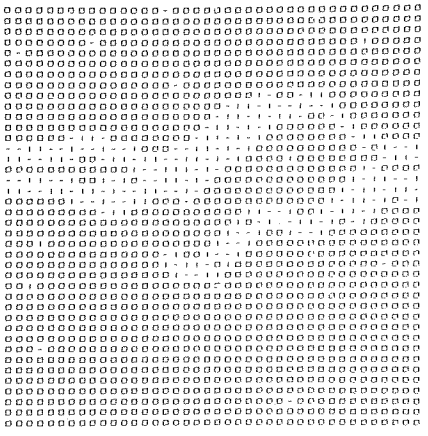

(6)

Fig. 18

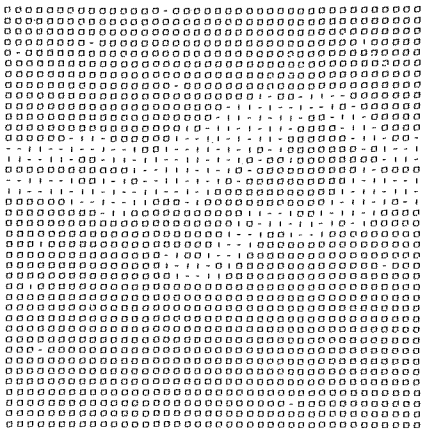

(7)

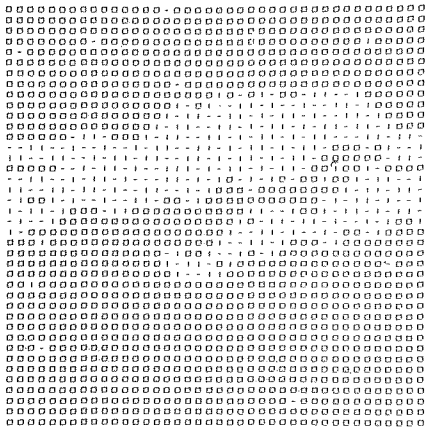

(10)

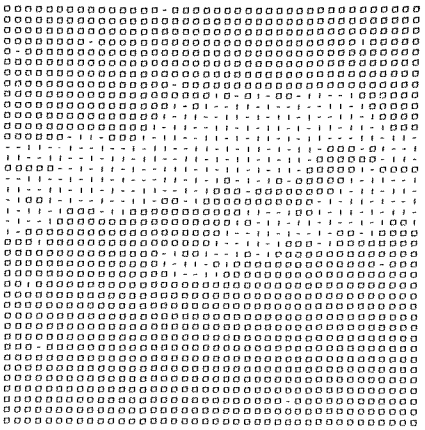

(8)

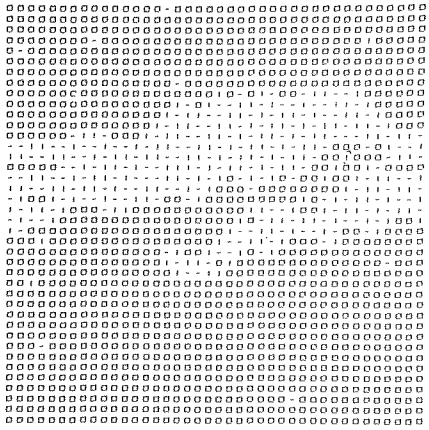

(11)

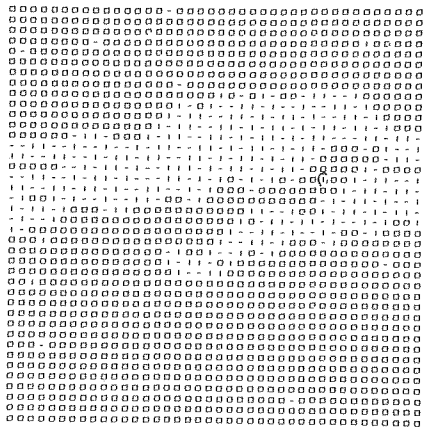

(9)

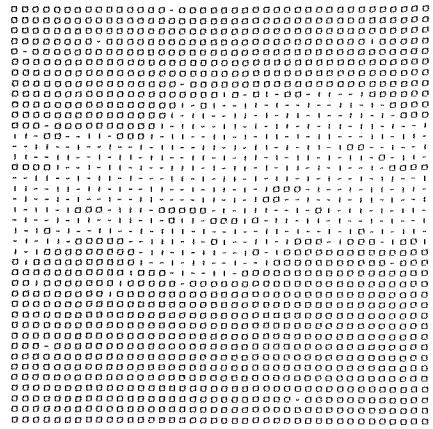

(12)

Fig. 18

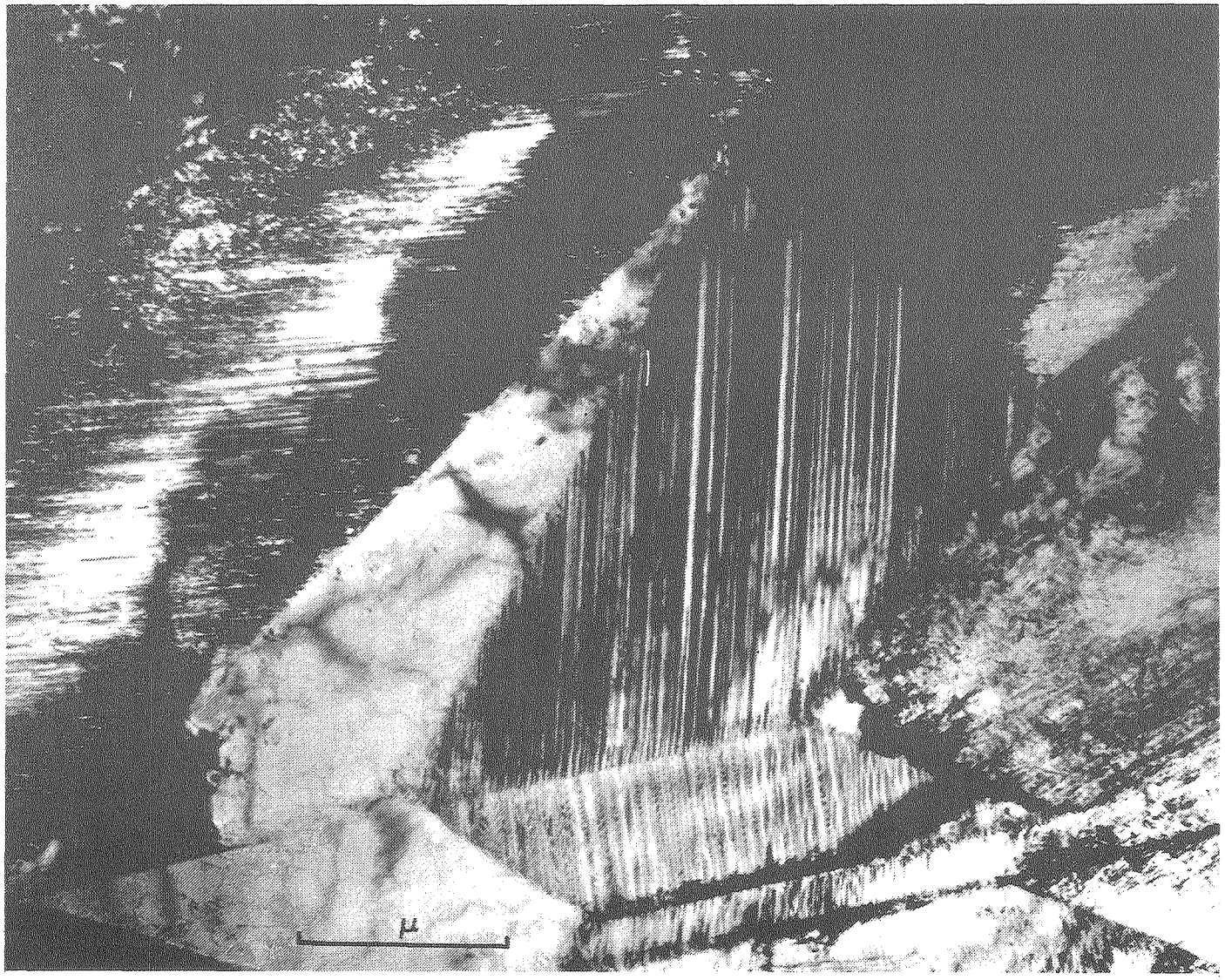

Fig. 19

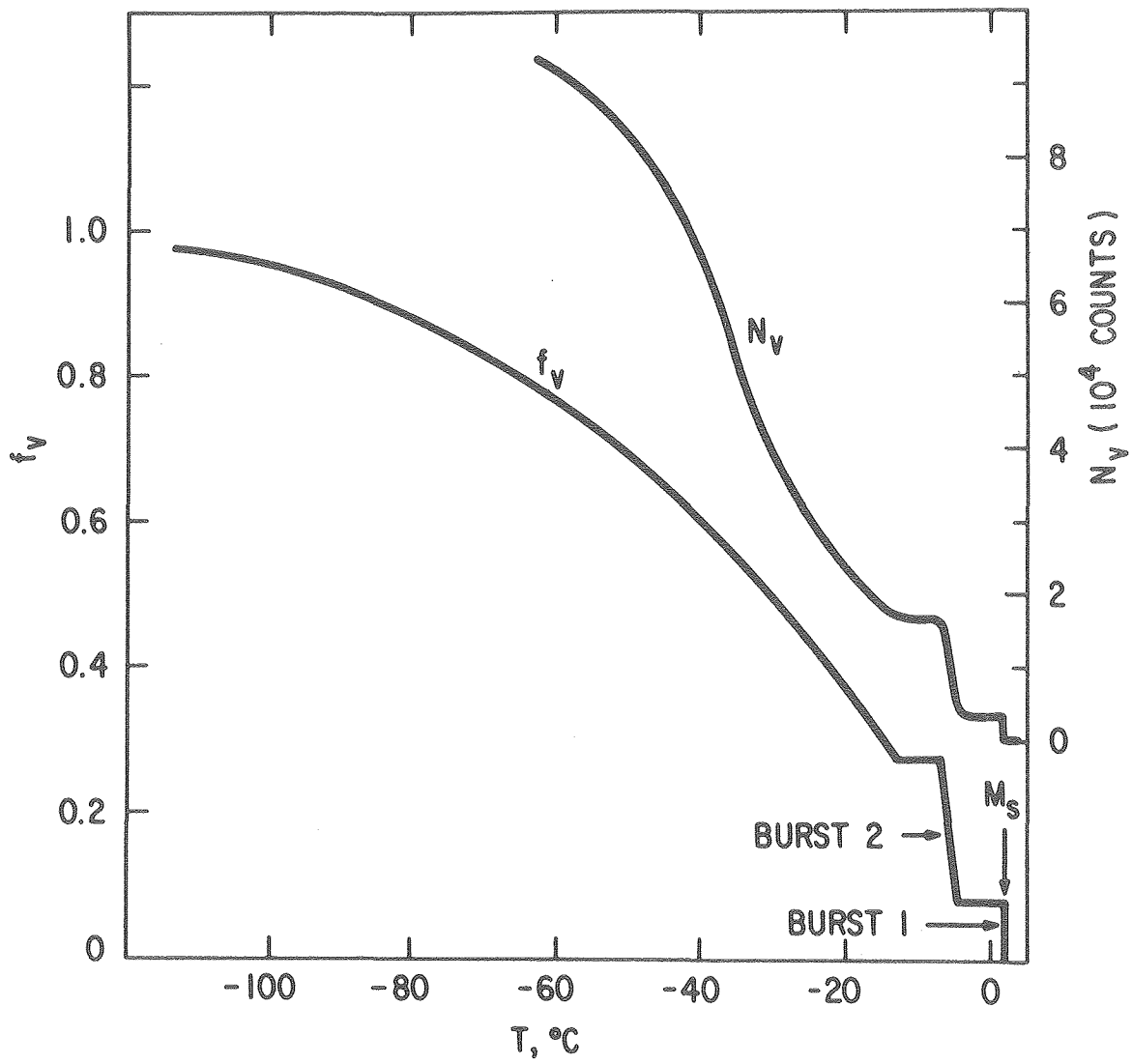

XBL 791-8170

Fig. 20

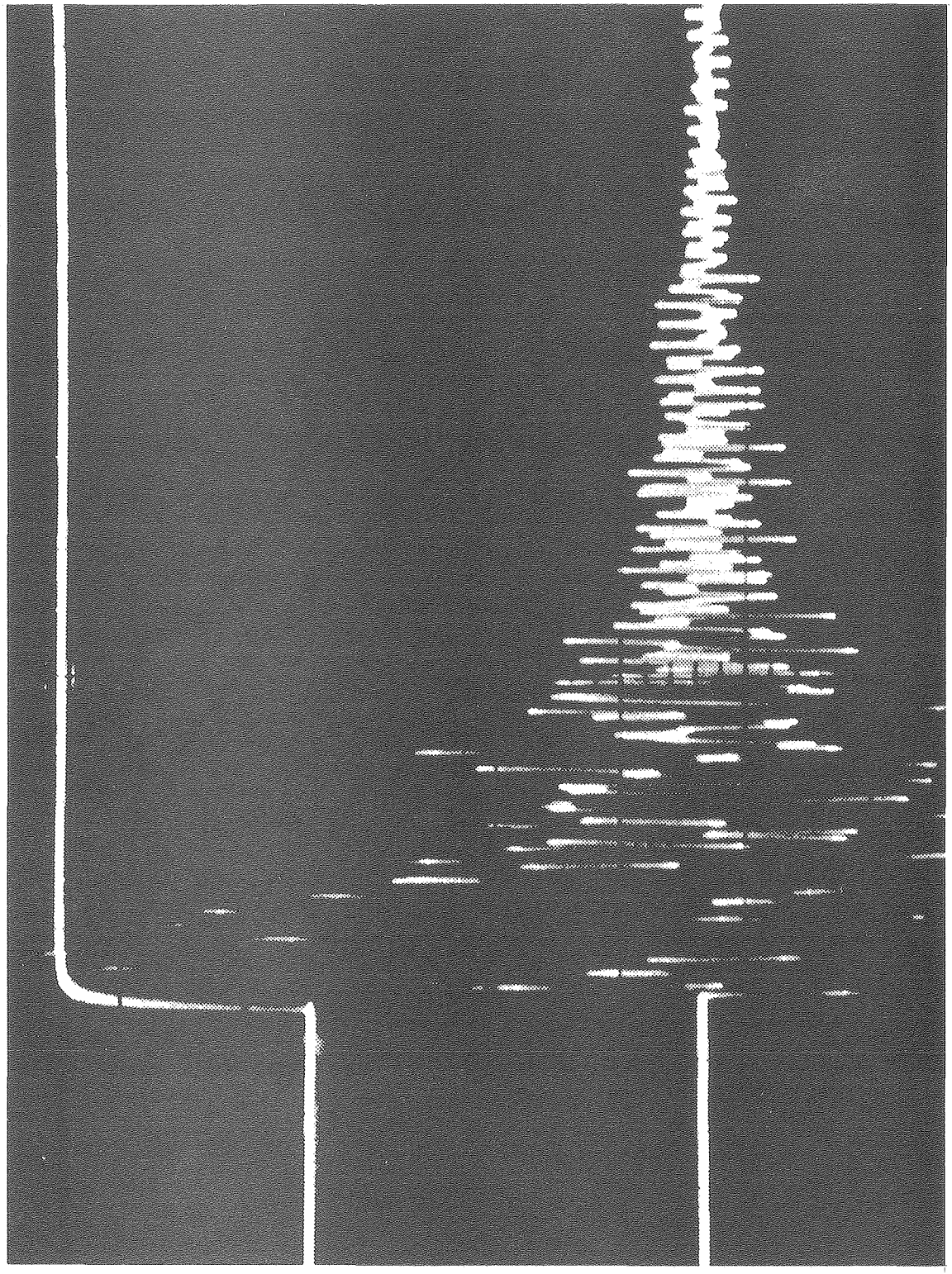

Fig. 21

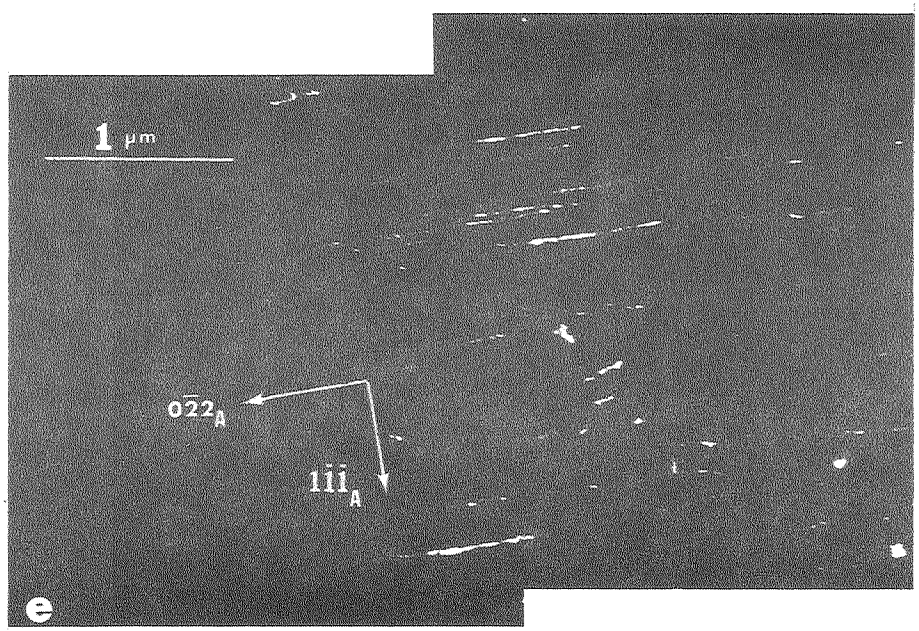

Fig. 22

This report was done with support from the Department of Energy. Any conclusions or opinions expressed in this report represent solely those of the author(s) and not necessarily those of The Regents of the University of California, the Lawrence Berkeley Laboratory or the Department of Energy.

Reference to a company or product name does not imply approval or recommendation of the product by the University of California or the U.S. Department of Energy to the exclusion of others that may be suitable.

TECHNICAL INFORMATION DEPARTMENT
LAWRENCE BERKELEY LABORATORY
UNIVERSITY OF CALIFORNIA
BERKELEY, CALIFORNIA 94720